SACY-1 DEAD-Box Helicase Links the Somatic Control of Oocyte Meiotic Maturation to the Sperm-to-Oocyte Switch and Gamete Maintenance in *Caenorhabditis elegans*

Seongseop Kim, J. Amaranath Govindan,[1] Zheng Jin Tu,[2] and David Greenstein[3]
Department of Genetics, Cell Biology and Development, University of Minnesota, Minneapolis, Minnesota 55455

ABSTRACT In sexually reproducing animals, oocytes arrest at diplotene or diakinesis and resume meiosis (meiotic maturation) in response to hormones. In *Caenorhabditis elegans*, major sperm protein triggers meiotic resumption through a mechanism involving somatic $G\alpha_s$–adenylate cyclase signaling and soma-to-germline gap-junctional communication. Using genetic mosaic analysis, we show that the major effector of $G\alpha_s$–adenylate cyclase signaling, protein kinase A (PKA), is required in gonadal sheath cells for oocyte meiotic maturation and dispensable in the germ line. This result rules out a model in which cyclic nucleotides must transit through sheath-oocyte gap junctions to activate PKA in the germ line, as proposed in vertebrate systems. We conducted a genetic screen to identify regulators of oocyte meiotic maturation functioning downstream of $G\alpha_s$–adenylate cyclase–PKA signaling. We molecularly identified 10 regulatory loci, which include essential and nonessential factors. *sacy-1*, which encodes a highly conserved DEAD-box helicase, is an essential germline factor that negatively regulates meiotic maturation. SACY-1 is a multifunctional protein that establishes a mechanistic link connecting the somatic control of meiotic maturation to germline sex determination and gamete maintenance. Modulatory factors include multiple subunits of a CoREST-like complex and the TWK-1 two-pore potassium channel. These factors are not absolutely required for meiotic maturation or its negative regulation in the absence of sperm, but function cumulatively to enable somatic control of meiotic maturation. This work provides insights into the genetic control of meiotic maturation signaling in *C. elegans*, and the conserved factors identified here might inform analysis in other systems through either homology or analogy.

IN sexually reproducing animals, cells of the germ line form gametes, which unite at fertilization and establish a heritable link between generations. Meiosis halves the number of chromosomes contributed by each gamete thereby ensuring the embryo inherits two full sets of chromosomes. Meiosis and germline sex determination are closely coordinated to ensure fertility (reviewed by Kimble and Crittenden 2007; Ewen and Koopman 2010; Murray *et al.* 2010). During development germ cells must adopt a sexual fate so as to differentiate either as sperm or oocytes. Sex-specific timing in the meiotic process is commonly observed: spermatocytes proceed through the meiotic divisions in an uninterrupted fashion, whereas oocytes almost invariably arrest once, and sometimes twice, depending on the species. Oocyte meiotic maturation is defined by the transition between diakinesis and metaphase of meiosis I and is accompanied by nuclear envelope breakdown, rearrangement of the cortical cytoskeleton, and meiotic spindle assembly (Masui and Clarke 1979). While the timing of the meiotic divisions with respect to fertilization varies among species, maturation promoting factor (MPF), CDK1/cyclin B, is a universal regulator of oocyte meiotic cell cycle progression (reviewed by Ferrell *et al.* 2009; Von Stetina and Orr-Weaver 2011). By contrast, the mechanisms by which the meiotic maturation process is regulated and integrated within the oogenic program are comparatively less well understood. Maternal age-related defects in the oocyte meiotic maturation process represent the largest single source of birth defects and infertility in

doi: 10.1534/genetics.112.143271
Manuscript received June 27, 2012; accepted for publication August 4, 2012
Available freely online through the author-supported open access option.
Supporting information is available online at http://www.genetics.org/lookup/suppl/doi:10.1534/genetics.112.143271/-/DC1.
[1]Present address: Department of Molecular Biology, Massachusetts General Hospital, Simches Research Center, Boston, MA 02114.
[2]Present address: Division of Biomedical Statistics and Informatics, Department of Health Sciences Research, Mayo Clinic, 200 1st St. SW, Rochester, MN 55905.
[3]Corresponding author: Department of Genetics, Cell Biology and Development, University of Minnesota, 4-208 MCB, 420 Washington Ave. SE, Minneapolis, MN 55455. E-mail: green959@umn.edu

developed countries, which motivates studies in both mammalian and invertebrate model systems (reviewed by Hassold and Hunt 2009).

The nematode *Caenorhabditis elegans* has emerged as a useful model for studying the regulation of oocyte meiotic maturation by intercellular signaling (reviewed by Han *et al.* 2010; Von Stetina and Orr-Weaver 2011; Kim *et al.* 2013). *C. elegans* hermaphrodites possess two U-shaped gonad arms that produce sperm during the last larval stage and oocytes during adulthood (Figure 1A). Oocyte meiotic maturation, ovulation, and fertilization occur iteratively in an assembly line-like fashion approximately every 23 min (McCarter *et al.* 1999). By contrast, strong loss-of-function (lf) mutations in sex-determination genes that feminize the germ line such that exclusively oocytes are produced, cause meiotic maturation to occur infrequently (approximately every 8 hr) and thus oocytes stack up in the gonad arm (McCarter *et al.* 1999). Mating of these females to males restores normal rates of meiotic maturation, ovulation, and fertilization (McCarter *et al.* 1999). These experiments (McCarter *et al.* 1999) and related observations (Ward and Carrel 1979) provided evidence that sperm produce a diffusible signal that promotes oocyte meiotic maturation and oocyte production. Subsequently, a biochemical purification of the maturation-inducing signal from sperm revealed that the major sperm proteins (MSPs) are sufficient to promote oocyte meiotic maturation and gonadal sheath cell contraction (Miller *et al.* 2001). MSPs appear to be released from sperm using an unconventional vesicle budding mechanism (Kosinski *et al.* 2005). MSPs were originally shown to function as the chief cytoskeletal element in the actin-independent amoeboid locomotion of nematode sperm (Italiano *et al.* 1996; Miao *et al.* 2003; reviewed by Roberts and Stewart 2012). MSPs were proposed to function as central elements of a sperm-sensing mechanism that couples meiotic maturation and fertilization rates to sperm availability, thereby ensuring efficient progeny production and utilization of resources (Miller *et al.* 2003).

MSP triggers multiple molecular readouts of meiotic maturation, including activation of the MPK-1 mitogen-activated protein kinase (MAPK) (Miller *et al.* 2001), which is required for normal meiotic maturation (Lee *et al.* 2007). MSP also promotes the reorganization of the oocyte microtubule cytoskeleton (Harris *et al.* 2006), the localization of the AIR-2 Aurora B protein kinase to chromatin (Govindan *et al.* 2009), and the remodeling of oocyte ribonucleoprotein particles (Jud *et al.* 2008). In addition, MSP promotes the actomyosin-dependent cytoplasmic flows that drive oocyte growth and require the continued presence of sperm (Wolke *et al.* 2007; Nadarajan *et al.* 2009). In this regard, MSP might function in part by promoting the phosphorylation of the MLC-4 regulatory light chain of NMY-2 nonmuscle myosin (Nadarajan *et al.* 2009). Thus far, all described outcomes of MSP signaling in the germ line require $G\alpha_s$–adenylate cyclase activity in the gonadal sheath cells that surround oocytes (Govindan *et al.* 2009). Genetic mosaic analysis established that genotypically wild-type oocytes, which are surrounded by gonadal sheath cells that lack $G\alpha_s$ or adenylate cyclase activity, behave as if they do not receive the MSP signal (Govindan *et al.* 2009). Further, activation of $G\alpha_s$–adenylate cyclase signaling in the gonadal sheath cells is sufficient to drive meiotic maturation at robust rates in the absence of sperm (Govindan *et al.* 2006, 2009).

A key question is how $G\alpha_s$–adenylate cyclase signaling in gonadal sheath cells promotes oocyte meiotic maturation in response to the MSP signal. Part of the answer to this question is that the gonadal sheath cells form gap junctions with oocytes (Hall *et al.* 1999), and these gap junctions function to inhibit meiotic maturation when sperm are absent (Govindan *et al.* 2006, 2009; Whitten and Miller 2007; T. Starich and D. Greenstein, unpublished results). A loss-of-function mutation in the *inx-22* gene, which encodes the gap junction protein INX-22, suppresses *gsa-1(lf)* sterility (*gsa-1* encodes $G\alpha_s$; Govindan *et al.* 2009). Here we use genetic analysis to delineate the molecular mechanisms by which somatic $G\alpha_s$–adenylate cyclase signaling promotes oocyte meiotic maturation. We use genetic mosaic analysis to show that the protein kinase A (PKA) target of $G\alpha_s$–adenylate cyclase signaling is required in gonadal sheath cells for oocyte meiotic maturation. Not only is PKA activity in the germ line dispensable for meiotic maturation, but PKA does not function in the germ line as a negative regulator of MPF activation, as observed in vertebrate systems (Maller and Krebs 1977; Lincoln *et al.* 2002; Han *et al.* 2005; Pirino *et al.* 2009; Oh *et al.* 2010). This genetic result rules out a model in which cyclic nucleotides must move through sheath-oocyte gap junctions to regulate meiotic maturation via PKA activity in the *C. elegans* germ line, as has been proposed in vertebrate systems (Anderson and Albertini 1976; Sela-Abramovich *et al.* 2006; Norris *et al.* 2008, 2009).

acy-4 encodes the adenylate cyclase that is required in gonadal sheath cells for oocyte meiotic maturation (Govindan *et al.* 2009). To identify new regulators of oocyte meiotic maturation that function downstream of somatic $G\alpha_s$–ACY-4–PKA signaling, we conducted a genetic screen for **s**uppressor of ***acy-4(lf)*** sterility (Sacy) mutations. We characterized 66 Sacy mutations in at least 17 genes. By using whole-genome sequencing and other positional cloning tools, together with an analysis of previously isolated mutations, we molecularly identified 10 Sacy loci. The centerpiece of our analysis is *sacy-1*, which encodes a highly conserved DEAD-box helicase that functions in the germ line downstream of PKA signaling. Genetic analysis reveals that SACY-1 mediates multiple functions necessary for *C. elegans* reproduction: it is a strong negative regulator of oocyte meiotic maturation; it is a component of the germline sex-determination system, functioning in the hermaphrodite sperm-to-oocyte switch; and it is required to prevent necrotic cell death of gametes. Thus, *sacy-1* links the somatic control of meiotic maturation to germline sex determination and the maintenance of oocyte quality. In addition, our genetic screen identified multiple components of a CoREST-

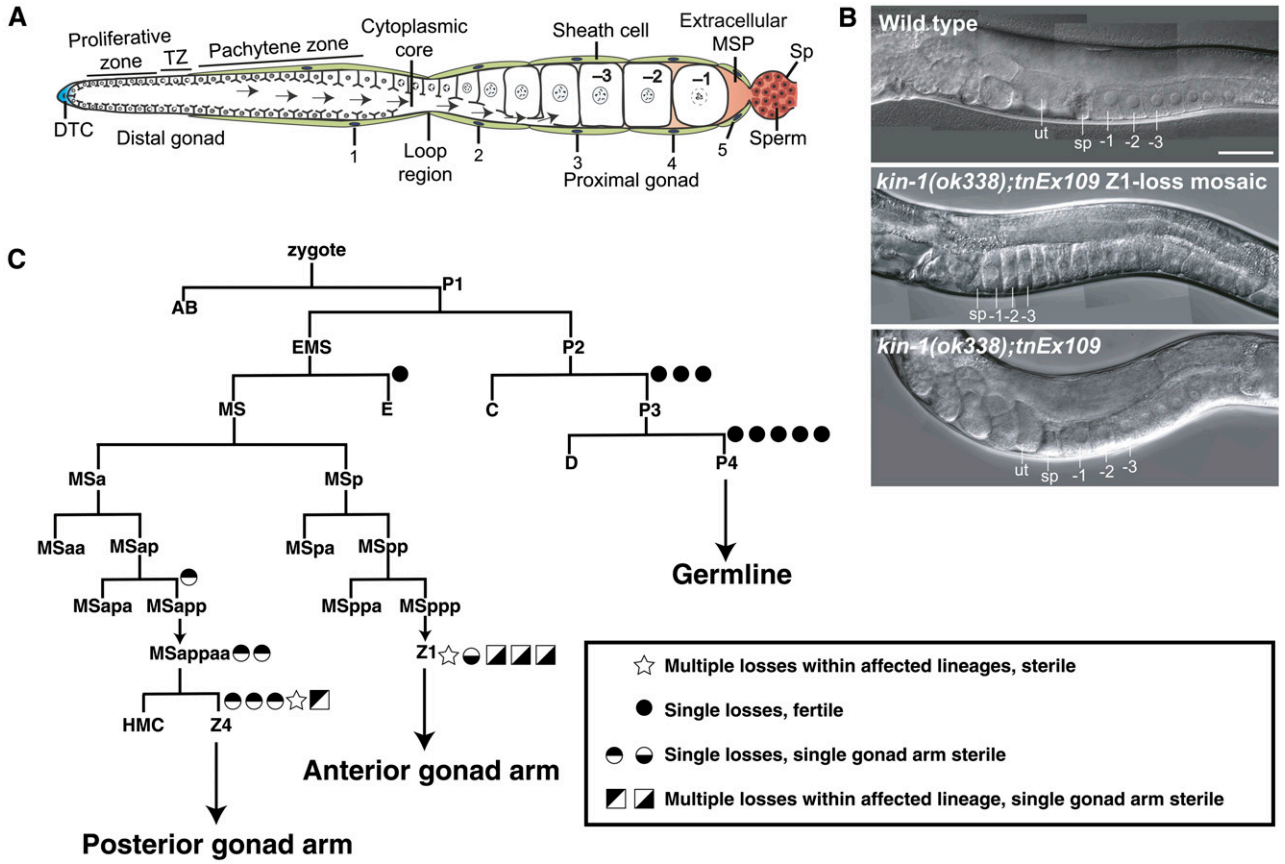

Figure 1 *kin-1* is required in the gonadal sheath cells for oocyte meiotic maturation. (A) An adult hermaphrodite gonad arm. Germline stem cells proliferate near the distal tip cell (DTC) and then enter meiosis as they move proximally. Oocytes grow by receiving cytoplasmic flow (arrows) and progress to the diakinesis stage of meiotic prophase I prior to undergoing meiotic maturation (at the −1 position) in response to MSP secreted from sperm in the spermatheca (sp). Five pairs of gonadal sheath cells surround the germ line in each gonad arm. (B) DIC images showing that loss of *kin-1(+)* function in the somatic gonad prevents meiotic maturation, causing oocytes to stack up in the gonad arm despite the presence of sperm. This genetic mosaic resulted from a complex loss within the Z1 lineage, such that the anterior sheath cells and the anterior DTC were mutant for *kin-1*, but a few spermathecal cells were *kin-1(+)* (the mosaic is displayed with anterior to the right). By contrast, wild-type and *kin-1(ok338); tnEx109* gonad arms are fertile; embryos are observed in the uterus (ut). Bar, 50 μm. (C) Genetic mosaic analysis of *kin-1* in meiotic maturation. Derivation of the somatic gonad and the germ line, the points in the lineage where the *kin-1(+)* array was lost and the resulting phenotypes are indicated (3378 animals were screened). Circles represent single mosaic animals, with array losses at the indicated position. Squares and stars indicate animals with complex losses affecting the somatic gonad (Figure S2). We did not recover losses of the *kin-1(+)* array in EMS or MS, similar to what was observed in the genetic mosaic analysis of *gsa-1* (Govindan *et al.* 2009).

like complex and the TWK-1 two-pore domain potassium channel, which we show function in the germline and somatic gonad, respectively. Genetic evidence suggests that CoREST and TWK-1 likely function cumulatively to regulate meiotic maturation. This work provides a foundation for unraveling the genetic control of meiotic maturation signaling in *C. elegans*. The insights gained may prove informative in the analysis of systems less amenable to forward genetic approaches.

Materials and Methods

Strains

C. elegans were cultured using standard methods at 20° (Brenner 1974), except as otherwise noted. OP50-1, a streptomycin-resistant OP50 derivative, was used for routine strain maintenance and nematode growth medium (NGM) contained 200 μg/ml streptomycin sulfate added before autoclaving. Streptomycin was omitted for all experiments using HT115(DE3), and their respective controls. Alleles generated in this study are described in Table 1, and the molecular changes identified are listed in the Supporting Information, Table S1. In addition, the following mutations were used: LGI: *pde-6(ok3410)*, *gsa-1(pk75)*, *fog-1(e2121)*, *dpy-5(e61)*, *tom-1(ok188)*, *tom-1(ok2437)*, *tom-1(ok285)*, *tom-1(tm4724)*, *let-605(h312)*, *dpy-14(e188)*, *sacy-1(tm5503)*, *unc-15(e1402)*, *unc-13(e450)*, *unc-13(e1091)*, *pbrm-1(gk1195)*, *rrf-1(pk1417)*, *spr-4(by105)*, *fog-3(q470)*, *lin-11(n566)*, *spr-5(ar197)*, *spr-5(by134)*, *kin-1(ok338)*, and *uev-1(ok2610)*; LG II: *tra-2(e2020)* and *rrf-3(pk1426)*; LGIII: *ced-4(n1162)*, *unc-32(e189)*, and *unc-119(ed3)*; LGIV: *unc-33(mn407)*, *unc-24(e138)*, *oma-1(zu405te33)*, *spr-2(ar199)*, *spr-2(ar211)*, *spr-2(tm4802)*, *fem-3(e1996)*, *fem-3(q20)*, *him-8(tm611)*, *dpy-20(e1282)*, and *ced-3(n717)*; LGV: *unc-46(e177)*, *acy-4*

Table 1 Complementation groups of Sacy mutations

Linkage group	Gene	Alleles[a]
I	*pde-6*	*tn1237*, *tn1242*, *tn1336*, *ok3410*
	tom-1[b]	*tn1454*, *tn1463*, *ok2437*
	sacy-1	*tn1385*, *tn1391*, *tn1440*
	twk-1[c]	*tn1397*, *tn1398*, *tn1403*
	spr-4	*tn1383*, *tn1402*, *tn1404*, *tn1438*, *tn1444*, *tn1467*, *by105*
	spr-5[c]	*tn1378*, *tn1379*, *tn1394*, *ar197*, *by134*
	uev-1[d]	*tn1381*, *tn1382*, *ok2610*
	Unassigned	*tn1389*, *tn1390*, *tn1392*, *tn1393*, *tn1395*, *tn1415*, *tn1416*, *tn1418*, *tn1419*, *tn1434*, *tn1441*, *tn1442*, *tn1445*, *tn1446*, *tn1464*, *tn1471*
II	*sacy-2*	*tn1401*, *tn1410*, *tn1421*
	Unassigned	*tn1424*, *tn1428*, *tn1432*, *tn1451*, *tn1452*, *tn1469*
III	*sacy-3*	*tn1396*, *tn1408*, *tn1412*, *tn1414*, *tn1422*, *tn1437*
	Unassigned	*tn1449*, *tn1456*
IV	*spr-2*[e]	*tn1380*, *tn1436*, *ar211*, *tm4802*
	sacy-4	*tn1387*, *tn1413*, *tn1431*, *tn1468*
	Unassigned	*tn1386*, *tn1455*
V	Unassigned	*tn1409*
X	Unassigned	*tn1384*, *tn1388*

[a] *tn* alleles were isolated in this study; the independently isolated alleles listed suppress *acy-4(lf)* sterility and fail to complement at least one *tn* allele. In addition, previously isolated mutations in *spr-1* and *spr-3* suppress *acy-4(lf)* sterility (see text). *inx-22(tm1661)*, *ceh-18(mg57)*, and *vab-1(dx31)* do not suppress *acy-4(lf)* sterility (Govindan *et al.* 2009; S. Kim, J. A. Govindan, and D. Greenstein, unpublished results).

[b] *tom-1* encodes the *C. elegans* tomosyn ortholog (Dybbs *et al.* 2005; Gracheva *et al.* 2006). In addition to the alleles listed, other *tom-1* alleles were tested (*ok188*, *ok285*, and *tm4724*) but found not to suppress *acy-4(lf)* sterility (Figure S1).

[c] Oocytes stack in the gonad arms of *twk-1(tn1397); fog-2(oz40)* and *spr-5(by134); fog-2(oz40)*, as they do in *fog-2(oz40)* females, indicating that neither *twk-1* nor *spr-5* is a negative regulator of meiotic maturation in the absence of sperm.

[d] *uev-1* encodes a ubiquitin-conjugating enzyme variant (Jones *et al.* 2002; Kramer *et al.* 2010).

[e] *spr-2(ar199)* mutation does not suppress *acy-4(lf)* sterility.

(ok1806), *unc-68(e540)*, *oma-2(te51)*, *spr-1(gk734)*, *unc-23 (e25)*, *fog-2(oz40)*, and *fog-2(q71)*; LGX: *spr-3(by108)* and *spr-3(ok2525)*. The following rearrangements, deficiencies, duplications, and extrachromosomal arrays were used: *hT2 [dpy-18(h662)*; *bli-4(e937)]* (I; III), *hT2[bli-4(e937) let-? (q782) qIs48]* (I; III), *nT1[qIs51]* (IV; V), *sDp2*(I; f), *qDf16*, *tnEx31 [gsa-1(+) sur-5*::*gfp]*, *tnEx37[acy-4(+) sur-5*::*gfp]*, *tnEx109 [kin-1(+) sur-5*::*gfp]*, *tnEx131[acy-1*::*gfp rol-6(su1006d)]*, *tnEx133[acy-2*::*gfp rol-6(su1006d)]*, *tnEx134[acy-3*::*gfp rol-6(su1006d)]*, *tnEx159[gfp*::*sacy-1 unc-119(+)]*, *tnEx175 [twk-1*::*gfp rol-6(su1006d)]*, *tnEx180[twk-1(+) sur-5*::*gfp]*, *tnEx181[twk-1*::*gfp str-1*::*gfp]*, *tnEx188[twk-1(*ΔC284*)*::*gfp str-1*::*gfp]*. The genotypes of strains used in this study are listed in Table S2.

Isolation of suppressor of acy-4(lf) sterility (Sacy) mutations

L4-stage *acy-4(ok1806)*; *tnEx37* animals were mutagenized with 50 mM ethyl methanesulfonate (EMS) (Brenner 1974). GFP^+ F_1 animals were cultured individually and fertile GFP^- animals were sought in the F_2 generation. Approximately 20,000 haploid genomes were screened and 63 suppressors had sufficient brood sizes to be analyzed further. Brood sizes are expressed as mean ± SD. All Sacy mutations were outcrossed to the parental strain and were recessive. Mutations analyzed in detail were outcrossed at least five times, or as otherwise noted. The polymerase chain reaction verified that all suppressor strains retained the *acy-4 (ok1806)* deletion, and did not contain a wild-type copy of the *acy-4* gene or *gfp* sequences (oligonucleotides used in this study are listed in Table S3). *pde-6* alleles were identified as EMS-induced mutations in N2 that suppressed sterility following *gsa-1(RNAi)*. The three *pde-6* alleles failed to complement for this property, but exhibited normal RNAi responses with *unc-22* and *pos-1* triggers.

Genetic mapping and molecular identification of Sacy mutations

Assignment to linkage groups used SNP mapping (Davis *et al.* 2005) with crosses to DG2574, which was generated by introgressing the *acy-4(ok1806)* mutation, balanced by *tnEx37*, into the CB4856 Hawaiian background using 10 backcrosses. It proved difficult to fine map many of the Sacy mutations in the Hawaiian background, possibly because complex genetic interactions between Bristol and Hawaiian loci modified the penetrance of *acy-4(lf)* (S. Kim, J. A. Govindan, and D. Greenstein, unpublished results). In addition, more than half of Sacy mutations localize to LGI and thus the documented incompatibility between Bristol and Hawaiian strains caused by the *peel-1/zeel-1* system (Seidel *et al.* 2008) might have distorted the mapping results. Therefore, we utilized a strategy combining complementation testing, whole-genome sequencing, and transgenic rescue. Complementation tests were conducted between Sacy mutations mapping to the same linkage group. Briefly, *trans*-heterozygotes *sacy(a)/sacy(b)*; *acy-4(ok1806)*; *tnEx37* were constructed and the fraction of GFP^- fertile progeny was measured and compared to the parental strains. Because Sacy mutations might exhibit nonallelic noncomplementation, these assignments are viewed as provisional unless validated

by sequencing of multiple alleles, transgenic rescue, or suppression of *acy-4(lf)* sterility by other available alleles.

Whole-genome sequencing for mutant identification was conducted on Illumina GAIIx and HiSeq2000 instruments according to the manufacturer's instructions. The average depth of coverage was ~49-fold. Data were analyzed using MAQGene (Bigelow *et al.* 2009). Candidate Sacy mutations in independently isolated alleles were identified and confirmed by Sanger sequencing. Phylogenetic analysis was conducted as described (Dereeper *et al.* 2008).

Transgenic rescue and expression studies

Transgenic animals expressing translational *gfp* fusions were generated using recombineering (Warming *et al.* 2005; Tursun *et al.* 2009) and either microinjection (Stinchcomb *et al.* 1985) or biolistic transformation (Praitis *et al.* 2001). To create C-terminal TWK-1::GFP fusions, fosmid WRM0616aE06 was used. To generate a C-terminal truncation of TWK-1::GFP (TWK-1ΔC284::GFP), *Escherichia coli* GalK was first inserted before Thr284, and then GalK and the C terminus of TWK-1 (residues 284–451) were deleted using recombineering. The C-terminal truncated *twk-1*::*gfp* and controls were directly injected into *twk-1(tn1397)/unc-13(e51)*; *acy-4(ok1806)/nT1[qIs51]* animals, and several transgenic lines expressing the *str-1*::*gfp* co-injection marker were established. The transgene arrays were tested for rescuing *twk-1(+)* function in *twk-1(tn1397)*; *acy-4(ok1806)* animals by restoring *acy-4(lf)* sterility. Fosmid WRM0640aH10 was used to generate an N-terminal GFP::SACY-1 fusion. Cre-mediated recombination was used to introduce the *unc-119* gene (Zhang *et al.* 2008) into the fosmid for biolistic transformation. A *gfp*::*sacy-1*–expressing extrachromosomal array (*tnEx159*) was crossed into *sacy-1* mutant backgrounds and tested for rescue. To generate C-terminal GFP fusions to ACY-1, ACY-2, and ACY-3, we used fosmids WRM067dG12, WRM0638bH07, and WRM0618cF11, respectively. Fusion constructs were injected into the wild type with *rol-6(su1006d)* as co-injection marker. Transgenes were then crossed into the *spr-5(by134)* mutant background.

Genetic mosaic analysis

Genetic mosaic analysis for *kin-1* was performed using a rescuing *kin-1(+)* extrachromosomal array, *tnEx109[kin-1(+) sur-5*::*gfp]*, carrying the cell autonomous *sur-5*::*gfp* marker (Yochem *et al.* 1998). *kin-1(ok338)*, *sacy-1(tn1385) kin-1(ok338)*, *spr-5(by134) kin-1(ok338)*, and *twk-1(tn1397) kin-1(ok338)* animals bearing *tnEx109* were used for the analysis. To identify genetic mosaics with array losses in the somatic gonad, young adult hermaphrodites were examined on a Zeiss Axioskop using DIC and fluorescence microscopy with a 100× Plan-Apochromat (numerical aperature, N.A. 1.4) objective lens. To determine the point of array loss in animals exhibiting mosaic expression of the *sur-5*::*gfp* marker, the following cells were routinely examined: distal tip cell (DTC), gonadal sheath, spermatheca, coelomocytes, the head mesodermal cell (HMC), body wall muscles, hyp11, intestine, excretory cell, B, F, K, DVA, DVC, and the germ line (the presence of GFP^+ progeny could only be scored if at least one gonad arm was fertile). To identify germline-loss mosaics, L4 hermaphrodites were cultured individually. Animals producing entire broods of GFP^- progeny were further examined by fluorescence microscopy. Unfertilized oocytes laid by *kin-1(ok338)* germline mosaics were counted over the first 6 days of adulthood. For *twk-1*, genetic mosaics were identified in similar fashion using *twk-1(tn1397)*; *acy-4(ok1806)/nT1[qIs51]*; *tnEx180[twk-1(+) sur-5*::*gfp]* as the parent strain. *twk-1(tn1397)* somatic gonad mosaics were fertile in the affected gonad arm, but germline mosaics could not be sought. For genetic mosaic analysis of the *sacy-1(tm5503)* gamete degeneration phenotype, we used *sacy-1(tm5503)*; *unc-119(ed3)*; *tnEx159[gfp*::*sacy-1 unc-119(+)]*. Coordinated (non-Unc) animals showing the *sacy-1(tm5503)* gamete degeneration phenotype were sought and analyzed by DIC and fluorescence microscopy.

RNA interference

All RNA interference (RNAi) experiments were conducted at 22° using injection (Fire *et al.* 1998) or feeding (Timmons and Fire 1998), as modified (Govindan *et al.* 2006).

Immunohistochemistry and microscopy

TWK-1::GFP was detected in dissected and fixed (Finney and Ruvkun 1990) gonads using mouse monoclonal anti-GFP antibodies (Abcam; 1:500). Rhodamine phalloidin (Sigma; 1:200) was used to detect actin. MSP and RME-2 were detected in dissected gonads as described (Kosinski *et al.* 2005), using mouse monoclonal anti-MSP antibody 4A5 (1:300) and rabbit anti–RME-2 antibody (Grant and Hirsh 1999; kindly provided by B. Grant, Rutgers University, 1:50). Secondary antibodies were Alexa 488-conjugated goat antimouse (Life Technologies, 1:500), Cy3-conjugated goat antimouse (Jackson ImmunoResearch, 1:500), and Alexa 488-conjugated goat antirabbit (Life Technologies, 1:500). Acridine orange was used to stain apoptotic germ cells (Gumienny *et al.* 1999) and necrotic gametes in *ced-3(n717)* and *ced-4(n1162)* mutant backgrounds. Adult hermaphrodites (18–24 hr post-L4) were cultured for 1 hr on 8 ml of OP50-1–seeded NGM to which 0.5 ml of M9 containing acridine orange (20 μg/ml) was added. After staining, worms were transferred to fresh medium for 1 hr and then analyzed by fluorescence microscopy. Prior to microscopy, worms were kept in the dark. DIC and fluorescent images were acquired on a Zeiss motorized Axioplan 2 microscope with either 40× Plan-Neofluar (N.A. 1.3) or 63× Plan-Apochromat (N.A. 1.4) objective lenses using a AxioCam MRm camera and AxioVision software.

Results

kin-1 is required in the gonadal sheath cells for oocyte meiotic maturation

$G\alpha_s$–ACY-4 signaling is required in the gonadal sheath cells for oocyte meiotic maturation (Govindan *et al.* 2009). cAMP-

dependent PKA is a canonical downstream effector of $G\alpha_s$–adenylate cyclase signaling. In *C. elegans*, the catalytic and regulatory subunits of PKA are encoded by *kin-1* and *kin-2*, respectively (Gross *et al.* 1990; Lu *et al.* 1990). The KIN-2 regulatory subunit functions by binding and inactivating the catalytic subunit in the absence of cAMP; binding of cAMP to KIN-2 alleviates its inhibition of KIN-1 activity (reviewed by Taylor *et al.* 1990). In a female genetic background, a *kin-2* reduction-of-function (rf) mutation or *kin-2(RNAi)* derepress oocyte meiotic maturation and MAPK activation in oocytes in the absence of sperm (Govindan *et al.* 2006). Further, *kin-2 (ce179rf)* suppresses the sterility caused by a strong loss-of-function mutation in *acy-4* (Govindan *et al.* 2009). *kin-2 (RNAi)* experiments using the *rrf-1* genetic background, which is sensitive to RNAi in the germ line but resistant in the somatic gonad (Sijen *et al.* 2001; Kumsta and Hansen 2012), suggested that *kin-2* functions in the soma to inhibit meiotic maturation in the absence of sperm (Govindan *et al.* 2006). Because cyclic nucleotides have been suggested to move through gap junctions to regulate PKA activity in oocytes in mammalian systems (Sela-Abramovich *et al.* 2006; Norris *et al.* 2009), we sought to assess directly the involvement and focus of action of the kinase in meiotic maturation in *C. elegans* using genetic mosaic analysis.

We conducted genetic mosaic analysis using the *kin-1 (ok338)* deletion allele. The *kin-1(ok338)* allele deletes conserved subregions III–VI of the catalytic domain (Hanks *et al.* 1988) and introduces a frameshift before subregion VII, which generates multiple stop codons in all known isoforms. *kin-1(ok338)* exhibits a larval lethal phenotype apparently identical to that caused by an absence of $G\alpha_s$ in the strong loss-of-function *gsa-1(pk75)* allele (Korswagen *et al.* 1997). We rescued *kin-1(ok338)* lethality using an extrachromosomal array bearing a wild-type copy of the gene linked to a cell-autonomous nuclear GFP marker. Approximately 98% of *kin-1(ok338)*; *tnEx109[kin-1(+) sur-5*::*gfp]* animals reaching the L4 stage are fertile (n = 595) and segregate GFP-expressing fertile animals, non–GFP-expressing arrested larvae, and genetic mosaics. Loss of *kin-1(+)* function in germline lineages (P3 and P4; Figure 1C) did not affect viability or fertility. Thus, *kin-1* is not required in the germ line for meiotic maturation. The progeny of germline mosaic animals (n = 26) arrested as L1 larvae, recapitulating the *kin-1(ok338)* zygotic phenotype.

To assess whether *kin-1* might function in the germ line to inhibit meiotic maturation, as in vertebrate systems (Maller and Krebs 1977; Mehlmann 2005), we asked whether oocytes continue to undergo meiotic maturation and ovulation upon the depletion of sperm through self-fertilization in germline mosaics. We observed that *kin-1(ok338)* germline mosaics produced a total of 10 ± 14 unfertilized oocytes (n = 15) as compared to 14 ± 21 unfertilized oocytes (n = 18) for nonmosaic siblings ($P > 0.5$, Student's t-test). Thus, *kin-1(+)* function is dispensable in the germ line both for meiotic maturation and also for its inhibition when sperm are absent or limiting.

Next, we sought array losses in the MS lineage, which gives rise to the somatic cells of the gonad. Array losses within the MS lineage cause sterility within a gonad arm (Figure 1B). The fertility of a specific gonad arm (anterior or posterior) depends on the *kin-1* genotype of that gonad arm. For the animal to be completely sterile, independent losses were needed affecting both gonad arms (Figure 1C). *kin-1(+)* somatic gonad-loss mosaics exhibit sterility because oocytes fail to undergo meiotic maturation, ovulation, and fertilization, phenocopying *acy-4(lf)* mutants (Govindan *et al.* 2009). Complex losses found within the sheath-spermathecal lineages suggest that *kin-1* is needed in the gonadal sheath cells, not in the spermatheca, for meiotic maturation (Figure S2).

Genetic and molecular identification of suppressor of acy-4(lf) sterility mutations

To identify new regulators of oocyte meiotic maturation that might function downstream of somatic $G\alpha_s$–ACY-4–PKA signaling, we conducted a forward genetic screen for mutations that suppress the sterility of *acy-4(ok1806)* mutants (Figure 2A; Table 1). We identified 63 suppressors from ~20,000 mutagenized haploid genomes and an additional three suppressors from a related screen (see *Materials and Methods*). We refer to these suppressors as Sacy mutants (**s**uppressor of ***acy-4(lf)*** mutant sterility). All isolated Sacy mutations are recessive. The brood sizes of the Sacy mutants in the *acy-4(lf)* background are variable and smaller than those of the wild type (~10–90 progeny *vs.* 339 ± 31 (n = 37); Figure 2B). Linkage analysis and complementation testing indicate that the 66 suppressors represent at least 17 genes (Table 1).

Molecular identification of Sacy genes, an overview

We used a combination of positional cloning and whole-genome sequencing to identify 8 of 17 Sacy loci identified in our screen (Figures 3 and 4; Table 1). Based on their molecular identities, strong loss-of-function phenotypes, and likely modes of action, there appear to be several pathways that function cumulatively to affect the regulation of meiotic maturation downstream of PKA. Among these pathways, *sacy-1* acts as a strong negative regulator of meiotic maturation and provides a mechanistic connection to the fundamental germline processes of sex determination and gamete maintenance. We will first describe *sacy-1*, followed by the nonessential Sacy loci.

SACY-1 DEAD-box helicase functions in the germ line downstream of KIN-1 and is a negative regulator of meiotic maturation in the absence of sperm

Whole-genome sequencing identified three noncomplementing alleles (*tn1385*, *tn1391*, and *tn1440*) mapping to the center of LGI as missense mutations in *H27M09.1*, which encodes a DEAD-box helicase related to *Drosophila* Abstrakt and human DDX41 (Figure 4). We confirmed the missense mutations in *H27M09.1* using Sanger sequencing (Figure 4) and named *H27M09.1 sacy-1*. Whole-genome sequencing also identified independent tightly linked missense mutations

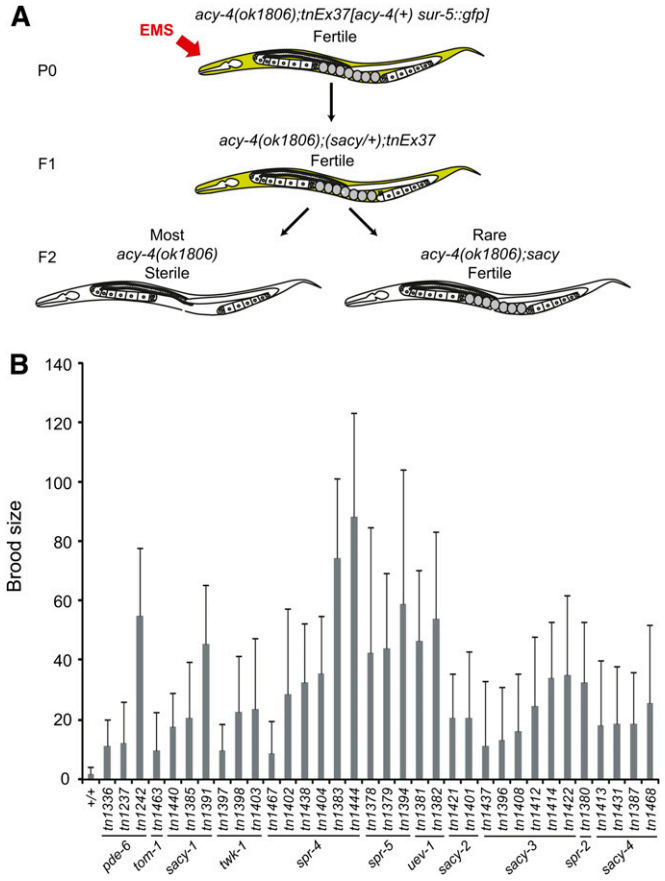

Figure 2 Genetic screen for *acy-4(lf)* suppressor mutations. (A) *acy-4 (ok1806)* animals possessing an extrachromosomal *acy-4(+)* array (green) were mutagenized, and F_1 progeny were cultured individually. Cultures containing fertile animals not possessing the extrachromosomal array (nongreen animals) were sought in the F_2 generation. (B) Brood sizes of Sacy mutants, measured in the *acy-4(ok1806)* background. Brood sizes of *pde-6* alleles were measured in a *unc-46(e177) acy-4(ok1806)* background. At least 10 hermaphrodites were scored for each genotype. Error bars represent one standard deviation.

in *pbrm-1* in *tn1385* and *tn1440*. *pbrm-1* encodes a polybromo protein that likely regulates chromatin structures and transcription during development of the gonad (Shibata *et al.* 2012). Several lines of evidence indicate that mutations in *sacy-1*, not *pbrm-1*, are responsible for *acy-4(lf)* suppression. We separated the two *sacy-1* mutations (*tn1385* and *tn1440*) from the *pbrm-1* mutations (*tn1475* and *tn1476*, respectively) by recombination with closely linked markers. The *sacy-1* mutations were able to suppress *acy-4 (lf)* sterility individually, but the *pbrm-1* mutations exhibited no activity as *acy-4(lf)* suppressors. Further, we examined a *pbrm-1(gk1195)* deletion allele and found that *pbrm-1 (gk1195)*; *acy-4(ok1806)* double mutants are sterile and exhibit the *acy-4(lf)* meiotic maturation defect (Table S4). Increased suppression of *sacy-1(rf)*; *acy-4(lf)* by *pbrm-1* mutations was also not consistently observed (Table S4). Moreover, *sacy-1(RNAi)* suppresses *acy-4(lf)* sterility (Figure 5A). To assess whether RNAi depletion of *sacy-1* function in the germ line or somatic gonad mediates the suppression of *acy-4(lf)* sterility, we conducted RNAi experiments in the somatic gonad RNAi-deficient *rrf-1(pk1417)* genetic background. *sacy-1(RNAi)* using *rrf-1(pk1417)*; *acy-4(ok1806)*; *tnEx37* suppresses *acy-4(lf)* sterility in the F_1 generation (Figure 5A). Thus, reduction of *sacy-1* function in the germ line suppresses *acy-4(lf)* sterility. We used recombineering and biolistic transformation to generate an N-terminal GFP::SACY-1 fusion within the fosmid context (Figure 4C) and assessed its rescuing activity (Figure 5, C and D). The GFP::SACY-1 fusion rescues *acy-4(lf)* suppression (Figure 5C). We observed that GFP::SACY-1 is expressed in most or all germline and somatic cells and localizes to the nucleus and cytoplasm (Figure 4C).

Structural and bioinformatic studies show that DEAD-box RNA helicases contain a highly conserved core helicase domain containing ATP and RNA binding sites (Linder and Jankowsky 2011). Each of the three missense *sacy-1* alleles changes a highly conserved glycine residue to an arginine residue in either the DEAD-box or helicase domains (Figure 4B). *tn1385* results in a G533R substitution in motif VI, which contributes to ATP binding and hydrolysis (Linder 2006). The R534 residue adjacent to the *tn1385* mutation site interacts with the γ-phosphate of ATP (Schutz *et al.* 2010). *tn1440* results in G331R in motif Ib, which contributes to RNA binding (Schutz *et al*, 2010). *tn1391* results in G473R in a region between motifs IV and V, which is surface exposed in the crystal structure of the human ortholog DDX41 (Schutz *et al.* 2010).

When separated from the *acy-4(ok1806)* mutation, each *sacy-1* missense allele was comparably viable and fertile as the wild type. For example, *sacy-1(tn1385)* has a brood size of 349 ± 77 (n = 35), compared to a wild-type brood size of 339 ± 31 (n = 37, P value = 0.49). When placed in *trans* to the deficiency *qDf16*, which deletes *sacy-1*, each missense allele was viable and fertile. Interestingly, when the *sacy-1* missense alleles were treated with *sacy-1(RNAi)* by feeding, we observed increased levels of embryonic lethality compared to the wild type (Figure 5B). Since the wild type is relatively impervious to *sacy-1(RNAi)* (Figure 5B; ~10% lethality with the full-length dsRNA trigger), an off-target RNAi effect seems an insufficient explanation for the experimental observation. Further, *sacy-1* dsRNA triggers that target different portions of the cDNA also cause high levels of embryonic lethality specifically in the *sacy-1* missense alleles (Figure 5B). BLAST searches indicate that these dsRNA triggers are highly specific to *sacy-1*. It seems unlikely that the *sacy-1* missense alleles have an enhanced sensitivity to RNAi because even *rrf-3(pk1426)* mutants, which exhibit enhanced RNAi responses (Sijen *et al.* 2001), only exhibit a moderate increase in embryonic lethality after *sacy-1 (RNAi)* (Figure 5B). While we are unable to completely exclude the possibility that off-target effects might contribute to the embryonic lethality observed following *sacy-1(RNAi)*, an analysis of the strong loss-of-function *sacy-1(tm5503)* allele (Figure 4A) shows it to be an essential gene with a zygotic sterile phenotype (see below). Thus, we conclude

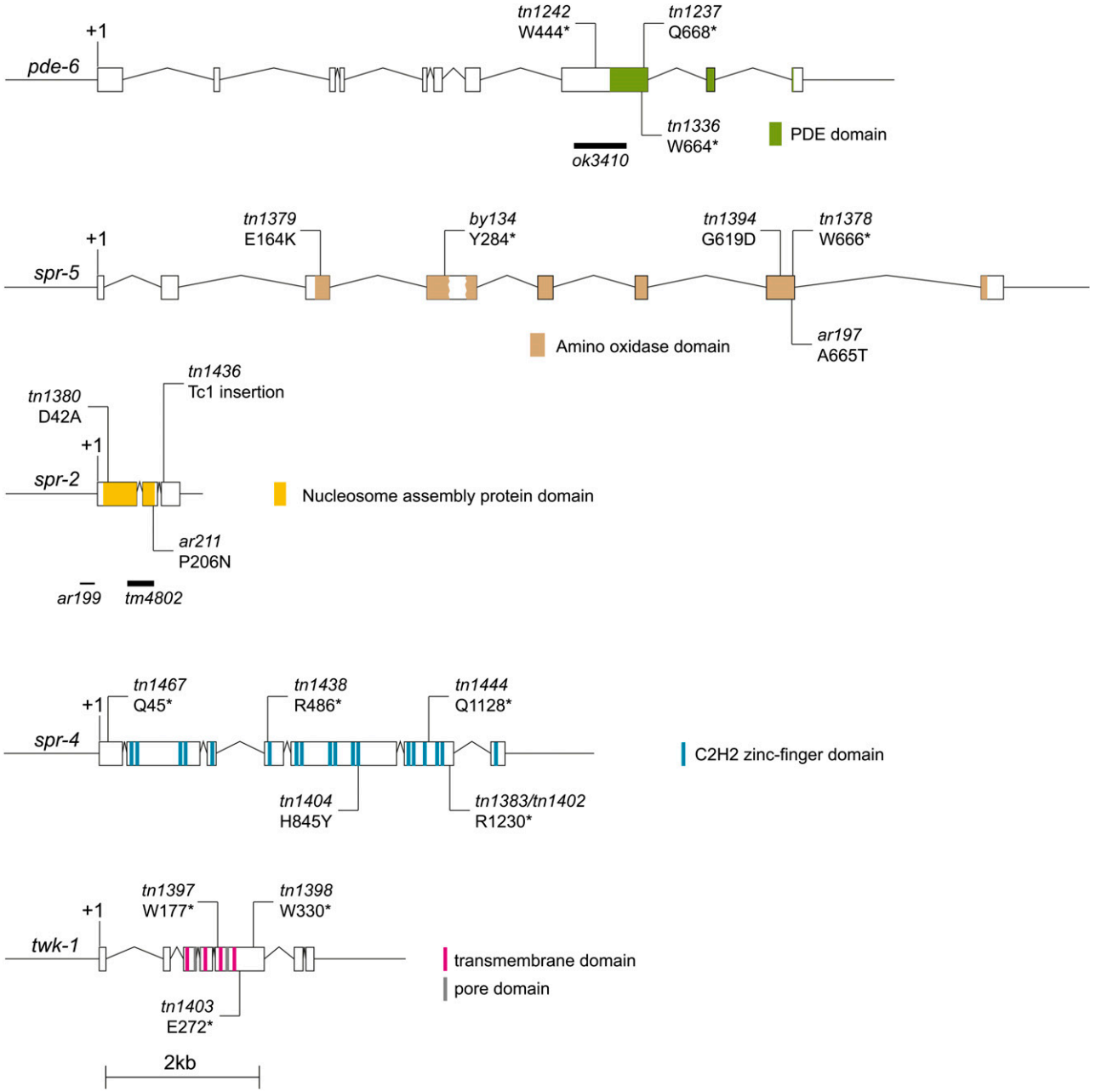

Figure 3 Molecular identification of Sacy mutations in *pde-6*, *twk-1*, and CoREST genes. Newly identified Sacy mutations (*tn* alleles) and independently isolated mutant alleles that suppress *acy-4(lf)* sterility are shown (asterisks indicate premature stop codons).

that the *sacy-1* mutant alleles isolated as *acy-4(lf)* suppressors are reduction-of-function alleles.

To determine whether *sacy-1* is a negative regulator of oocyte meiotic maturation in the absence of sperm, we feminized the strongest of the missense alleles, *tn1385*, by making double mutants with mutations affecting germline sex determination [*e.g.*, *fog-1(e2121)*, *fog-2(oz40)*, *fog-3(q470)*, and *fem-3(e1996)*]. In all cases we observed increased numbers of oocytes in the uterus (Figure S3B), indicating that *sacy-1* is a negative regulator of meiotic maturation. To test whether *sacy-1* functions downstream of $G\alpha_s$–ACY-4–PKA signaling, we removed *kin-1(+)* function from the somatic gonad in genetic mosaics generated in a *sacy-1(tn1385)* genetic background. We observed that all genetic mosaics that lost *kin-1(+)* function in somatic gonadal lineages were fertile (Table 2). Thus, *sacy-1* functions in the germ line downstream of $G\alpha_s$–ACY-4–PKA signaling. Additional *sacy-1* mutant phenotypes are now described.

sacy-1 functions in the hermaphrodite sperm-to-oocyte switch

We serendipitously found that *sacy-1(tn1385)* strongly suppresses the self-sterility caused by *fog-2(oz40)* (Table 3), a strong loss-of-function mutation (Y29stop) in *fog-2*, which

Figure 4 *sacy-1* mutations suppress *acy-4(lf)* sterility. (A) *sacy-1* alleles isolated as *acy-4(lf)* suppressor mutations are shown. The *sacy-1(tm5503)* deletion is underlined. (B) *C. elegans* SACY-1 is highly conserved. ClustalW alignment of SACY-1, *Drosophila* Abstrakt (Irion and Leptin 1999; Schmucker *et al.* 2000), and human DDX41. SACY-1 and Abstrakt share 54% (323/603) identity and 70% (424/603) similarity; SACY-1 and DDX41 share 60% (318/533) identity and 75% (401/533) similarity. *sacy-1* mutant alleles (triangles) and the DEAD box (boxed in red) are indicated. Ce_SACY-1 (NP_491962.1), Dm_Abstrakt (NP_524220.1), and Hs_DDX41 (NP_057306.2) were used for the analysis. Conserved domains [DEAD-box domain (DEADc), helicase domain (HELICc), and zinc finger domain (ZnF)] and motifs (Q, I, Ia, Ib, II, III, IV, V, and VI) are indicated (Henn *et al.* 2012). (C) Rescuing GFP::SACY-1 fusion (*tnEx159*) is broadly expressed in the nuclei and cytoplasm of most or all cells. Embryos (e), spermatheca (sp), oocytes (−1, −2, and −3). Bar, 50 μm.

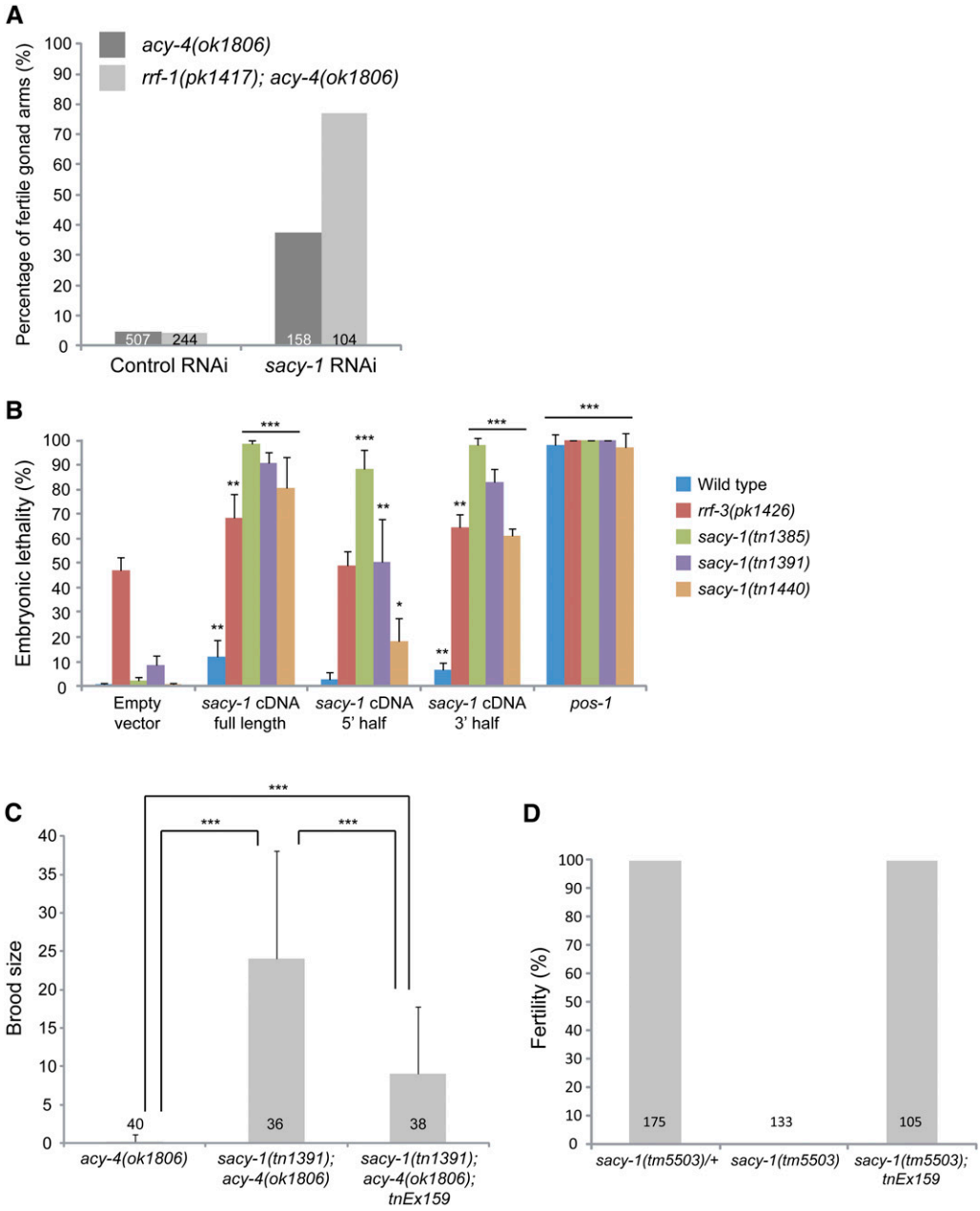

Figure 5 *acy-4(lf)* suppressor mutations in *sacy-1* reduce but do not eliminate gene function. (A) *sacy-1* RNAi suppresses *acy-4 (lf)* sterility. *sacy-1* dsRNAs were injected into the *acy-4(ok1806)* hermaphrodites bearing an *acy-4*–rescuing array and non–array-bearing F_1 progeny were scored by DIC microscopy. *sacy-1* RNAi also suppresses *acy-4(lf)* sterility in the *rrf-1(pk1417)* background, suggesting that *sacy-1* likely functions in the germ line. The numbers of gonad arms scored are indicated. (B) *sacy-1*–feeding RNAi induces embryonic lethality. L1-stage larvae were fed bacterial food expressing the indicated dsRNAs and embryonic lethality was scored in the F_1 generation. The embryonic lethality is enhanced in *sacy-1* mutants, as compared to the wild type. Three independent experiments were conducted and the error bars represent one standard deviation. At least 400 embryos were analyzed for each experimental condition. $*P < 0.05$, $**P < 0.01$, $***P < 0.001$ compared to the empty vector RNAi controls using Student's *t*-test. (C) GFP::SACY-1 (*tnEx159*) partially rescues *sacy-1 (tn1391)* for suppression of *acy-4 (lf)* sterility. *tnEx159[gfp::sacy-1 unc-119(+)]* itself does not reduce fertility because *sacy-1(tn1391); acy-4(ok1806)*; *tnEx159*; *tnEx37 [acy-4(+) sur-5::gfp]* hermaphrodites have a brood size of 105 ± 67 (n = 27). The numbers of animals scored are indicated. (D) GFP::SACY-1 rescues the sterility of the *sacy-1(tm5503)* deletion allele.

encodes an F-box protein required for spermatogenesis in *C. elegans* hermaphrodites but not males (Schedl and Kimble 1988; Clifford *et al.* 2000; Nayak *et al.* 2005). Suppression of *fog-2(oz40)* self-sterility required that the *sacy-1(tn1385)* reduction-of-function mutation be present both maternally and zygotically (Table 3; $m_{rf}z_{rf}$). *sacy-1(tn1385)* also strongly suppressed the self-sterility of *fog-2(q71)* (Table 3), another strong loss-of-function *fog-2* mutation (W148stop; Clifford *et al.* 2000). The two weaker *sacy-1* missense alleles, *tn1391* and *tn1440*, also suppressed the self-sterility of *fog-2(oz40)* and *fog-2(q71)* to varying degrees (Table 3). The suppression of *fog-2* sterility appears to involve a reinstatement of the hermaphrodite sperm-to-oocyte switch in the absence of *fog-2* function because the suppressed animals appear indistinguishable from wild-type hermaphrodites, and they exclusively produce oocytes in the adult stage. The suppression of *fog-2(lf)* self-sterility by the *sacy-1* missense alleles appears to reflect a loss of *sacy-1* function because *sacy-1(RNAi)* also suppresses *fog-2(oz40)* sterility (Table 3). *sacy-1(RNAi)* in the *rrf-1(pk1417)*; *fog-2(oz40)* background, in which the RNAi response is compromised in the somatic gonad but not the germ line, results in efficient suppression of *fog-2* self-sterility (Table 3), suggesting that *sacy-1* functions in the germ line as a component of the sperm-to-oocyte switch.

Genetic analysis has identified many of the key genes that control sex determination in *C. elegans* (Figure 6; reviewed by Ellis and Schedl 2007; Kimble and Crittenden 2007). Therefore we assessed whether *sacy-1(tn1385)* suppresses the self-sterility of strong loss-of-function mutations in *fem-3*, *fog-1*,

Table 2 *sacy-1*, *spr-5*, and *twk-1* are epistatic to *kin-1*

Genotype[a]	Fertile/total gonad arms	Number of animals screened
kin-1(ok338)	0/13	1822
sacy-1(tn1385) kin-1(ok338)	10/10	1105
spr-5(by134) kin-1(ok338)	12/12	1600
twk-1(tn1397) kin-1(ok338)	11/11	1297

[a] Epistasis tests were conducted in the respective double mutant backgrounds by analyzing genetic mosaics with losses of the *kin-1(+)*-rescuing array in the somatic gonad lineage. Genetic mosaics were sought in animals bearing the *tnEx109[kin-1 (+) sur-5::gfp]* extrachromosomal array. The genotype refers to the somatic cells of a gonad arm in the genetic mosaics.

and *fog-3*. In these experiments we ensured that the *sacy-1 (tn1385)* reduction-of-function mutation was both maternally and zygotically homozygous, but in no case did we find evidence for suppression (Table 3). Biochemical studies established that FOG-2 can form a ternary complex with the KH-domain protein GLD-1 and the 3′-UTR of *tra-2* (Clifford *et al.* 2000), consistent with the proposal that GLD-1 binds the *tra-2* 3′-UTR to mediate translational repression as a key element of the hermaphrodite sperm-to-oocyte switch (Jan *et al.* 1999). Therefore, we examined whether *sacy-1(RNAi)* could suppress germline feminization and self-sterility caused by the *tra-2 (e2020)* dominant mutation that deletes GLD-1 binding sites within the *tra-2* 3′-UTR (Jan *et al.* 1999; Clifford *et al.* 2000). We found that *sacy-1(RNAi)* was unable to suppress the self-sterility of *tra-2(e2020)* mutants (Table 3). Taken together, these results suggest that *sacy-1* functions in the hermaphrodite sperm-to-oocyte switch upstream of *tra-2*.

sacy-1 prevents necrotic cell death of gametes

The analysis thus far relied on weak reduction-of-function *sacy-1* alleles recovered as *acy-4(lf)* suppressors. To address whether *sacy-1* plays essential roles during oogenesis, we analyzed the *sacy-1(tm5503)* deletion allele generated by S. Mitani. *sacy-1(tm5503)* results from a 619-bp deletion that removes the entire second and third exons and a portion of the fourth (Figure 4A). Potential unspliced or alternatively spliced messages are either predicted to be out of frame or to lack conserved regions of the DEAD-box domain. *sacy-1(tm5503)* homozygous hermaphrodites produced from heterozygous parents develop to adulthood but are sterile. The *gfp*::*sacy-1* transgene fully rescues the sterility (Figure 5D). *sacy-1(tm5503)* adult hermaphrodites do not produce fertilized embryos (Table 4); instead they contain oocytes and sperm that become vacuolated and appear to degenerate (Figure 7). We conducted a time-course analysis to examine the onset and progression of gamete degeneration. By DIC microscopy, we observed a mixture of small and large vacuoles in sperm and oocytes on day 1 of adulthood. With time these vacuoles appeared to grow in size or fuse (Figure 8B and Figure S4). Ultimately, we observed the gonad arms to contain gamete remnants in which Brownian

Table 3 *sacy-1* functions in the hermaphrodite sperm-to-oocyte switch

	sacy-1			
Genotype	Maternal	Zygotic	Fertility[a] (%)	Number scored[b]
fog-2(oz40)	WT	WT	0	241
fog-2(q71)	WT	WT	0	175
sacy-1(tn1385); fog-2(oz40)	rf	rf	76[c]	206
sacy-1(tn1385); fog-2(oz40)	WT	rf	0	182
sacy-1(tn1385)/+; fog-2(oz40)	rf	WT	0[d]	72
sacy-1(tn1391); fog-2(oz40)	rf	rf	16	244
sacy-1(tn1440); fog-2(oz40)	rf	rf	30	236
sacy-1(tn1385); fog-2(q71)	rf	rf	49	162
sacy-1(tn1391); fog-2(q71)	rf	rf	12	192
sacy-1(tn1440); fog-2(q71)	rf	rf	10	164
fog-2(oz40); control RNAi[e]	WT	WT	0	1116
fog-2(oz40); *sacy-1* RNAi	RNAi	RNAi	49[f]	792
rrf-1(pk1417); fog-2(oz40); *sacy-1* RNAi	RNAi	RNAi	71[g]	753
tra-2(e2020gf); *sacy-1* RNAi	RNAi	RNAi	0	74
sacy-1(tn1385); fem-3(e1996)	rf	rf	0	290
fog-1(e2121) sacy-1(tn1385)	rf	rf	0	342
sacy-1(tn1385) fog-3(q470)	rf	rf	0	348

[a] Fertility was scored on a per-animal basis, except for the RNAi experiments, in which case fertility was scored on a per-gonad arm basis because *sacy-1(RNAi)* in *fog-2(oz40)* or *rrf-1(pk1417); fog-2(oz40)* backgrounds caused a gamete degeneration phenotype in 3–4% of gonad arms. This gamete degeneration phenotype was the same as that caused by *sacy-1(tm5503)*.
[b] Number scored refers to gonad arms for RNAi experiments and animals for the remainder.
[c] Brood size of fertile animals was 194 ± 88 (n = 40).
[d] *sacy-1(tn1385); fog-2(oz40)* females were crossed to *gsa-1(pk75)/hT2[qIs48]; fog-2(oz40)* males and GFP$^+$ XX progeny were analyzed. The *hT2* balancer contains an insertion of a *myo-2*::*gfp*.
[e] *Cbr-lin-12* dsRNA were used as a negative control RNAi (Felix 2007).
[f] Brood size of fertile animals was 172 ± 94 (n = 42).
[g] Brood size of fertile animals was 148 ± 71 (n = 40).

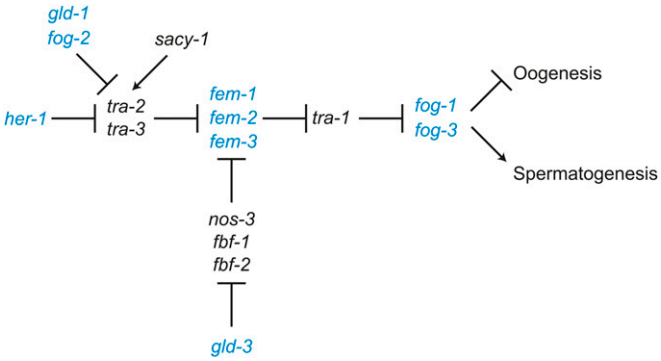

Figure 6 The *C. elegans* germline sex-determination pathway (genes promoting the male and female fate are shown in blue and black, respectively). The data in Table 3 suggest that *sacy-1* promotes the oocyte fate antagonistically to *fog-2*, which promotes spermatogenesis.

motion was observed to occur in residual cytoplasm. We also observed a similar sperm degeneration phenotype in *sacy-1(tm5503)* adult males (Figure 7A), which were never observed to sire cross-progeny. The somatic gonad appeared to develop normally in *sacy-1(tm5503)* hermaphrodites and males. We sought genetic mosaics using the *sacy-1(tm5503)*; *unc-119(ed3)*; *tnEx159[gfp::sacy-1 unc-119(+)]* strain in which the rescuing GFP::SACY-1 fusion is expressed in most or all germline and somatic cells and serves as a cell-autonomous marker for mosaic analysis. The *unc-119(ed3)* genetic background was utilized as a marker for the AB lineage so as to identify rare non-Unc mosaics showing the *sacy-1(tm5503)* gamete degeneration phenotype. We found four genetic mosaics with P1 losses, a single mosaic with a P3 loss (this animal had an independent loss within the C lineage), and two mosaics with P4 losses (Figure 7B; $n > 40{,}000$). This result indicates that *sacy-1(+)* function is required in the germ line to prevent gamete degeneration.

To address whether gamete degeneration in *sacy-1(tm5503)* is dependent on the apoptotic pathway, we examined double mutants between *sacy-1(tm5503)* and *ced-3(n717)* or *ced-4(n1162)*. Both *ced-3* and *ced-4* are required for apoptosis (Ellis and Horvitz 1986); *ced-3* encodes a caspase (Yuan *et al.* 1993) and *ced-4* encodes an Apaf-1–like protein (Yuan and Horvitz 1992). Using DIC microscopy, we observed gamete degeneration in 99% of *sacy-1(tm5503)*; *ced-3(n717)* adult hermaphrodite gonad arms ($n = 150$) and in all *sacy-1(tm5503)*; *ced-4(n1162)* gonad arms ($n = 108$). Further, we used acridine orange staining to examine early degenerating gametes. We observed that acridine orange stains early degenerating gametes in the proximal gonad of *sacy-1(tm5503)*; *ced-3(n717)* double mutants, as well as *sacy-1(tm5503)* single mutant hermaphrodites (Figure 9). Apparently, the sheath cells might engulf and acidify some of these degenerating gametes. These results indicate that gamete degeneration in *sacy-1(tm5503)* is independent of the chief apoptotic effectors.

As a test of whether gamete degeneration in *sacy-1(tm5503)* mutant hermaphrodites involves necrotic cell death, we examined a *sacy-1(tm5503)*; *unc-68(e540)* double mutant. *unc-68* encodes the ryanodine receptor (Maryon *et al.* 1996) and an *unc-68* mutation was found to reduce the penetrance of necrotic cell death (Xu *et al.* 2001). We found that the *unc-68(e540)* mutation decreased the penetrance of gamete degeneration; whereas all *sacy-1(tm5503)* gonad arms failed to produce fertilized embryos, 20% of *sacy-1(tm5503)*; *unc-68(e540)* gonad arms produced fertilized embryos (Table 4). The fertilized embryos in *sacy-1(tm5503)*; *unc-68(e540)* animals failed to hatch. As controls, we tested mutations in *unc-24*, *unc-32*, and *unc-33*, but found that none were as effective as *unc-68(e540)* in ameliorating *sacy-1(tm5503)* gamete degeneration (Table 4). We did observe that 8% of gonad arms were fertile in *sacy-1(tm5503)*; *unc-33(mn407)* animals (Table 4). *unc-33* encodes a microtubule-binding CRMP protein that is exclusively expressed in neurons and is required for normal axon guidance and elongation (Maniar *et al.* 2012). The slight reduction of gamete necrosis in *sacy-1(tm5503)*; *unc-33(mn407)* animals might be a secondary physiological consequence of their slow growth.

Table 4 *unc-68(e540)* partially suppresses the *sacy-1(tm5503)* gamete necrosis phenotype

Genotype	Fertility[a] (%)	Number of gonad arms scored
sacy-1(tm5503)	0	266
sacy-1(tm5503); unc-68(e540)	20	258
sacy-1(tm5503); unc-24(e138)	0	208
sacy-1(tm5503); unc-32(e189)	3	232
sacy-1(tm5503); unc-33(mn407)	8	136

[a] Day-1 adults were examined by DIC microscopy. Gonad arms producing fertilized embryos were scored as fertile although the embryos failed to hatch.

Germline feminization delays the onset of gamete degeneration and reveals sacy-1 as a strong negative regulator of meiotic maturation

We next investigated the genetic requirements for gamete degeneration in *sacy-1(tm5503)* hermaphrodites. Feminization with strong loss-of-function mutations in the sex determination pathway, *fog-2(oz40)*, *fem-3(e1996)*, *fog-1(e2121)*, or *fog-3(q470)*, delayed the time of onset and the severity of oocyte degeneration in *sacy-1(tm5503)* females (Figure 8 and Figure S3; S. Kim and D. Greenstein, unpublished results). By contrast, masculinization of the germ line using a gain-of-function mutation in *fem-3* (Barton *et al.* 1987) did not suppress gamete degeneration; we observed vacuolated and morphologically abnormal sperm in *sacy-1(tm5503)*; *fem-3(q20gf)* animals (Figure S5). Upon mating, *sacy-1(tm5503)* females produce embryos that arrest without properly undergoing morphogenesis and fail to hatch. We did not explore the basis for this embryonic lethality further. We did not observe mating to wild-type males to overtly increase the penetrance or severity of oocyte degeneration. Possibly, the presence of mutant sperm in the gonad arm might potentiate oocyte degeneration. While the physiological basis for the

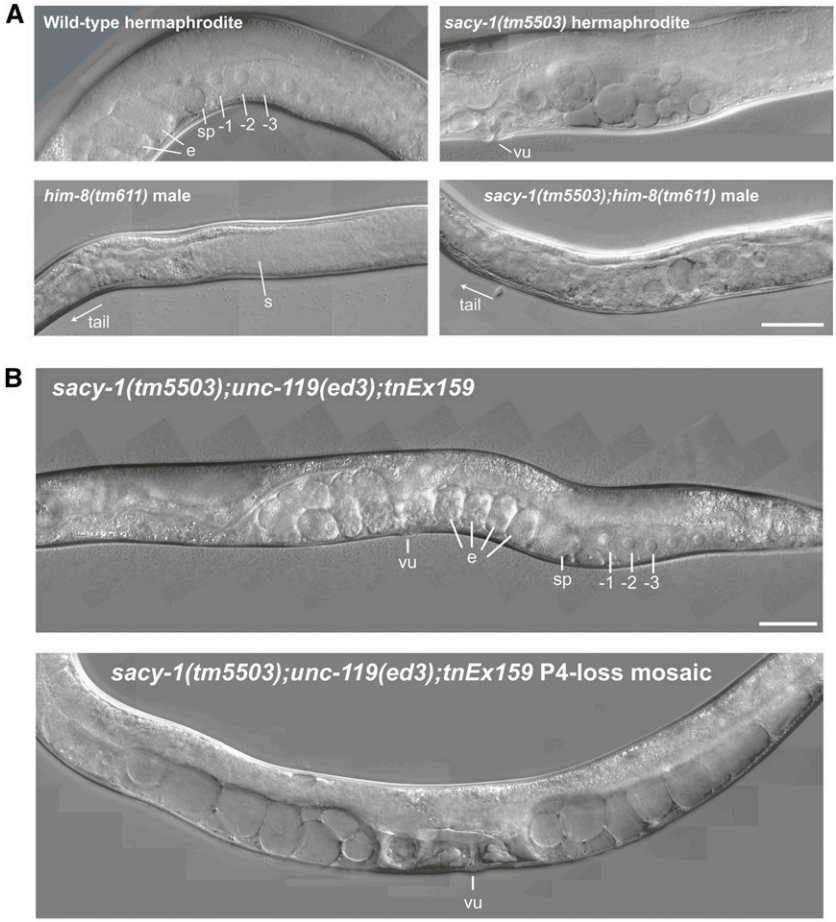

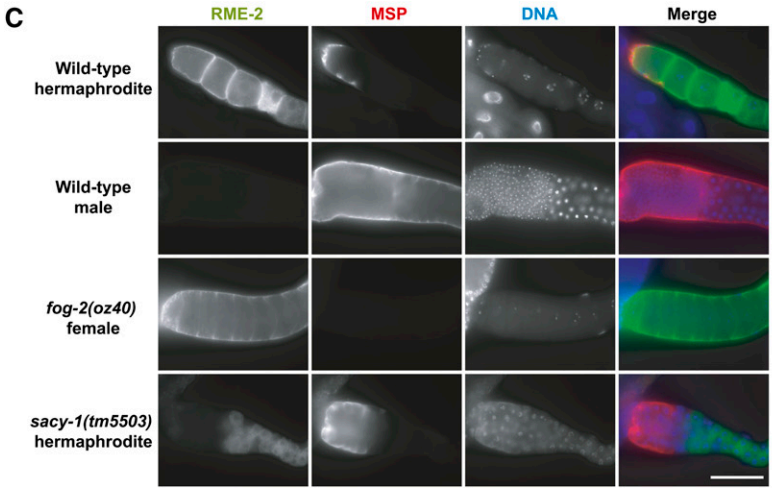

Figure 7 *sacy-1* is required for gamete maintenance. (A) *sacy-1(tm5503)* adult hermaphrodites and males produce gametes that degenerate. Embryos (e), spermatheca (sp), oocytes (−1, −2, and −3), vulva (vu), sperm (s). (B) *sacy-1* functions in the germ line to prevent gamete necrosis. GFP::SACY-1 fusion rescues *sacy-1(tm5503)* sterility (top). A genetic mosaic that lost GFP::SACY-1 in the primordial germ cell P4 exhibits gamete necrosis and is sterile (bottom). (C) *sacy-1 (tm5503)* hermaphrodites produce male and female gametes that ultimately degenerate. The yolk receptor RME-2 and MSP were used for markers of oocyte and sperm fates, respectively. Proximal is to the left. Bars, 50 μm.

delayed onset of oocyte degeneration upon germline feminization is unclear, this phenomenon proved useful in that it enabled us to examine oocytes and embryos produced by *sacy-1(tm5503)* females. In all female backgrounds tested, we observed oocytes in *sacy-1(tm5503)* females to undergo meiotic maturation and ovulation at apparently high rates; the uterus filled with unfertilized oocytes (Figure 8A and Figure S3C). We also observed apparently defective ovulation in *sacy-1(tm5503)* females such that the gonad arms often contained endomitotic oocytes. We confirmed that MSP was undetectable in *sacy-1(tm5503)* females as expected (Figure S6). Thus, *sacy-1* is a strong negative regulator of oocyte meiotic maturation in the absence of sperm.

Since only reduction-of-function *sacy-1* alleles were recovered as *acy-4(lf)* suppressors, we wished to determine the genetic behavior of a loss-of-function *sacy-1* allele. Thus, we conducted genetic epistasis analysis between *acy-4* and *sacy-1* using strong loss-of-function alleles of both genes. In a hermaphrodite background, we observed gamete degeneration in all *sacy-1(tm5503)*; *acy-4(ok1806)* animals

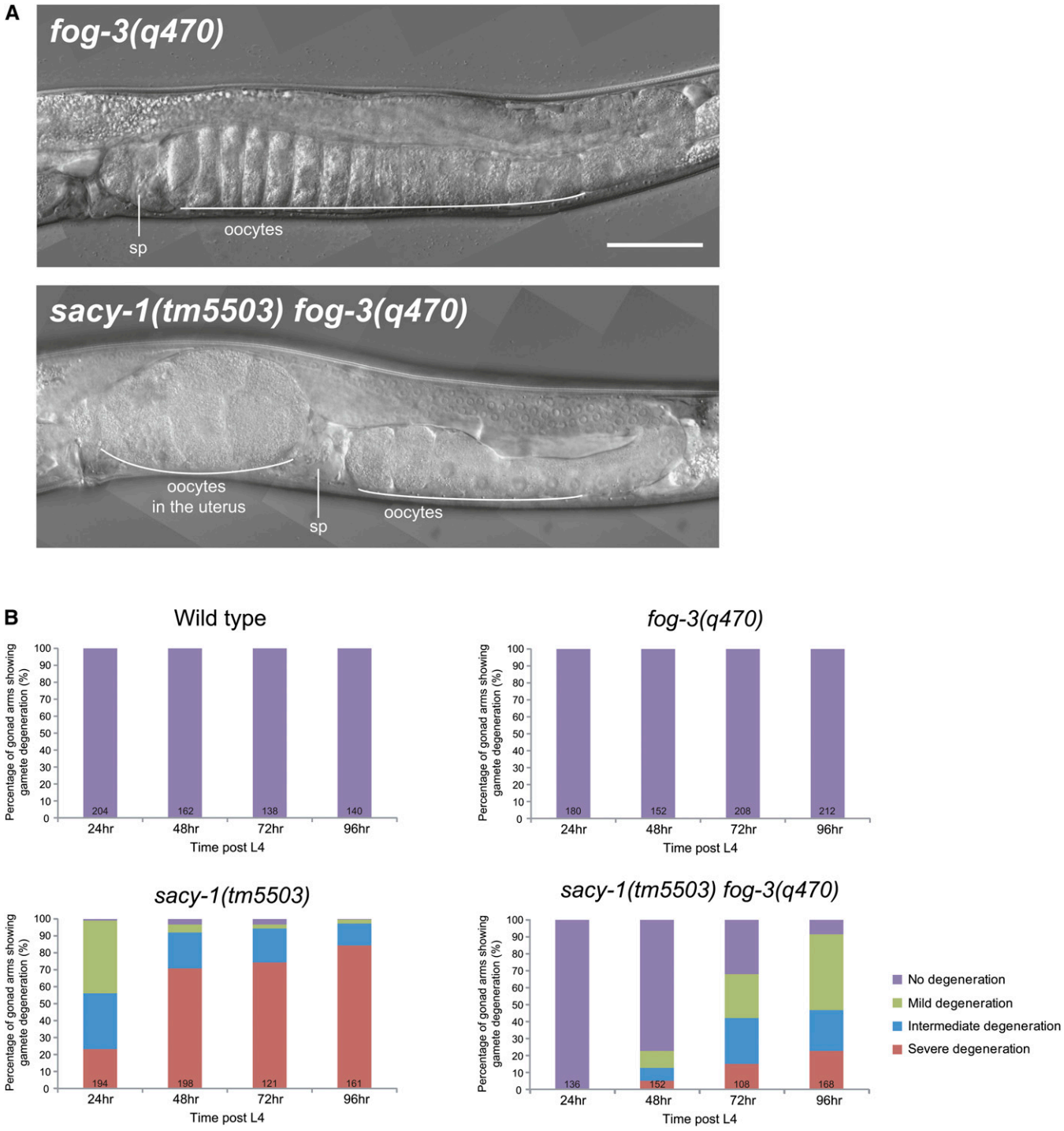

Figure 8 Germline feminization delays the onset of oocyte necrosis in *sacy-1(tm5503)* mutants. (A) Oocytes in *fog-3(q470)* females stack within the gonad arm, and the uterus and spermatheca (sp) are empty (top). In *sacy-1(tm5503) fog-3(q470)* females, oocytes undergo meiotic maturation despite the absence of sperm, and the uterus fills with unfertilized oocytes (bottom). Bar, 50 μm. (B) Feminization of the gonad delays the onset of oocyte necrosis. A time-course analysis of gamete degeneration conducted over the first 4 days of adulthood. The numbers of gonad arms scored are indicated. The severity of degeneration was scored using a qualitative scale. Representative images illustrative of the scoring criteria are shown in Figure S4.

examined (n = 94). Therefore gamete degeneration is independent of *acy-4* signaling. We therefore employed germline-feminizing mutations to overcome the gamete degeneration phenotype in conducting epistasis experiments between *sacy-1* and *acy-4*. In a *sacy-1(tm5503) fog-3(q470)*; *acy-4(ok1806)* background, we observed oocyte meiotic maturation to occur constitutively; however, ovulation typically failed and endomitotic oocytes accumulated in the gonad arm (Figure S7). All examined *sacy-1(tm5503) fog-3(q470)*; *acy-4(ok1806)* gonad arms contained endomitotic oocytes (n = 42), in contrast

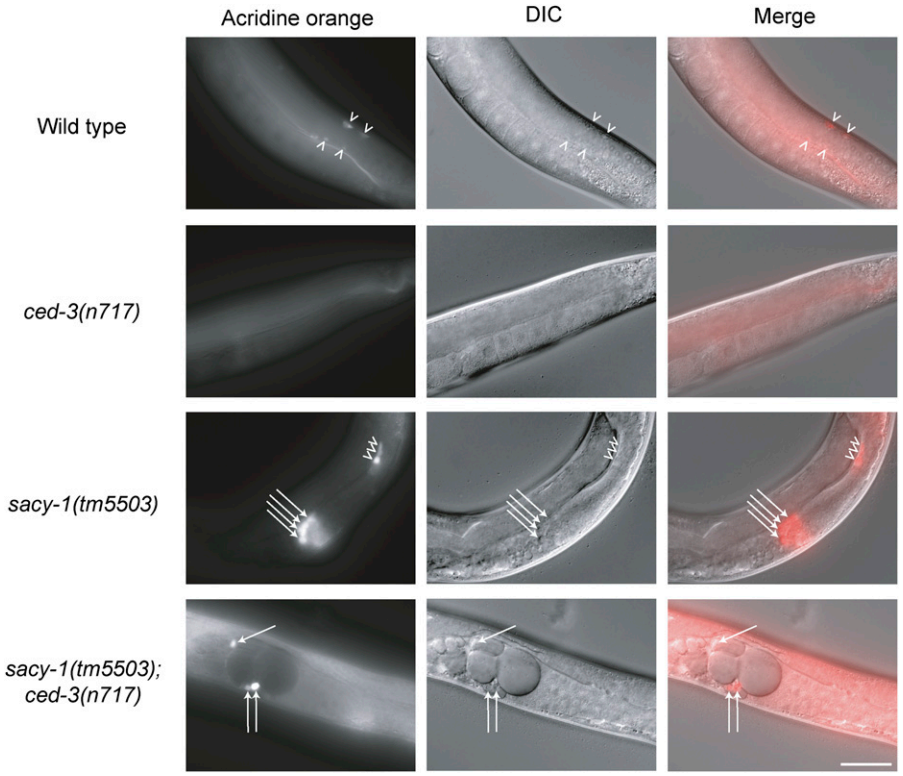

Figure 9 The gamete degeneration phenotype in *sacy-1(tm5503)* is independent of apoptosis. Acridine orange was used to identify germ cells dying by apoptosis or necrosis. Wild-type and *sacy-1(tm5503)* hermaphrodites exhibit apoptotic germ cells in the gonadal loop region (arrowheads), but *ced-3(n717)* hermaphrodites do not. *sacy-1(tm5503)* and *sacy-1(tm5503); ced-3(n717)* hermaphrodites exhibit acridine orange staining in the proximal gonad arm (arrows) that appears to coincide with degenerating gametes. This proximal acridine orange staining is not observed in wild-type hermaphrodites. Proximal is to the left. Bar, 50 μm.

to *fog-3(q470)*; *acy-4(ok1806)* gonad arms, which exclusively contained oocytes arrested in diakinesis ($n = 43$). Thus, *sacy-1(lf)* is epistatic to *acy-4(lf)* for meiotic maturation, as was also observed for the reduction-of-function alleles.

Since *sacy-1* is a strong negative regulator of oocyte meiotic maturation, we investigated epistasis with *oma-1* and *oma-2*, which encode TIS-11 zinc-finger proteins that are redundantly required for oocyte meiotic maturation (Detwiler *et al.* 2001). In a hermaphrodite background, we observed gamete degeneration in *sacy-1(tm5503)*; *oma-1(zu405te33)*; *oma-2(te51)* animals. By contrast, in a *sacy-1(tm5503) fog-3(q470)*; *oma-1(zu405te33)*; *oma-2(te51)* females, we observed that oocyte degeneration was markedly delayed. We observed that diakinesis-stage oocytes failed to undergo meiotic maturation and ovulation and accumulated in the gonad arms of all quadruple mutant female animals examined ($n = 30$). Thus, *oma-1* and *oma-2* appear to function downstream or in parallel to *sacy-1* in the regulation of meiotic maturation.

Multiple nonessential Sacy genes mediate the somatic control of oocyte meiotic maturation

In contrast to *sacy-1*, which is an essential gene, we now describe seven nonessential Sacy loci (*pde-6*, *spr-1–5*, and *twk-1*) that affect the regulation of meiotic maturation by somatic $G\alpha_s$–adenylate cyclase–PKA signaling.

PDE-6 phosphodiesterase is a negative regulator of meiotic progression: We isolated *pde-6* mutations in a related screen for mutations that suppress sterility following *gsa-1 (RNAi)* yet exhibit normal RNAi responses and are viable and fertile. From this screen, only mutations from a single complementation group, represented by *tn1237*, *tn1242*, and *tn1336*, suppress *acy-4(lf)* sterility. One of these mutations, *tn1237*, was tested and also found to suppress the sterility caused by mosaic loss of *gsa-1* activity in the somatic gonad, as expected (Table S5A). A combination of whole-genome and Sanger sequencing identified independent nonsense mutations in each *pde-6* allele (Figure 3). We also found that the *pde-6(ok3410)* deletion allele suppresses *acy-4(ok1806)* sterility and fails to complement *tn1237* for suppression of *acy-4(lf)* sterility. *pde-6* encodes a phosphodiesterase and the mutant alleles introduce stop codons prior to or within the coding sequence for the PDE domain (Figure 3), suggesting they represent strong loss-of-function alleles. The likely human ortholog of PDE-6 is PDE8 (Figure S8), the high-affinity cAMP-specific phosphodiesterase, which specifically lowers cAMP levels via phosphodiester bond hydrolysis (Fisher *et al.* 1998; Soderling *et al.* 1998). The chromatin localization of the AIR-2 Aurora B kinase in proximal oocytes is a marker for graded MSP responses (Schumacher *et al.* 1998; Govindan *et al.* 2009). In an *acy-4(+)* background, the *pde-6(tn1237)* mutation extends AIR-2::GFP chromatin localization distally (Table S5B), suggesting that an enhancement in $G\alpha_s$–ACY-4–PKA signaling in gonadal sheath cells results in a heightened MSP response in oocytes.

Mutations of multiple CoREST components suppress acy-4 (lf) sterility: Three noncomplementing alleles, *tn1378*, *tn1379*, and *tn1394*, map to the right end of LGI and define

the gene *spr-5* (Figure 3). Using *tn1394*, we genetically mapped the *acy-4(lf)* suppression to the interval between SNPs *haw14129* and *haw14136*, which contains two genes, *spr-5* and *Y48G10A.6*. Previously isolated *spr-5* mutations, the strong loss-of-function allele, *by134*(Y284stop) (Eimer *et al.* 2002; Nottke *et al.* 2011), and *ar197*(A665T) (Jarriault and Greenwald 2002), also suppress *acy-4(ok1806)* sterility and fail to complement *tn1394* for suppression. Consistent with this gene identification, injection of *spr-5* dsRNA into *acy-4(ok1806)*; *tnEx37[acy-4(+) sur-5*::*gfp]* hermaphrodites suppresses *acy-4(lf)* sterility in the F_1 generation (Figure S9). *spr-5(RNAi)* experiments conducted in the somatic gonad RNAi-deficient *rrf-1(pk1417)*; *acy-4(ok1806)* background indicate that *spr-5* depletion in the germ line results in meiotic maturation in the absence of *acy-4* (Figure S9). *spr-5* by itself does not appear to function as a negative regulator of meiotic maturation in the absence of sperm because oocytes stack in the gonad arm in *spr-5(by134)*; *fog-2(oz40)* females (Table 1).

spr-5 and other *spr* genes were originally identified as suppressors of the *sel-12* presenilin mutant egg-laying defect (Wen *et al.* 2000; Eimer *et al.* 2002; Jarriault and Greenwald 2002; Lakowski *et al.* 2003; reviewed by Lakowski *et al.* 2006). The *spr* genes encode multiple chromatin-modifying components that might constitute a *C. elegans* CoREST-like complex, similar to mammalian CoREST (**core**pressor for element-1–**s**ilencing **t**ranscription factor; reviewed by Lakowski *et al.* 2006). *spr-5* encodes an H3K4me2 demethylase that is thought to contribute to transcriptional repression by remodeling chromatin structure (Eimer *et al.* 2002; Jarriault and Greenwald 2002; Katz *et al.* 2009). *spr-5* mutations have been shown to confer a mortal germline phenotype after more than ~20 generations (Katz *et al.* 2009) and to exhibit modest defects in meiotic DNA double-strand break repair (Nottke *et al.* 2011). Suppression of *acy-4(lf)* sterility is observed in the first generation in which *spr-5* mutations become homozygous and is efficient in subsequent generations. We have not examined germline mortality in these strains in detail, but did observe declines in fecundity after many generations, consistent with prior findings. *spr-5* mutations bypass the *sel-12* presenilin requirement for egg laying by derepressing *hop-1* presenilin expression (Eimer *et al.* 2002). Therefore, we considered the possibility that *spr-5* mutations might bypass the requirement of *acy-4* for meiotic maturation via derepression of other adenylate cyclase(s) in the gonadal sheath cells. We generated C-terminal GFP fusions for ACY-1, ACY-2, and ACY-3 using fosmid recombineering and compared their expression in the wild type and *spr-5* mutants. We observed apparently identical expression patterns in the wild type and *spr-5* mutants and in no case did we observe expression of an adenylate cyclase other than *acy-4* in the gonadal sheath cells (S. Kim and D. Greenstein, unpublished results). As a more direct test, we conducted genetic mosaic analysis of *kin-1* in an *spr-5* mutant background. We observed that loss of *kin-1(+)* activity in the somatic gonad in the *spr-5(by134)* genetic background resulted in fertility, in contrast to the wild-type background (Table 2). Thus, *spr-5* functions downstream or in parallel to *kin-1*, consistent with a function in the germ line. Prior work identified >100 genes upregulated in *spr-5* mutant gonads (Nottke *et al.* 2011). We tested whether RNAi of any of these candidate genes might restore *acy-4(lf)* sterility to *spr-5(by134)*; *acy-4(ok1806)* mutants, but in no case was such a result obtained. Possibly *spr-5* might regulate genes not identified by the microarray analysis or multiple pathways might contribute to the suppression of *acy-4(lf)* sterility.

During this analysis, we observed that unlike the wild type, *acy-4(ok1806)* worms exhibit a growth defect on standard nematode growth medium with the bacterial strain HT115(DE3) as a food source, as opposed to OP50-1. Under these conditions, *acy-4(ok1806)* animals exhibit larval lethality or arrest, or they grow slowly and appear grossly unhealthy (Figure S10). This phenotype is rescued by an *acy-4(+)* extrachromosomal array (*tnEx37*), indicating that an absence of *acy-4* activity prevents normal growth on the HT115 (DE3) food source. This is an unexpected result because HT115(DE3) is a high-quality food source for *C. elegans* (Brooks *et al.* 2009; Y. You, personal communication). We found that *spr-5(by134)* also suppresses the *acy-4(ok1806)* HT115 growth defect: double mutant animals are viable and fertile with HT115 as a food source, as they are on standard OP50 bacterial strains. While the basis for this unusual phenotype remains to be determined, we nonetheless screened all Sacy mutants and found two additional loci that suppress the HT115 growth defect. Genetic mapping and DNA sequencing established that these two Sacy genes are *spr-2* and *spr-4* (Figure 3; Table 1). We therefore tested independently isolated alleles of *spr* loci and found that *spr-2(ar211)* and *spr-2(tm4802)* suppress *acy-4(ok1806)* sterility and the HT115 growth defect. We did, however, observe that *spr-2(ar199)* failed to suppress *acy-4(lf)* sterility. Interestingly, *spr-2(ar199)* specifically eliminates the expression of SPR-2 in somatic cells after the 50-cell stage (A. Gontijo and B. Lakowski, personal communication), consistent with a role for CoREST function in the germ line downstream of *kin-1*. Similarly, we observed that *spr-4(by105)* suppresses *acy-4(ok1806)* sterility and the HT115 growth defect. We did not isolate *spr-3* mutant alleles in our screen, yet both *spr-3(ok2525)* and *spr-3(by108)* suppress *acy-4(ok1806)* sterility. Neither of these *spr-3* alleles suppresses the HT115 growth defect. We constructed *acy-4(ok1806) spr-1(gk734)* double mutants and observed that they were fertile and suppressed for the HT115 growth defect (Figure S10). These results suggest that a CoREST-like complex has a function in the germ line that participates in the regulation of oocyte meiotic maturation by the somatic gonad and sperm signaling. Further, the observation that mutations in *spr-1*, *spr-2*, *spr-4*, and *spr-5* suppress the *acy-4(lf)* HT115 growth defect suggests that CoREST-like complex genes and *acy-4* might coordinately function in additional processes besides oocyte meiotic maturation.

A two-pore domain potassium (TWIK) channel functions in sheath cells downstream of KIN-1 to regulate meiotic maturation: Whole-genome sequencing identified three noncomplementing alleles (*tn1397*, *tn1398*, and *tn1403*) mapping to the center of LGI as nonsense mutations in *twk-1*, which encodes a TWIK channel (Figure 3). *tn1398* and *tn1403* introduce stop codons after the fourth transmembrane domain (W330stop and E272stop, respectively) and *tn1397* introduces a stop codon after the second transmembrane domain (Figure 3; W177stop). The crystal structures of TWIK channels suggest that all four transmembrane helices likely participate in the formation of a functional channel complex (Brohawn *et al.* 2012; Miller and Long 2012). *tn1397* is therefore a strong loss-of-function allele. *tn1397*, but not *tn1398* or *tn1403*, exhibits an adult-onset paralyzed uncoordinated (Unc) phenotype in a wild-type genetic background. Thus, *tn1398* and *tn1403* must reduce but not eliminate *twk-1* function. Interestingly, *twk-1(tn1397)*; *acy-4(ok1806)* animals do not exhibit an adult-onset Unc phenotype. Thus, *twk-1* mutant alleles are recessive suppressors of *acy-4(lf)* sterility, and *acy-4(ok1806)* is a recessive suppressor of the *twk-1(tn1397)* movement defect. To test whether *twk-1* mutations are causal for the suppression of *acy-4(lf)* sterility and the adult-onset Unc phenotype, we conducted rescue tests by introducing a *twk-1* fosmid clone, WRM0616aE06, into *twk-1(tn1397)*; *acy-4(ok1806)*/+ and *twk-1(tn1397)* genetic backgrounds, respectively. *twk-1(tn1397)*; *acy-4(ok1806)* animals bearing the *twk-1(+)* extrachromosomal array were sterile and exhibited the *acy-4(lf)* defect in meiotic maturation (Table S6A). Further, we also observed rescue of the *twk-1(tn1397)* Unc phenotype (Table S6B). The suppression of the *twk-1(tn1397)* Unc phenotype by *acy-4(lf)* is partially affected by *spr-5(+)* function because 23% (n = 95) of *twk-1(tn1397) spr-5(by134)*; *acy-4(ok1806)* animals exhibit the adult-onset Unc phenotype as compared to 0% of *twk-1(tn1397)*; *acy-4(ok1806)* adults (n = 93). Thus, *acy-4*, *spr-5*, and *twk-1* genetically interact in a separate biological context.

In *C. elegans*, high-copy extrachromosomal arrays generated by microinjection, as done for *twk-1*, are typically silenced in the germ line (Kelly *et al.* 1997). To test more definitively whether *acy-4(ok1806)* sterility requires *twk-1(+)* function in the somatic gonad, we conducted genetic mosaic analysis of *acy-4(lf)* suppression. We sought fertile genetic mosaics among *twk-1(tn1397)*; *acy-4(ok1806)*; *tnEx180[twk-1(+) sur-5*::*gfp]* animals, produced by *acy-4(ok1806)*/+ heterozygous parents using *nT1[qIs51]* as a dominantly marked balancer chromosome for *acy-4(ok1806)*. Two genetic mosaics with losses in the EMS founder cell, which is a precursor to the somatic gonad (Figure 1C), were fertile in both gonad arms. These genetic mosaics produced GFP-containing progeny, indicating that their germ lines were *twk-1(+)*. A third genetic mosaic animal resulted from complex losses within the Z1 lineage (Figure S11). This animal was fertile in the anterior gonad arm, but was sterile in the posterior gonad arm. All gonadal sheath cells in the anterior gonad arm of this mosaic were *twk-1(tn1397)* mutant, but the germline and several anterior spermathecal cells were *twk-1(+)*. A fourth genetic mosaic, resulting from a loss in the Z4 somatic gonadal precursor cell (and some cells within the C lineage; see Figure 1C), was fertile in the posterior gonad arm, but not the anterior gonad arm. The germ line of this animal was also *twk-1(+)*. We conclude that *twk-1* functions downstream of *acy-4* in the somatic gonad to regulate meiotic maturation.

To examine TWK-1 expression, we used recombineering to fuse GFP to the C terminus of TWK-1 within the fosmid context and generated transgenic lines in wild-type and *twk-1* mutant backgrounds. The *twk-1*::*gfp* extrachromosomal arrays rescued both *acy-4(lf)* suppression and *twk-1* Unc phenotypes (Table S6A), indicating that the TWK-1::GFP fusion protein is functional *in vivo* and might represent the endogenous expression pattern. TWK-1::GFP is expressed in the gonadal sheath cells, the distal tip cell, and a few unidentified neurons, but is not expressed in spermathecal cells (Figure 10). TWK-1 is not itself a strong negative regulator of meiotic maturation as oocytes in unmated *twk-1(tn1397)*; *fog-2(oz40)* females stack in the gonad arm and do not exhibit elevated rates of meiotic maturation (Table 1). To test whether *twk-1* functions downstream or in parallel to somatic PKA signaling needed for oocyte meiotic maturation, we conducted genetic mosaic analysis in *twk-1(tn1397) kin-1(ok338)*; *tnEx109[kin-1(+) sur-5*::*gfp]* animals, similar to what was done for *sacy-1* and *spr-5*. All genetic mosaics that lost *kin-1(+)* function in somatic gonadal lineages were fertile (Table 2). Thus, *twk-1* is epistatic to *kin-1* for oocyte meiotic maturation. Taken together, these data suggest that TWK-1 has a function in gonadal sheath cells that contributes to the regulation of meiotic maturation by $G\alpha_s$–ACY-4–PKA signaling.

TWIK channels conduct potassium ions across the plasma membrane to control the negative resting potential of excitable cells. The finding that TWK-1 functions downstream or in parallel to PKA signaling provides additional evidence that the sheath cells play a critical role in regulating *C. elegans* oocyte meiotic maturation. TWK-1 has several human homologs, including TREK-1 and TREK-2 (Figure S12A). Application of intracellular cAMP or stimulation of a $G\alpha_s$-coupled receptor block TREK-1 and TREK-2 channel activity (Patel *et al.* 1998; Lesage *et al.* 2000). Interestingly, electrophysiological studies found that C-terminal truncation of TREK-1 shortly after the fourth transmembrane domain renders the channel insensitive to cAMP inhibition and thus constitutively open (Patel *et al.* 1998). Multiple PKA phosphorylation sites in the C terminus were shown to mediate cAMP regulation of the channel (Patel *et al.* 1998; Murbartian *et al.* 2005; Kang *et al.* 2007). We therefore considered the possibility that TWK-1 C terminus might play an essential regulatory function. However, *twk-1(tn1403)* and *twk-1(tn1398)* reduce but do not eliminate *twk-1* activity and are predicted to truncate the protein at positions 272

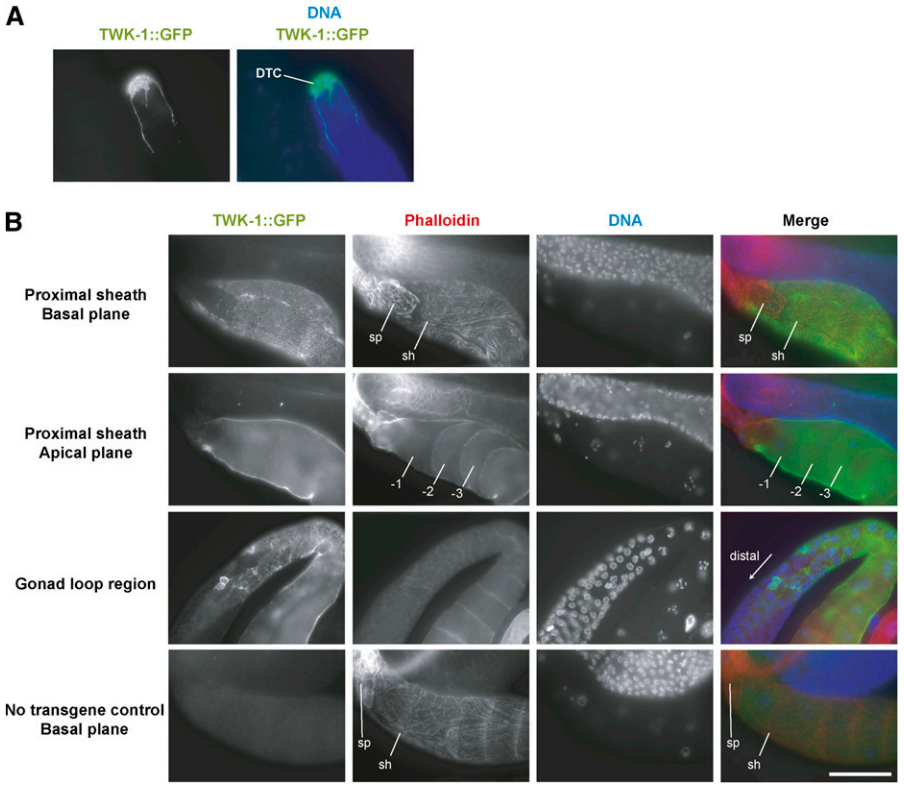

Figure 10 Expression of TWK-1::GFP in the somatic gonad. Immunostaining of TWK-1::GFP in dissected and fixed gonads using anti-GFP antibodies. TWK-1::GFP is expressed in the distal tip cell (DTC) (A) and the gonadal sheath cells (sh), but not spermathecal cells (sp) (B). Phalloidin was used to detect actin in the proximal gonadal sheath cells and the spermatheca. Identical exposure times were used to acquire GFP images. Proximal oocytes (−1, −2, and −3). Bar, 50 μm.

and 330, respectively (Figure S12). Thus, the TWK-1 channel must retain some function in the absence of the C terminus. As a further test of whether the C terminus of TWK-1 is essential for function, we asked whether a TWK-1 C-terminal truncation (ΔC284) could rescue the strongest loss-of-function allele, *twk-1(tn1397)*. We chose the position of the C-terminal TWK-1 deletion to correspond to the TREK-1 deletion that renders the channel constitutively open. We observed that TWK-1ΔC284::GFP could mediate function for both oocyte maturation and motility (Figure S12B). Another possibility is that the regulation of the channel via the C terminus might be important for closing the channel to facilitate meiotic maturation. If so, then a constitutively open channel, resulting from a C-terminal truncation, might confer a dominant disruptive effect on the meiotic maturation and ovulation process. Such an effect is predicted to be most evident with increased dosage achieved through expression from high-copy arrays. Since TWK-1ΔC284::GFP is functional in rescue assays, it seems unlikely that regulation of TWK-1 by PKA, if it exists in this system, plays an essential role. Alternatively, the C-terminal deletion might produce offsetting effects by concomitantly reducing function and removing inhibitory regulation. Further studies will be needed to assess whether PKA plays a direct role in regulating TWK-1 in the meiotic maturation process.

Sacy genes might act cumulatively downstream of somatic cAMP signaling

Sacy mutations enable partial fertility in the absence of somatic adenylate cyclase signaling, but in no case is fertility restored to wild-type levels. Possibly, Sacy genes might define cumulatively acting pathways that enable somatic control of meiotic maturation to ensure optimal rates of progeny production and sperm utilization. To begin to address this issue, we asked whether mutations in *twk-1* or *sacy-1* might increase *acy-4(lf)* brood sizes in combination with a strong-loss-of-function mutation in *spr-5*. This analysis is complicated by the fact that the strongest loss-of-function mutations in both *twk-1* and *sacy-1* confer pleiotropic phenotypes that can negatively impact fertility. Nonetheless, we observed that the weak mutations, *sacy-1(tn1440)* and *twk-1(tn1403)*, further increased brood sizes in the *spr-5 (by134)*; *acy-4(ok1806)* genetic background (Table 5). While not definitive, these results are consistent with the idea that brood size is a complex function of multiple pathways downstream of *acy-4*. In the case of *spr-5* and *twk-1*, genetic and molecular analyses are consistent with the idea the two pathways might act in combination, but that neither is essential for reproduction. By contrast, genetic analysis of *sacy-1* suggests that it functions as a major regulator of oogenesis and a strong negative regulator of meiotic maturation, possibly representing a downstream integrator of the upstream signaling pathways.

Discussion

Suppressor genetics and the somatic control of oocyte meiotic maturation

Oocyte meiotic maturation is a conserved biological process required for sexual reproduction of animals. For the most

Table 5 Evidence for cumulative action of Sacy mutations in the suppression of *acy-4(lf)* sterility

Genotype	Brood size (± SD)	Number of animals scored
acy-4(ok1806)	1 (± 2)	30
spr-5(by134); acy-4(ok1806)	81 (± 35)	40
twk-1(tn1403); acy-4(ok1806)	32 (± 25)	36
sacy-1(tn1440); acy-4(ok1806)	20 (± 19)	39
twk-1(tn1403) spr-5(by134); acy-4(ok1806)	128* (± 46)	40
sacy-1(tn1440) spr-5(by134); acy-4(ok1806)	108* (± 52)	40

* $P < 0.01$ compared to *spr-5(by134); acy-4(ok1806)* using Student's *t*-test.

part, our understanding in this area largely derives from biochemical and cell biological studies. For example, classical biochemical studies in amphibian oocytes led to the discovery of maturation promoting factor (Masui and Markert 1971). By contrast, comparably fewer forward genetic approaches have been undertaken. Historically, research studies on animal oocytes have benefited greatly from a diversity of experimental systems, including organisms less amenable to forward genetic analyses. Here we have taken the approach of screening for mutations that impact the regulation of the meiotic maturation process in *C. elegans*.

A tried-and-true approach in developmental genetics is to screen for mutations in which the developmental process of interest is disrupted—here oocyte meiotic maturation. Thus far, comparably few single gene mutations have been described that result in a block in oocyte meiotic maturation. Any mutation that completely feminizes the adult hermaphrodite gonad significantly blocks the process because of the absence of the MSP signal for meiotic maturation (McCarter *et al.* 1999; Miller *et al.* 2001). By contrast, strong loss-of-function mutations in *acy-4* block meiotic maturation despite the presence of sperm (Govindan *et al.* 2009). The relatively few single gene mutations found to date that completely block meiotic maturation likely stems from a combination of factors. Meiotic maturation occurs in the adult stage and depends on signaling and cell cycle factors, such as *cdk-1*, *gsa-1*, or *kin-1*, which play earlier developmental roles (Boxem *et al.* 1999; Govindan *et al.* 2006, 2009). Further, genetic redundancy, as observed for *oma-1* and *oma-2* (Detwiler *et al.* 2001), might contribute to the robustness of the genetic network. Here we have taken advantage of epistasis in genetic pathways to isolate *acy-4(lf)* sterility suppressor mutations. Two technological advances enabled this approach. The first is the wide availability of deletion alleles isolated by the *C. elegans* Knockout Consortia (Moerman and Barstead 2008; S. Mitani, unpublished results). Many deletion alleles remove functional or catalytic domains in proteins, as does the *acy-4(ok1806)* deletion we used for screening. This consideration makes it less likely that intragenic or informational suppressors might be isolated. Further, the availability of deletion alleles of many genes facilitates gene identification and the analysis of strong loss-of-function alleles. A second enabling technology is whole-genome sequencing for mutant identification (Hillier *et al.* 2008; Sarin *et al.* 2008). In the current instance, this technology made it possible to determine the molecular identities of Sacy genes defined by multiple alleles, in the face of an inability to fine map many of the mutations by conventional means.

A salient feature of oocyte meiotic maturation signaling pathways in many organisms is that the somatic gonad exerts a controlling influence on the germ line. For example, it has long been known that removal of fully grown mammalian oocytes from antral follicles triggers meiotic resumption (Pincus and Enzmann 1935; Edwards 1965). Further, luteinizing hormone promotes meiotic resumption through activation of $G\alpha_s$–adenylate cyclase–PKA signaling in mural granulosa cells, thereby regulating a cascade of paracrine and gap-junctional signaling pathways, which ultimately results in lowering intra-oocyte cAMP levels to trigger MPF activation (reviewed by Sun *et al.* 2009; Downs 2010). In mammals, somatic gonadal control of meiotic maturation, in part, provides a means to link reproduction to pituitary hormone control. By contrast, in *C. elegans*, control by the somatic gonad provides a means to link oocyte meiotic maturation to sperm availability. In *C. elegans*, somatic $G\alpha_s$–adenylate cyclase–PKA signaling is required for all described germline responses to the MSP hormone (Govindan *et al.* 2009; this work; Figure 11). Further, $G\alpha_s$–adenylate cyclase–PKA pathway activation can drive meiotic maturation at high rates in the absence of sperm (Govindan *et al.* 2006, 2009), approaching ~50% of the maximal hermaphrodite rate, depending on the specific method of pathway activation.

In this work, we used suppressor genetics to ask two questions: (1) What are the molecular pathways that impose and mediate somatic control of meiotic maturation? (2) What happens to reproduction when signaling is perturbed? We identified mutations in at least 17 Sacy genes that enable partial fertility in the absence of somatic adenylate cyclase signaling. Cumulatively, we molecularly characterized mutations in 10 Sacy genes (*sacy-1*, *pde-6*, *spr-1*–*5*, *twk-1*, *tom-1*, and *uev-1*). In no case was fertility restored to wild-type levels, however. Given the scale of the suppressor screen, it seems doubtful that any viable single gene mutation can fully restore the fertility of *acy-4(lf)* hermaphrodites to wild-type levels. We identified two classes of mutations. The first class of suppressor is exemplified by *sacy-1*, which encodes a highly conserved DEAD-box helicase. While we recovered reduction-of-function *sacy-1* alleles as *acy-4(lf)* suppressor mutations, our screens could not recover strong loss-of-function *sacy-1* alleles because of its essential functions

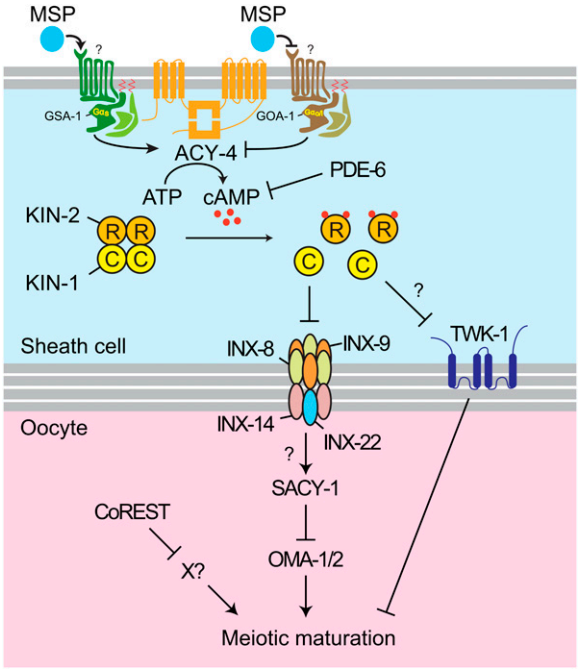

Figure 11 Model for the control of oocyte meiotic maturation in *C. elegans*. MSP signaling for oocyte meiotic maturation requires $G\alpha_s$–ACY-4–PKA activity in the gonadal sheath cells. PDE-6 and TWK-1 may function in the gonadal sheath cells as negative regulators of meiotic maturation. The gonadal sheath cells inhibit meiotic maturation in part via gap-junctional communication involving the innexins INX-8 and INX-9 in the gonadal sheath cells (T. Starich and D. Greenstein, unpublished data) and INX-14 and INX-22 in oocytes (Govindan *et al.* 2009). SACY-1 is a strong negative regulator of meiotic maturation that functions in the germ line upstream of, or in parallel to, the positive regulators OMA-1 and OMA-2. CoREST-like complex has a function in the germ line that is needed for the dependence of meiotic maturation on the $G\alpha_s$–ACY-4–PKA sheath cell pathway. For illustrative purposes, TWK-1 and sheath cell MSP binding activity are displayed in a localized fashion, though this is unlikely to be the case (Govidan *et al.* 2009; this work).

needed for gamete maintenance and embryogenesis. SACY-1 is a strong negative regulator of oocyte meiotic maturation in the absence of sperm, and it likely functions upstream of OMA-1 and OMA-2 (Figure 11), which are redundantly required for meiotic maturation (Detwiler *et al.* 2001). In contrast to SACY-1, the second suppressor class, exemplified by mutations affecting a CoREST-like complex and the TWK-1 two-pore potassium channel, is not absolutely required for meiotic maturation or its negative regulation in the absence of sperm (Figure 11). These genes and perhaps other Sacy loci appear to function cumulatively to enable somatic control of meiotic maturation.

Control of transcription and translation in the germ line and the regulation of meiotic maturation

Our findings suggest that CoREST-like chromatin regulators function in the germ line to ensure the somatic control of oocyte meiotic maturation. One potential model is that a CoREST-like complex prevents the germline expression of proteins that might interfere with the circuitry that establishes or maintains the dependence of meiotic maturation on somatic $G\alpha_s$–adenylate cyclase–PKA and MSP signaling. In this model, the role of CoREST in oocyte meiotic maturation would be reminiscent of the synthetic multivulval (SynMuv) genes in vulval development (Fay and Yochem 2007). The SynMuv genes establish a necessary precondition for vulval induction by repressing ectopic transcription of *lin-3*, which encodes the anchor cell signal (Cui *et al.* 2006; Saffer *et al.* 2011). SynMuv*B* genes define a chromatin regulatory pathway involving the Rb retinoblastoma ortholog LIN-35 (Lu and Horvitz 1998). Interestingly, *lin-35* and *spr-1* display a synthetic genetic interaction affecting gonadogenesis (Bender *et al.* 2007), suggesting that CoREST may mediate multiple functions needed for optimal germline development and reproduction. These functions might involve the regulation of transcription in the germ line.

By contrast, SACY-1 might function in post-transcriptional gene regulation important for the control of oocyte meiotic maturation, the hermaphrodite sperm-to-oocyte switch, and gamete maintenance. Genetic epistasis analysis suggests that *sacy-1* functions upstream of *oma-1* and *oma-2*. Since oocytes are transcriptionally quiescent (Starck 1977; Gibert *et al.* 1984; Schisa *et al.* 2001; Walker *et al.* 2007), and OMA-1 and OMA-2 are cytoplasmically localized (Detwiler *et al.* 2001), an attractive hypothesis is that these two TIS11 zinc-finger proteins regulate meiotic maturation at a post-transcriptional level. Indeed, OMA-1 and OMA-2 have been shown to repress the translation of several mRNAs in oocytes and embryos (Jadhav *et al.* 2008; Li *et al.* 2009; Guven-Ozkan *et al.* 2010). Our finding that SACY-1 functions as a component of the hermaphrodite sperm-to-oocyte switch likely upstream of *tra-2* is consistent with its potential involvement in post-transcriptional gene regulation (reviewed by Thomas *et al.* 2012). Both SACY-1 and its *Drosophila* ortholog Abstrakt are found in the nucleus and cytoplasm (Irion and Leptin 1999), and thus these factors might function at a variety of levels to impact gene expression. We suggest that SACY-1 is a positive factor for TRA-2 expression, perhaps playing a similar role as Abstrakt, which promotes expression of the Inscutable protein (Irion *et al.* 2004). If SACY-1 functions in a similar manner to regulate meiotic maturation, then it might function in part by promoting the translation of an inhibitory factor that restrains cell cycle progression. Interestingly, DDX41, the human ortholog of SACY-1, was recently found to be one of five genes recurrently mutated in patients with relapsing acute myeloid leukemia (Ding *et al.* 2012). DDX41 also functions in a signaling pathway that detects invading viral double-stranded DNA in the cytoplasm and initiates an antiviral response (Zhang *et al.* 2011), but other components of this innate immunity pathway appear not to be conserved in nematodes. Intriguingly, *sacy-1* is required to prevent the necrotic cell death of gametes. Therefore, *sacy-1* establishes a mechanistic link among three developmental processes critical for sexual reproduction: germline sex determination, somatic control of meiotic maturation, and preservation of gamete quality. The molecular genetic tools described in this

work will facilitate the dissection of these key reproductive processes.

Acknowledgments

We are grateful to Shohei Mitani and the *Caenorhabditis* Genetics Center for providing strains. We thank Monica Colaiácovo, Yang Shi, Alisson Gontijo, and Bernard Lakowski for sharing results prior to publication. We thank Bob Herman, Bernard Lakowski, Todd Starich, Caroline Spike, and Tatsuya Tsukamoto for many helpful suggestions, experimental advice, and comments on the manuscript. We thank Alexander Boyanov, Maria Doitsidou, Henry Bigelow, and Oliver Hobert for whole-genome sequencing using the GAIIX instrument and advice on installation of MAQGene. Whole-genome sequencing was also performed at the Biomedical Genomics Center of the University of Minnesota, with instrumentation supported by grant 1S10RR026342-01 from the National Center for Research Resources/National Institutes of Health (NIH). Analysis of whole-genome sequencing data was carried out using computing resources at the University of Minnesota Supercomputing Institute. This work was supported by NIH grants GM57173 and GM65115 to D.G.

Literature Cited

Anderson, E., and D. F. Albertini, 1976 Gap junctions between the oocyte and companion follicle cells in the mammalian ovary. J. Cell Biol. 71(2): 680–686.

Barton, M. K., T. B. Schedl, and J. Kimble, 1987 Gain-of-function mutations of *fem-3*, a sex-determination gene in *Caenorhabditis elegans*. Genetics 115(1): 107–119.

Bender, A. M., N. V. Kirienko, S. K. Olson, J. D. Esko, and D. S. Fay, 2007 *lin-35*/Rb and the CoREST ortholog *spr-1* coordinately regulate vulval morphogenesis and gonad development in *C. elegans*. Dev. Biol. 302(2): 448–462.

Bigelow, H., M. Doitsidou, S. Sarin, and O. Hobert, 2009 MAQGene: software to facilitate *C. elegans* mutant genome sequence analysis. Nat. Methods 6(8): 549.

Boxem, M., D. G. Srinivasan, and S. van den Heuvel, 1999 The *Caenorhabditis elegans* gene *ncc-1* encodes a *cdc2*-related kinase required for M phase in meiotic and mitotic cell divisions, but not for S phase. Development 126(10): 2227–2239.

Brenner, S., 1974 The genetics of *Caenorhabditis elegans*. Genetics 77(1): 71–94.

Brohawn, S. G., J. del Marmol, and R. MacKinnon, 2012 Crystal structure of the human K2P TRAAK, a lipid- and mechano-sensitive K+ ion channel. Science 335(6067): 436–441.

Brooks, K. K., B. Liang, and J. L. Watts, 2009 The influence of bacterial diet on fat storage in *C. elegans*. PLoS ONE 4(10): e7545.

Clifford, R., M. H. Lee, S. Nayak, M. Ohmachi, F. Giorgini *et al.*, 2000 FOG-2, a novel F-box containing protein, associates with the GLD-1 RNA binding protein and directs male sex determination in the *C. elegans* hermaphrodite germ line. Development 127(24): 5265–5276.

Cui, M., J. Chen, T. R. Myers, B. J. Hwang, P. W. Sternberg *et al.*, 2006 SynMuv genes redundantly inhibit *lin-3/EGF* expression to prevent inappropriate vulval induction in *C. elegans*. Dev. Cell 10(5): 667–672.

Davis, M. W., M. Hammarlund, T. Harrach, P. Hullett, S. Olsen *et al.*, 2005 Rapid single nucleotide polymorphism mapping in *C. elegans*. BMC Genomics 6: 118.

Dereeper, A., V. Guignon, G. Blanc, S. Audic, S. Buffet *et al.*, 2008 Phylogeny.fr: robust phylogenetic analysis for the non-specialist. Nucleic Acids Res 36(Web Server issue): W465–469.

Detwiler, M. R., M. Reuben, X. Li, E. Rogers, and R. Lin, 2001 Two zinc finger proteins, OMA-1 and OMA-2, are redundantly required for oocyte maturation in *C. elegans*. Dev. Cell 1(2): 187–199.

Ding, L., T. J. Ley, D. E. Larson, C. A. Miller, D. C. Koboldt *et al.*, 2012 Clonal evolution in relapsed acute myeloid leukaemia revealed by whole-genome sequencing. Nature 481(7382): 506–510.

Downs, S. M., 2010 Regulation of the G2/M transition in rodent oocytes. Mol. Reprod. Dev. 77(7): 566–585.

Dybbs, M., J. Ngai, and J. M. Kaplan, 2005 Using microarrays to facilitate positional cloning: identification of tomosyn as an inhibitor of neurosecretion. PLoS Genet. 1(1): e2.

Edwards, R. G., 1965 Maturation in vitro of mouse, sheep, cow, pig, rhesus monkey and human ovarian oocytes. Nature 208 (5008): 349–351.

Eimer, S., B. Lakowski, R. Donhauser, and R. Baumeister, 2002 Loss of *spr-5* bypasses the requirement for the *C.elegans* presenilin *sel-12* by derepressing *hop-1*. EMBO J. 21(21): 5787–5796.

Ellis, H. M., and H. R. Horvitz, 1986 Genetic control of programmed cell death in the nematode *C. elegans*. Cell 44(6): 817–829.

Ellis, R., and T. Schedl, 2007 Sex determination in the germ line. WormBook 5: 1–13.

Ewen, K. A., and P. Koopman, 2010 Mouse germ cell development: from specification to sex determination. Mol. Cell. Endocrinol. 323(1): 76–93.

Fay, D. S., and J. Yochem, 2007 The SynMuv genes of *Caenorhabditis elegans* in vulval development and beyond. Dev. Biol. 306 (1): 1–9.

Felix, M. A., 2007 Cryptic quantitative evolution of the vulva intercellular signaling network in *Caenorhabditis*. Curr. Biol. 17 (2): 103–114.

Ferrell, J. E., Jr., J. R. Pomerening, S. Y. Kim, N. B. Trunnell, W. Xiong *et al.*, 2009 Simple, realistic models of complex biological processes: positive feedback and bistability in a cell fate switch and a cell cycle oscillator. FEBS Lett. 583(24): 3999–4005.

Finney, M., and G. Ruvkun, 1990 The *unc-86* gene product couples cell lineage and cell identity in *C. elegans*. Cell 63(5): 895–905.

Fire, A., S. Xu, M. K. Montgomery, S. A. Kostas, S. E. Driver *et al.*, 1998 Potent and specific genetic interference by double-stranded RNA in *Caenorhabditis elegans*. Nature 391(6669): 806–811.

Fisher, D. A., J. F. Smith, J. S. Pillar, S. H. St Denis, and J. B. Cheng, 1998 Isolation and characterization of PDE8A, a novel human cAMP-specific phosphodiesterase. Biochem. Biophys. Res. Commun. 246(3): 570–577.

Gibert, M. A., J. Starck, and B. Beguet, 1984 Role of the gonad cytoplasmic core during oogenesis of the nematode *Caenorhabditis elegans*. Biol. Cell 50(1): 77–85.

Govindan, J. A., H. Cheng, J. E. Harris, and D. Greenstein, 2006 Galphao/i and Galphas signaling function in parallel with the MSP/Eph receptor to control meiotic diapause in *C. elegans*. Curr. Biol. 16(13): 1257–1268.

Govindan, J. A., S. Nadarajan, S. Kim, T. A. Starich, and D. Greenstein, 2009 Somatic cAMP signaling regulates MSP-dependent oocyte growth and meiotic maturation in *C. elegans*. Development 136(13): 2211–2221.

Gracheva, E. O., A. O. Burdina, A. M. Holgado, M. Berthelot-Grosjean, B. D. Ackley *et al.*, 2006 Tomosyn inhibits synaptic vesicle priming in *Caenorhabditis elegans*. PLoS Biol. 4(8): e261.

Grant, B., and D. Hirsh, 1999 Receptor-mediated endocytosis in the *Caenorhabditis elegans* oocyte. Mol. Biol. Cell 10(12): 4311–4326.

Gross, R. E., S. Bagchi, X. Lu, and C. S. Rubin, 1990 Cloning, characterization, and expression of the gene for the catalytic subunit of cAMP-dependent protein kinase in *Caenorhabditis elegans*. Identification of highly conserved and unique isoforms generated by alternative splicing. J. Biol. Chem. 265(12): 6896–6907.

Gumienny, T. L., E. Lambie, E. Hartwieg, H. R. Horvitz, and M. O. Hengartner, 1999 Genetic control of programmed cell death in the *Caenorhabditis elegans* hermaphrodite germ line. Development 126(5): 1011–1022.

Guven-Ozkan, T., S. M. Robertson, Y. Nishi, and R. Lin, 2010 *zif-1* translational repression defines a second, mutually exclusive OMA function in germline transcriptional repression. Development 137(20): 3373–3382.

Hall, D. H., V. P. Winfrey, G. Blaeuer, L. H. Hoffman, T. Furuta *et al.*, 1999 Ultrastructural features of the adult hermaphrodite gonad of *Caenorhabditis elegans*: relations between the germ line and soma. Dev. Biol. 212(1): 101–123.

Han, S. J., R. Chen, M. P. Paronetto, and M. Conti, 2005 Wee1B is an oocyte-specific kinase involved in the control of meiotic arrest in the mouse. Curr. Biol. 15(18): 1670–1676.

Han, S. M., P. A. Cottee, and M. A. Miller, 2010 Sperm and oocyte communication mechanisms controlling *C. elegans* fertility. Dev. Dyn. 239(5): 1265–1281.

Hanks, S. K., A. M. Quinn, and T. Hunter, 1988 The protein kinase family: conserved features and deduced phylogeny of the catalytic domains. Science 241(4861): 42–52.

Harris, J. E., J. A. Govindan, I. Yamamoto, J. Schwartz, I. Kaverina *et al.*, 2006 Major sperm protein signaling promotes oocyte microtubule reorganization prior to fertilization in *Caenorhabditis elegans*. Dev. Biol. 299(1): 105–121.

Hassold, T., and P. Hunt, 2009 Maternal age and chromosomally abnormal pregnancies: what we know and what we wish we knew. Curr. Opin. Pediatr. 21(6): 703–708.

Henn, A., M. J. Bradley, and E. M. De La Cruz, 2012 ATP utilization and RNA conformational rearrangement by DEAD-box proteins. Annu Rev Biophys 41: 247–267.

Hillier, L. W., G. T. Marth, A. R. Quinlan, D. Dooling, G. Fewell *et al.*, 2008 Whole-genome sequencing and variant discovery in *C. elegans*. Nat. Methods 5(2): 183–188.

Irion, U., and M. Leptin, 1999 Developmental and cell biological functions of the *Drosophila* DEAD-box protein abstrakt. Curr. Biol. 9(23): 1373–1381.

Irion, U., M. Leptin, K. Siller, S. Fuerstenberg, Y. Cai *et al.*, 2004 Abstrakt, a DEAD box protein, regulates Insc levels and asymmetric division of neural and mesodermal progenitors. Curr. Biol. 14(2): 138–144.

Italiano, J. E., Jr., T. M. Roberts, M. Stewart, and C. A. Fontana, 1996 Reconstitution in vitro of the motile apparatus from the amoeboid sperm of Ascaris shows that filament assembly and bundling move membranes. Cell 84(1): 105–114.

Jadhav, S., M. Rana, and K. Subramaniam, 2008 Multiple maternal proteins coordinate to restrict the translation of *C. elegans nanos-2* to primordial germ cells. Development 135(10): 1803–1812.

Jan, E., C. K. Motzny, L. E. Graves, and E. B. Goodwin, 1999 The STAR protein, GLD-1, is a translational regulator of sexual identity in *Caenorhabditis elegans*. EMBO J. 18(1): 258–269.

Jarriault, S., and I. Greenwald, 2002 Suppressors of the egg-laying defective phenotype of *sel-12* presenilin mutants implicate the CoREST corepressor complex in LIN-12/Notch signaling in *C. elegans*. Genes Dev. 16(20): 2713–2728.

Jones, D., E. Crowe, T. A. Stevens, and E. P. Candido, 2002 Functional and phylogenetic analysis of the ubiquitylation system in Caenorhabditis elegans: ubiquitin-conjugating enzymes, ubiquitin-activating enzymes, and ubiquitin-like proteins. Genome Biol. 3(1): RESEARCH0002.

Jud, M. C., M. J. Czerwinski, M. P. Wood, R. A. Young, C. M. Gallo *et al.*, 2008 Large P body-like RNPs form in *C. elegans* oocytes in response to arrested ovulation, heat shock, osmotic stress, and anoxia and are regulated by the major sperm protein pathway. Dev. Biol. 318(1): 38–51.

Kang, D., C. Choe, E. Cavanaugh, and D. Kim, 2007 Properties of single two-pore domain TREK-2 channels expressed in mammalian cells. J. Physiol. 583(Pt 1): 57–69.

Katz, D. J., T. M. Edwards, V. Reinke, and W. G. Kelly, 2009 A *C. elegans* LSD1 demethylase contributes to germline immortality by reprogramming epigenetic memory. Cell 137(2): 308–320.

Kelly, W. G., S. Xu, M. K. Montgomery, and A. Fire, 1997 Distinct requirements for somatic and germline expression of a generally expressed *Caenorhabditis elegans* gene. Genetics 146(1): 227–238.

Kim, S., C. Spike, and D. Greenstein, 2013 Control of oocyte growth and meiotic maturation in *Caenorhabditis elegans*. Adv. Exp. Med. Biol. 757: 277–320.

Kimble, J., and S. L. Crittenden, 2007 Controls of germline stem cells, entry into meiosis, and the sperm/oocyte decision in *Caenorhabditis elegans*. Annu. Rev. Cell Dev. Biol. 23: 405–433.

Korswagen, H. C., J. H. Park, Y. Ohshima, and R. H. Plasterk, 1997 An activating mutation in a *Caenorhabditis elegans* G_s protein induces neural degeneration. Genes Dev. 11(12): 1493–1503.

Kosinski, M., K. McDonald, J. Schwartz, I. Yamamoto, and D. Greenstein, 2005 *C. elegans* sperm bud vesicles to deliver a meiotic maturation signal to distant oocytes. Development 132(15): 3357–3369.

Kramer, L. B., J. Shim, M. L. Previtera, N. R. Isack, M.-C. Lee *et al.*, 2010 UEV-1 is a ubiquitin-conjugating enzyme variant that regulates glutamate receptor trafficking in *C. elegans* neurons. PLoS ONE 5(12): e14291.

Kumsta, C., and M. Hansen, 2012 *C. elegans rrf-1* mutations maintain RNAi efficiency in the soma in addition to the germ line. PLoS ONE 7(5): e35428.

Lakowski, B., S. Eimer, C. Gobel, A. Bottcher, B. Wagler *et al.*, 2003 Two suppressors of *sel-12* encode C2H2 zinc-finger proteins that regulate presenilin transcription in *Caenorhabditis elegans*. Development 130(10): 2117–2128.

Lakowski, B., I. Roelens, and S. Jacob, 2006 CoREST-like complexes regulate chromatin modification and neuronal gene expression. J. Mol. Neurosci. 29(3): 227–239.

Lee, M. H., M. Ohmachi, S. Arur, S. Nayak, R. Francis *et al.*, 2007 Multiple functions and dynamic activation of MPK-1 extracellular signal-regulated kinase signaling in *Caenorhabditis elegans* germline development. Genetics 177(4): 2039–2062.

Lesage, F., C. Terrenoire, G. Romey, and M. Lazdunski, 2000 Human TREK2, a 2P domain mechano-sensitive K+ channel with multiple regulations by polyunsaturated fatty acids, lysophospholipids, and Gs, Gi, and Gq protein-coupled receptors. J. Biol. Chem. 275(37): 28398–28405.

Li, W., L. R. DeBella, T. Guven-Ozkan, R. Lin, and L. S. Rose, 2009 An eIF4E-binding protein regulates katanin protein levels in *C. elegans* embryos. J. Cell Biol. 187(1): 33–42.

Lincoln, A. J., D. Wickramasinghe, P. Stein, R. M. Schultz, M. E. Palko *et al.*, 2002 Cdc25b phosphatase is required for resumption of meiosis during oocyte maturation. Nat. Genet. 30(4): 446–449.

Linder, P., 2006 Dead-box proteins: a family affair–active and passive players in RNP-remodeling. Nucleic Acids Res. 34(15): 4168–4180.

Linder, P., and E. Jankowsky, 2011 From unwinding to clamping: the DEAD box RNA helicase family. Nat. Rev. Mol. Cell Biol. 12 (8): 505–516.

Lu, X., and H. R. Horvitz, 1998 *lin-35* and *lin-53*, two genes that antagonize a *C. elegans* Ras pathway, encode proteins similar to Rb and its binding protein RbAp48. Cell 95(7): 981–991.

Lu, X. Y., R. E. Gross, S. Bagchi, and C. S. Rubin, 1990 Cloning, structure, and expression of the gene for a novel regulatory subunit of cAMP-dependent protein kinase in *Caenorhabditis elegans*. J. Biol. Chem. 265(6): 3293–3303.

Maller, J. L., and E. G. Krebs, 1977 Progesterone-stimulated meiotic cell division in *Xenopus* oocytes. Induction by regulatory subunit and inhibition by catalytic subunit of adenosine 3′:5′-monophosphate-dependent protein kinase. J. Biol. Chem. 252 (5): 1712–1718.

Maniar, T. A., M. Kaplan, G. J. Wang, K. Shen, L. Wei *et al.*, 2012 UNC-33 (CRMP) and ankyrin organize microtubules and localize kinesin to polarize axon-dendrite sorting. Nat. Neurosci. 15(1): 48–56.

Maryon, E. B., R. Coronado, and P. Anderson, 1996 *unc-68* encodes a ryanodine receptor involved in regulating *C. elegans* body-wall muscle contraction. J. Cell Biol. 134(4): 885–893.

Masui, Y., and C. L. Markert, 1971 Cytoplasmic control of nuclear behavior during meiotic maturation of frog oocytes. J. Exp. Zool. 177(2): 129–145.

Masui, Y., and H. J. Clarke, 1979 Oocyte maturation. Int. Rev. Cytol. 57: 185–282.

McCarter, J., B. Bartlett, T. Dang, and T. Schedl, 1999 On the control of oocyte meiotic maturation and ovulation in *Caenorhabditis elegans*. Dev. Biol. 205(1): 111–128.

Mehlmann, L. M., 2005 Stops and starts in mammalian oocytes: recent advances in understanding the regulation of meiotic arrest and oocyte maturation. Reproduction 130(6): 791–799.

Miao, L., O. Vanderlinde, M. Stewart, and T. M. Roberts, 2003 Retraction in amoeboid cell motility powered by cytoskeletal dynamics. Science 302(5649): 1405–1407.

Miller, A. N., and S. B. Long, 2012 Crystal structure of the human two-pore domain potassium channel K2P1. Science 335(6067): 432–436.

Miller, M. A., V. Q. Nguyen, M. H. Lee, M. Kosinski, T. Schedl *et al.*, 2001 A sperm cytoskeletal protein that signals oocyte meiotic maturation and ovulation. Science 291(5511): 2144–2147.

Miller, M. A., P. J. Ruest, M. Kosinski, S. K. Hanks, and D. Greenstein, 2003 An Eph receptor sperm-sensing control mechanism for oocyte meiotic maturation in *Caenorhabditis elegans*. Genes Dev. 17(2): 187–200.

Moerman, D. G., and R. J. Barstead, 2008 Towards a mutation in every gene in *Caenorhabditis elegans*. Brief. Funct. Genomics Proteomics 7(3): 195–204.

Murbartian, J., Q. Lei, J. J. Sando, and D. A. Bayliss, 2005 Sequential phosphorylation mediates receptor- and kinase-induced inhibition of TREK-1 background potassium channels. J. Biol. Chem. 280(34): 30175–30184.

Murray, S. M., S. Y. Yang, and M. Van Doren, 2010 Germ cell sex determination: a collaboration between soma and germ line. Curr. Opin. Cell Biol. 22(6): 722–729.

Nadarajan, S., J. A. Govindan, M. McGovern, E. J. Hubbard, and D. Greenstein, 2009 MSP and GLP-1/Notch signaling coordinately regulate actomyosin-dependent cytoplasmic streaming and oocyte growth in *C. elegans*. Development 136(13): 2223–2234.

Nayak, S., J. Goree, and T. Schedl, 2005 *fog-2* and the evolution of self-fertile hermaphroditism in *Caenorhabditis*. PLoS Biol. 3 (1): e6.

Norris, R. P., M. Freudzon, L. M. Mehlmann, A. E. Cowan, A. M. Simon *et al.*, 2008 Luteinizing hormone causes MAP kinase-dependent phosphorylation and closure of connexin 43 gap junctions in mouse ovarian follicles: one of two paths to meiotic resumption. Development 135(19): 3229–3238.

Norris, R. P., W. J. Ratzan, M. Freudzon, L. M. Mehlmann, J. Krall *et al.*, 2009 Cyclic GMP from the surrounding somatic cells regulates cyclic AMP and meiosis in the mouse oocyte. Development 136(11): 1869–1878.

Nottke, A. C., S. E. Beese-Sims, L. F. Pantalena, V. Reinke, Y. Shi *et al.*, 2011 SPR-5 is a histone H3K4 demethylase with a role in meiotic double-strand break repair. Proc. Natl. Acad. Sci. USA 108(31): 12805–12810.

Oh, J. S., S. J. Han, and M. Conti, 2010 Wee1B, Myt1, and Cdc25 function in distinct compartments of the mouse oocyte to control meiotic resumption. J. Cell Biol. 188(2): 199–207.

Patel, A. J., E. Honore, F. Maingret, F. Lesage, M. Fink *et al.*, 1998 A mammalian two pore domain mechano-gated S-like K+ channel. EMBO J. 17(15): 4283–4290.

Pincus, G., and E. V. Enzmann, 1935 The comparative behavior of mammalian eggs in vivo and in vitro: I. the activation of ovarian eggs. J. Exp. Med. 62(5): 665–675.

Pirino, G., M. P. Wescott, and P. J. Donovan, 2009 Protein kinase A regulates resumption of meiosis by phosphorylation of Cdc25B in mammalian oocytes. Cell Cycle 8(4): 665–670.

Praitis, V., E. Casey, D. Collar, and J. Austin, 2001 Creation of low-copy integrated transgenic lines in *Caenorhabditis elegans*. Genetics 157(3): 1217–1226.

Roberts, T. M., and M. Stewart, 2012 Role of major sperm protein (MSP) in the protrusion and retraction of Ascaris sperm. Int Rev Cell Mol Biol 297: 265–293.

Saffer, A. M., D. H. Kim, A. van Oudenaarden, and H. R. Horvitz, 2011 The *Caenorhabditis elegans* synthetic multivulva genes prevent ras pathway activation by tightly repressing global ectopic expression of *lin-3* EGF. PLoS Genet. 7(12): e1002418.

Sarin, S., S. Prabhu, M. M. O'Meara, I. Pe'er, and O. Hobert, 2008 *Caenorhabditis elegans* mutant allele identification by whole-genome sequencing. Nat. Methods 5(10): 865–867.

Schedl, T., and J. Kimble, 1988 *fog-2*, a germ-line-specific sex determination gene required for hermaphrodite spermatogenesis in *Caenorhabditis elegans*. Genetics 119(1): 43–61.

Schisa, J. A., J. N. Pitt, and J. R. Priess, 2001 Analysis of RNA associated with P granules in germ cells of *C. elegans* adults. Development 128(8): 1287–1298.

Schmucker, D., G. Vorbruggen, P. Yeghiayan, H. Q. Fan, H. Jackle *et al.*, 2000 The *Drosophila* gene *abstrakt*, required for visual system development, encodes a putative RNA helicase of the DEAD box protein family. Mech. Dev. 91(1–2): 189–196.

Schumacher, J. M., A. Golden, and P. J. Donovan, 1998 AIR-2: an Aurora/Ipl1-related protein kinase associated with chromosomes and midbody microtubules is required for polar body extrusion and cytokinesis in *Caenorhabditis elegans* embryos. J. Cell Biol. 143(6): 1635–1646.

Schutz, P., T. Karlberg, S. van den Berg, R. Collins, L. Lehtio *et al.*, 2010 Comparative structural analysis of human DEAD-box RNA helicases. PLoS ONE 5(9). pii e12791.

Seidel, H. S., M. V. Rockman, and L. Kruglyak, 2008 Widespread genetic incompatibility in *C. elegans* maintained by balancing selection. Science 319(5863): 589–594.

Sela-Abramovich, S., I. Edry, D. Galiani, N. Nevo, and N. Dekel, 2006 Disruption of gap junctional communication within the ovarian follicle induces oocyte maturation. Endocrinology 147 (5): 2280–2286.

Shibata, Y., M. Uchida, H. Takeshita, K. Nishiwaki, and H. Sawa, 2012 Multiple functions of PBRM-1/Polybromo- and LET-526/Osa-containing chromatin remodeling complexes in *C. elegans* development. Dev. Biol. 361(2): 349–357.

Sijen, T., J. Fleenor, F. Simmer, K. L. Thijssen, S. Parrish *et al.*, 2001 On the role of RNA amplification in dsRNA-triggered gene silencing. Cell 107(4): 465–476.

Soderling, S. H., S. J. Bayuga, and J. A. Beavo, 1998 Cloning and characterization of a cAMP-specific cyclic nucleotide phosphodiesterase. Proc. Natl. Acad. Sci. USA 95(15): 8991–8996.

Starck, J., 1977 Radioautographic study of RNA synthesis in *Caenorhabditis elegans* (Bergerac Variety) oogenesis. Biol. Cell. 30: 181–182.

Stinchcomb, D. T., J. E. Shaw, S. H. Carr, and D. Hirsh, 1985 Extrachromosomal DNA transformation of *Caenorhabditis elegans*. Mol. Cell. Biol. 5(12): 3484–3496.

Sun, Q. Y., Y. L. Miao, and H. Schatten, 2009 Towards a new understanding on the regulation of mammalian oocyte meiosis resumption. Cell Cycle 8(17): 2741–2747.

Taylor, S. S., J. A. Buechler, and W. Yonemoto, 1990 cAMP-dependent protein kinase: framework for a diverse family of regulatory enzymes. Annu. Rev. Biochem. 59: 971–1005.

Thomas, C. G., G. C. Woodruff, and E. S. Haag, 2012 Causes and consequences of the evolution of reproductive mode in *Caenorhabditis* nematodes. Trends Genet. 28(5): 213–220.

Timmons, L., and A. Fire, 1998 Specific interference by ingested dsRNA. Nature 395(6705): 854.

Tursun, B., L. Cochella, I. Carrera, and O. Hobert, 2009 A toolkit and robust pipeline for the generation of fosmid-based reporter genes in *C. elegans*. PLoS ONE 4(3): e4625.

Von Stetina, J. R., and T. L. Orr-Weaver, 2011 Developmental control of oocyte maturation and egg activation in metazoan models. Cold Spring Harb. Perspect. Biol. 3(10): a005553.

Walker, A. K., P. R. Boag, and T. K. Blackwell, 2007 Transcription reactivation steps stimulated by oocyte maturation in *C. elegans*. Dev. Biol. 304(1): 382–393.

Ward, S., and J. S. Carrel, 1979 Fertilization and sperm competition in the nematode *Caenorhabditis elegans*. Dev. Biol. 73(2): 304–321.

Warming, S., N. Costantino, D. L. Court, N. A. Jenkins, and N. G. Copeland, 2005 Simple and highly efficient BAC recombineering using galK selection. Nucleic Acids Res. 33(4): e36.

Wen, C., D. Levitan, X. Li, and I. Greenwald, 2000 *spr-2*, a suppressor of the egg-laying defect caused by loss of *sel-12* presenilin in *Caenorhabditis elegans*, is a member of the SET protein subfamily. Proc. Natl. Acad. Sci. USA 97(26): 14524–14529.

Whitten, S. J., and M. A. Miller, 2007 The role of gap junctions in *Caenorhabditis elegans* oocyte maturation and fertilization. Dev. Biol. 301(2): 432–446.

Wolke, U., E. A. Jezuit, and J. R. Priess, 2007 Actin-dependent cytoplasmic streaming in *C. elegans* oogenesis. Development 134 (12): 2227–2236.

Xu, K., N. Tavernarakis, and M. Driscoll, 2001 Necrotic cell death in *C. elegans* requires the function of calreticulin and regulators of Ca(2+) release from the endoplasmic reticulum. Neuron 31 (6): 957–971.

Yochem, J., T. Gu, and M. Han, 1998 A new marker for mosaic analysis in *Caenorhabditis elegans* indicates a fusion between hyp6 and hyp7, two major components of the hypodermis. Genetics 149(3): 1323–1334.

Yuan, J., and H. R. Horvitz, 1992 The *Caenorhabditis elegans* cell death gene *ced-4* encodes a novel protein and is expressed during the period of extensive programmed cell death. Development 116(2): 309–320.

Yuan, J., S. Shaham, S. Ledoux, H. M. Ellis, and H. R. Horvitz, 1993 The *C. elegans* cell death gene *ced-3* encodes a protein similar to mammalian interleukin-1 beta-converting enzyme. Cell 75(4): 641–652.

Zhang, Y., L. Nash, and A. L. Fisher, 2008 A simplified, robust, and streamlined procedure for the production of *C. elegans* transgenes via recombineering. BMC Dev. Biol. 8: 119.

Zhang, Z., B. Yuan, M. Bao, N. Lu, T. Kim *et al.*, 2011 The helicase DDX41 senses intracellular DNA mediated by the adaptor STING in dendritic cells. Nat. Immunol. 12(10): 959–965.

Communicating editor: K. Kemphues

GENETICS

Supporting Information
http://www.genetics.org/lookup/suppl/doi:10.1534/genetics.112.143271/-/DC1

SACY-1 DEAD-Box Helicase Links the Somatic Control of Oocyte Meiotic Maturation to the Sperm-to-Oocyte Switch and Gamete Maintenance in *Caenorhabditis elegans*

Seongseop Kim, J. Amaranath Govindan, Zheng Jin Tu, and David Greenstein

DOI: 10.1534/genetics.112.143271

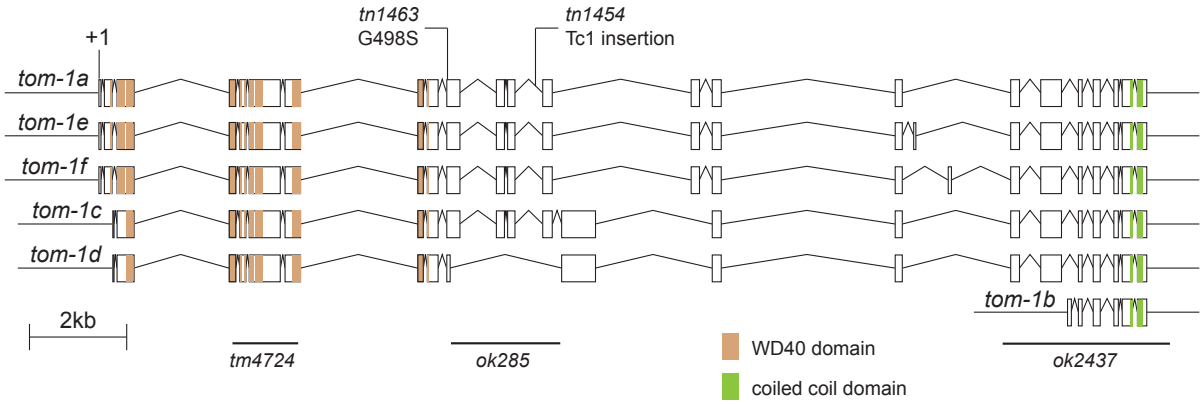

Figure S1 Location of Sacy alleles of *tom-1*. Each *tom-1* gene isoform is depicted. The start codon (+1) of the *tom-1a* gene isoform is indicated. Newly identified *tom-1 tn* alleles and the corresponding amino acid changes are shown. Deletion alleles are underlined. Apparently, *tom-1* is a complex locus and only *ok2437*, *tn1463*, and *tn1454* suppress *acy-4(lf)* sterility–the *tom-1* isoform(s) relevant to this observation are unclear.

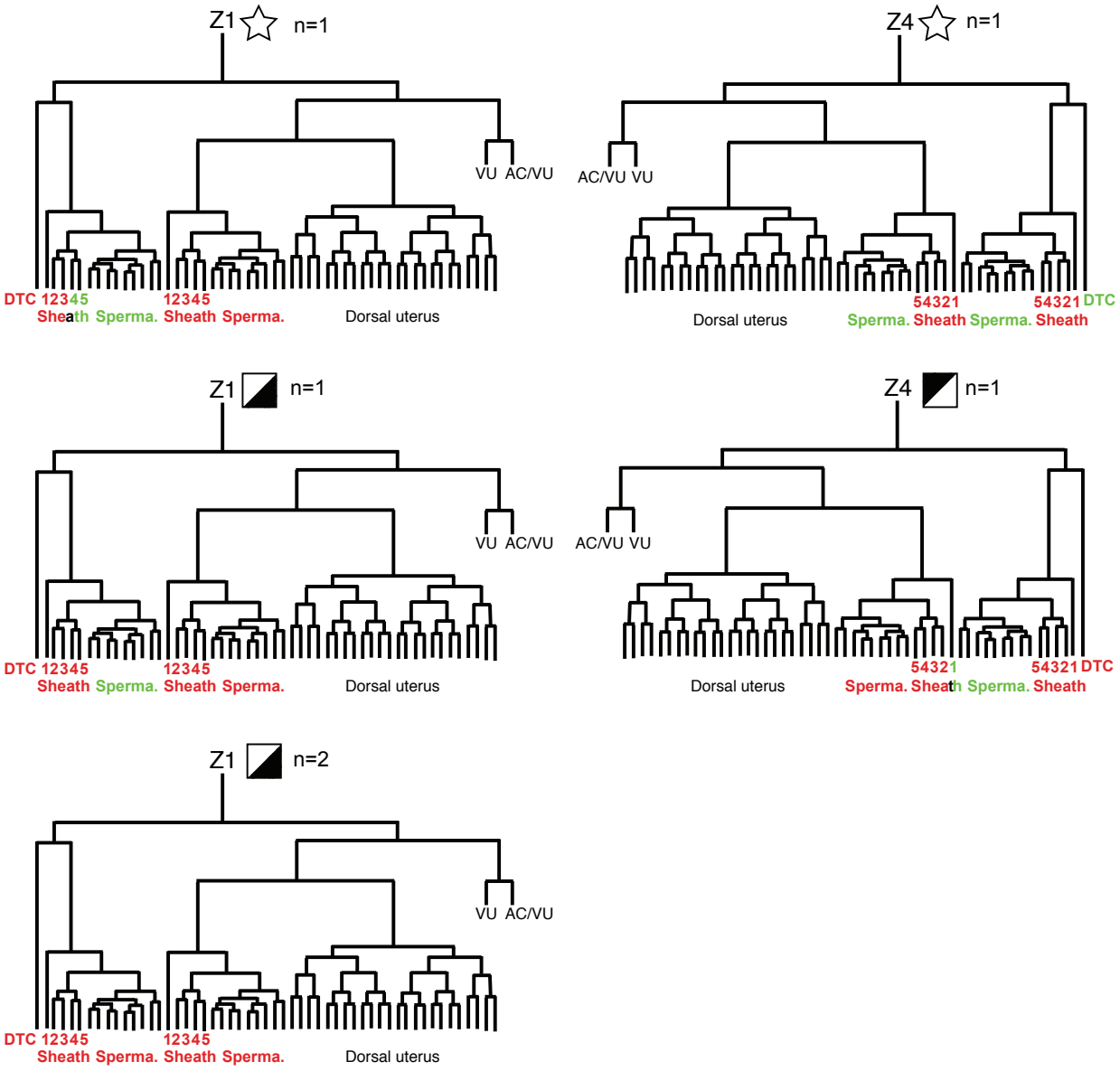

Figure S2 *kin-1* genetic mosaics with complex losses within the somatic gonadal cell lineages. Genetic-mosaic animals with complex losses of the *kin-1(+)* array in the somatic gonad (see Figure 1 in the main text) are described in more detail. Green characters represent the presence of the *kin-1(+)* array and red characters represent the absence of the *kin-1(+)* array. Uterine cells were not scored. One sterile genetic mosaic animal (star) resulted from multiple independent losses within both the Z1 and Z4 lineages. This animal is consistent with a requirement for *kin-1(+)* function in the gonadal sheath cells for meiotic maturation.

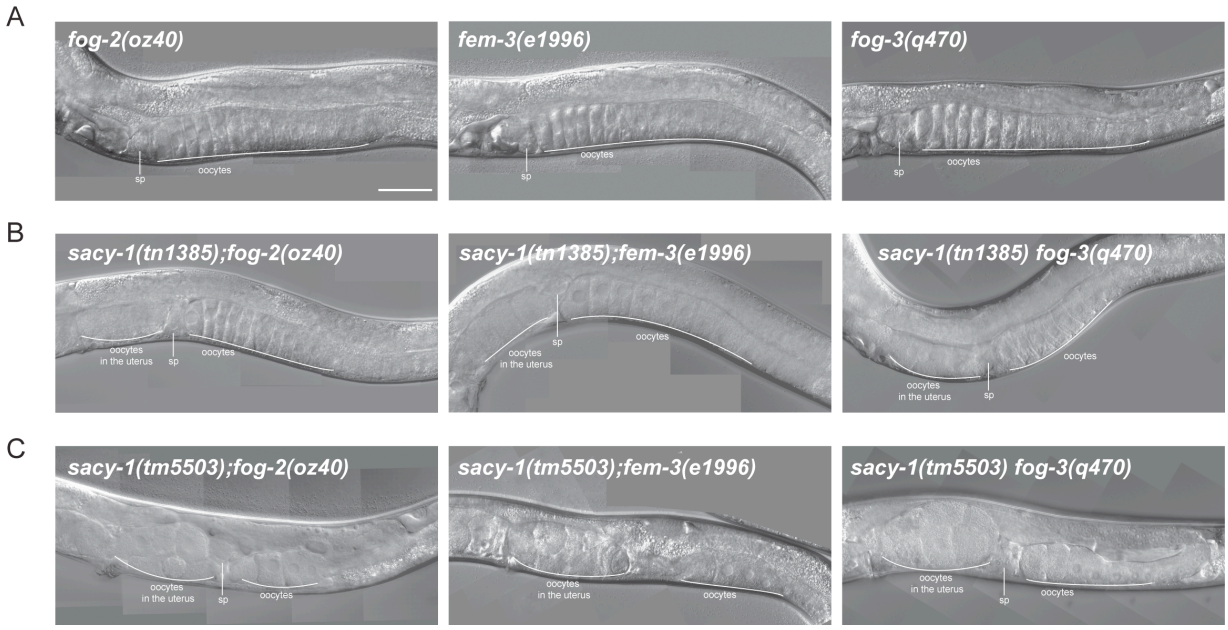

Figure S3 *sacy-1* is a negative regulator of oocyte meiotic maturation in the absence of sperm. (A) Control female mutants. Oocytes are stacked within the gonad arm and the uterus is empty. Spermatheca (sp). (B) *sacy-1(tn1385)* inhibits oocyte meiotic maturation in the absence of sperm. Oocytes undergo maturation and ovulation at an increased frequency and are observed in the uterus despite the absence of sperm. A similar phenotype was observed in *fog-1(e2121) sacy-1(tn1385)* females (S. Kim and D. Greenstein, unpublished results). (C) *sacy-1(tm5503)* is a strong negative regulator of oocyte meiotic maturation in the absence of sperm. Many unfertilized oocytes are observed in the uterus of *sacy-1(tm5503)* females, suggesting that *sacy-1* inhibits oocyte meiotic maturation in the absence of sperm. The frequent occurrence of defective ovulation in *sacy-1(tm5503)* females prevented us from directly measuring meiotic maturation rates. *fog-1(e2121) sacy-1(tm5503)* females exhibit a similar phenotype (S. Kim and D. Greenstein, unpublished results). All images were obtained from day-1 adults (24 hr post-L4) examined by DIC microscopy. *fog-3(q470)* and *sacy-1(tm5503) fog-3(q470)* images were duplicated from Figure 8 for comparison. Scale bar, 50 μm.

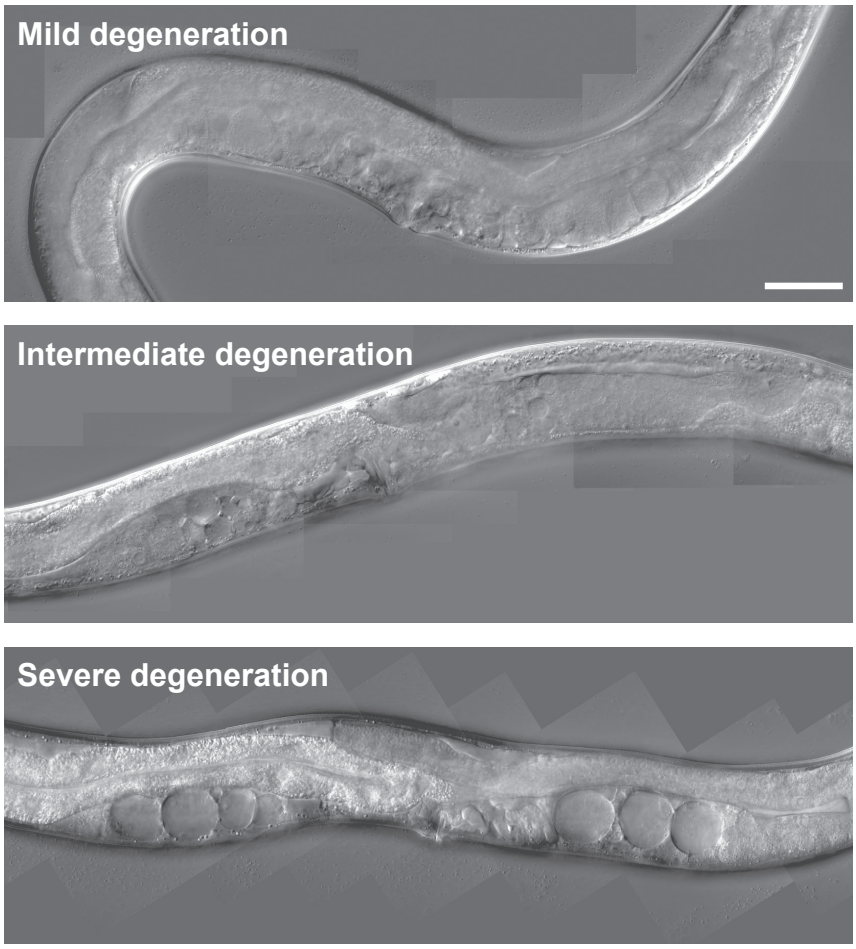

Figure S4 Representative DIC images of day-1 adults illustrating the qualitative scoring criteria used to evaluate the severity of the gamete degeneration phenotype of *sacy-1(tm5503)* hermaphrodites and females. Scale bar, 50 μm.

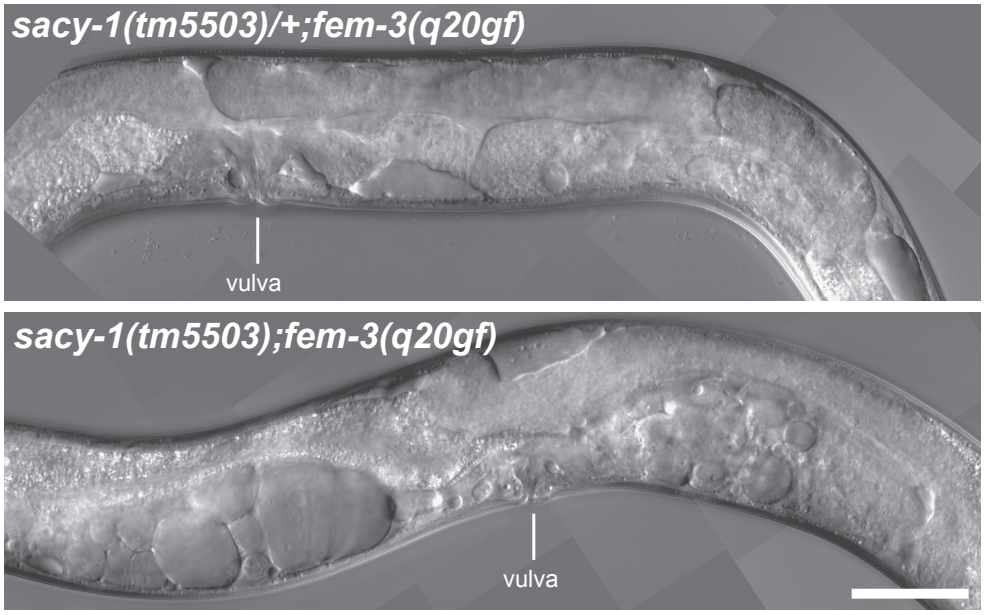

Figure S5 Masculinization of the hermaphrodite germ line does not suppress *sacy-1(tm5503)* gamete degeneration. A *sacy-1(tm5503); fem-3(q20gf)* hermaphrodite (bottom) exhibits the gamete degeneration phenotype. A *sacy-1(tm5503)/+; fem-3(q20gf)* hermaphrodite (top) produces excessive amounts of sperm. Scale bar, 50 μm.

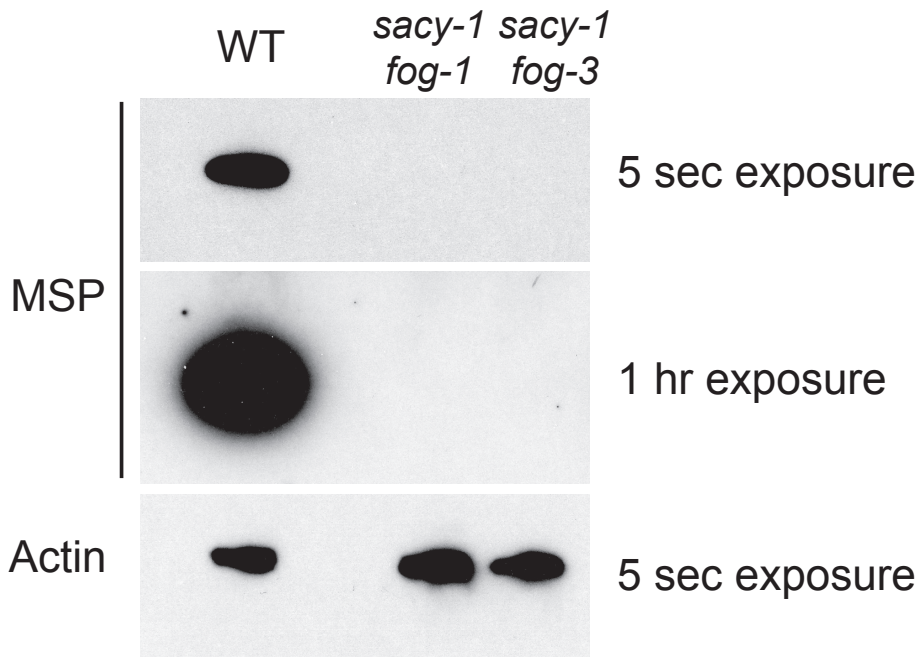

Figure S6 *sacy-1(tm5503)* females do not produce MSP. Western blot of MSP from wild-type (WT), *fog-1(e2121) sacy-1(tm5503)*, and *sacy-1(tm5503) fog-3(q470)* adults. Because oocyte meiotic maturation occurs frequently in *sacy-1(tm5503)* females despite the absence of MSP, *sacy-1* is a strong negative regulator of meiotic maturation. Ten animals of each genotype were lysed and immunoblotting was conducted using a rabbit C-terminal-specific anti-MSP antibody (C3196; 1:20,000) (Kosinski et al., 2005). Mouse anti-actin C4 antibody (Millipore; 1:20,000) served as a loading control.

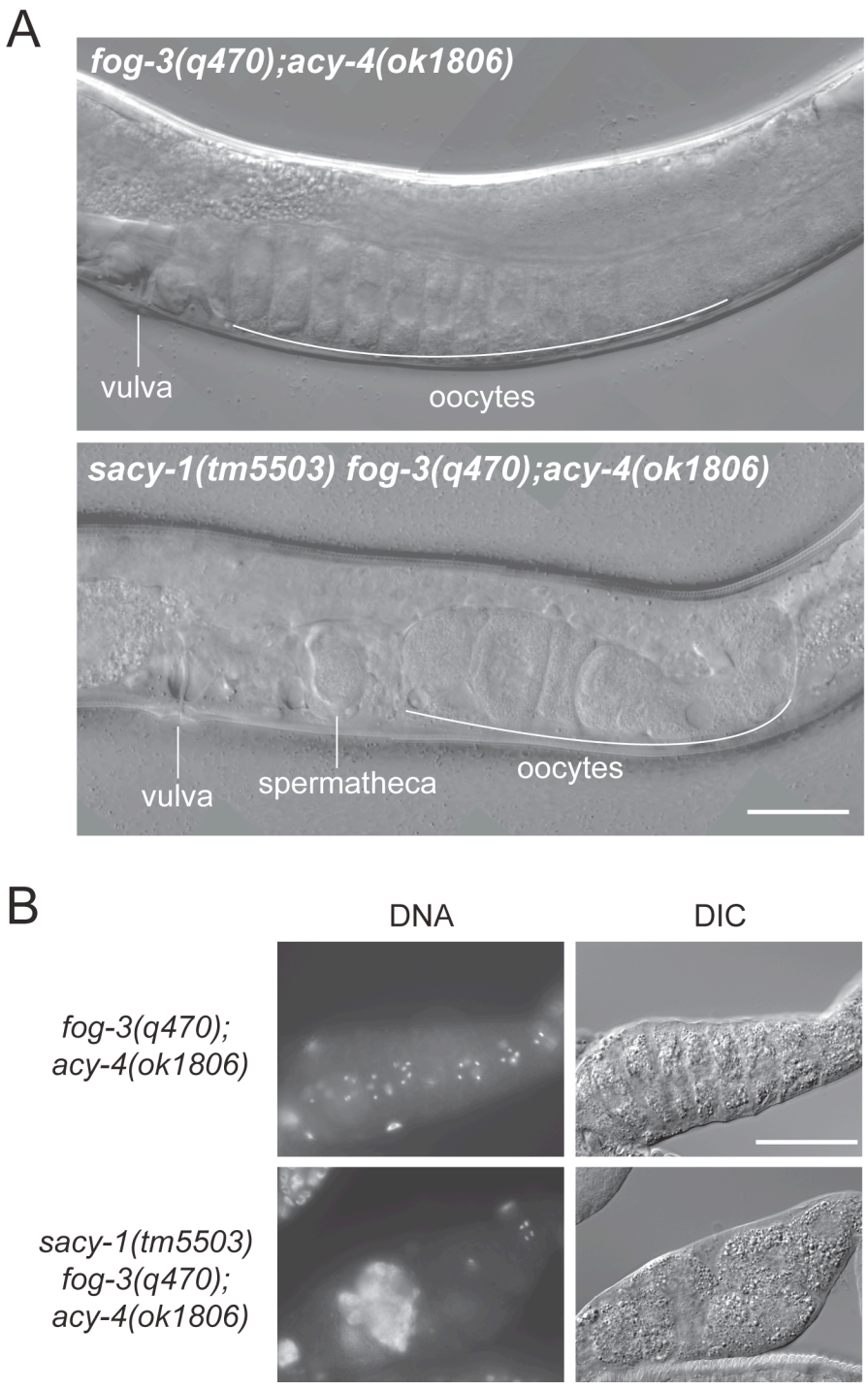

Figure S7 *sacy-1(tm5503)* is epistatic to *acy-4(ok1806)* for oocyte meiotic maturation. Oocyte meiotic maturation occurs frequently in *sacy-1(tm5503) fog-3(q470); acy-4(ok1806)* females, though ovulation often fails and endomitotic oocytes are observed in the gonad arm. In contrast, oocytes arrest in diakinesis in *fog-3(q470); acy-4(ok1806)* females. Day-1 adults were examined by DIC microscopy of living animals (A) and DNA was detected by DAPI staining of dissected and fixed gonads (B). Proximal is to the left side. Scale bar, 50 μm.

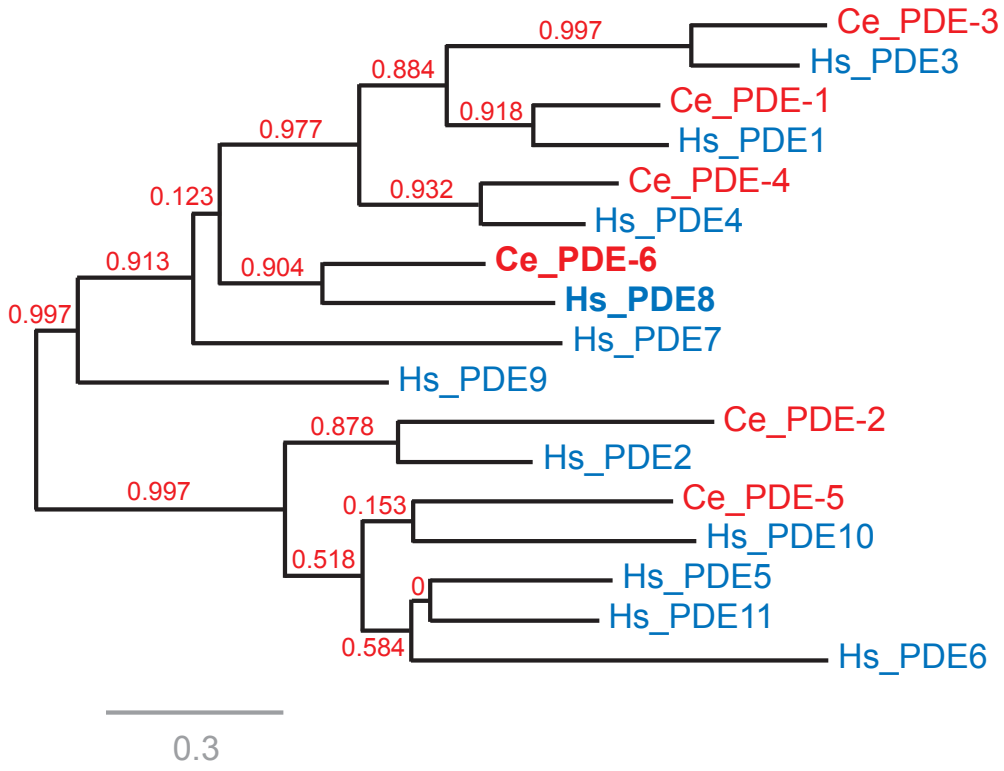

Figure S8 Phylogenetic comparison *C. elegans* and human phosphodiesterases. The likely human ortholog of *C. elegans* PDE-6 is PDE8, the high-affinity cAMP-specific phosphodiesterase. Red characters represent six *C. elegans* phosphodiesterases, and blue characters represent 11 human phosphodiesterases. The following amino acid sequences were used for the analysis; Ce_PDE-1 (NP_493343.1), Ce_PDE-2 (NP_001022705), Ce_PDE-3 (NP_871943.2), Ce_PDE-4 (NP_001040798.1), Ce_PDE-5 (NP_491544.2), Ce_PDE-6 (NP_490787.1), Hs_PDE1 (NP_000915.1), Hs_PDE2 (NP_002590.1), Hs_PDE3 (NP_000913.2), Hs_PDE4 (NP_001098101.1), Hs_PDE5 (NP_001074.2), Hs_PDE6 (NP_000274.2), Hs_PDE7 (NP_001229247.1), Hs_PDE8 (NP_001025024.1), Hs_PDE9 (NP_002597.1), Hs_PDE10 (NP_001124162.1), Hs_PDE11 (NP_058649.3).

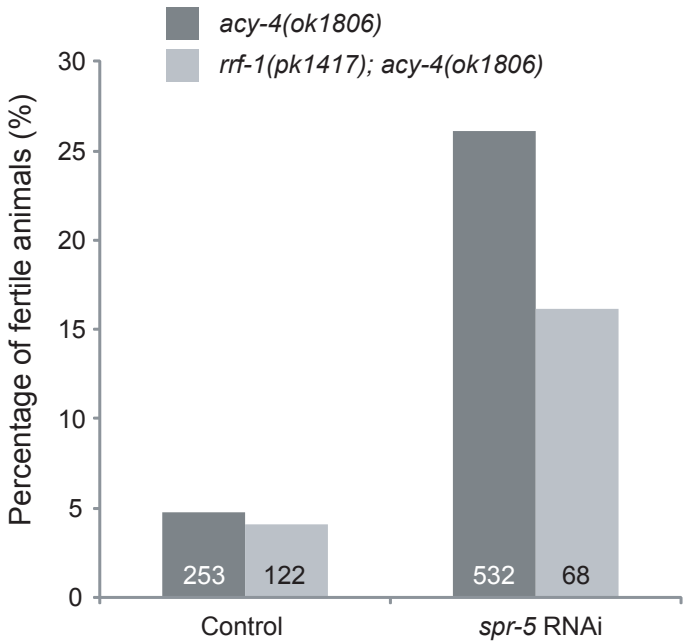

Figure S9 *spr-5* RNAi suppresses *acy-4(lf)* sterility. *spr-5* dsRNAs, or a buffer control, were injected into the gonad arms of *acy-4(ok1806); tnEx37[acy-4(+) sur-5::gfp]* or *rrf-1(pk1417); acy-4(ok1806); tnEx37[acy-4(+) sur-5::gfp]* adult hermaphrodites, and non-array-bearing F1 animals were scored by DIC microscopy for suppression of *acy-4(ok1806)* sterility. Fertile animals were defined as having more than two embryos in the spermathecae and/or uterus. The numbers of animals scored are indicated.

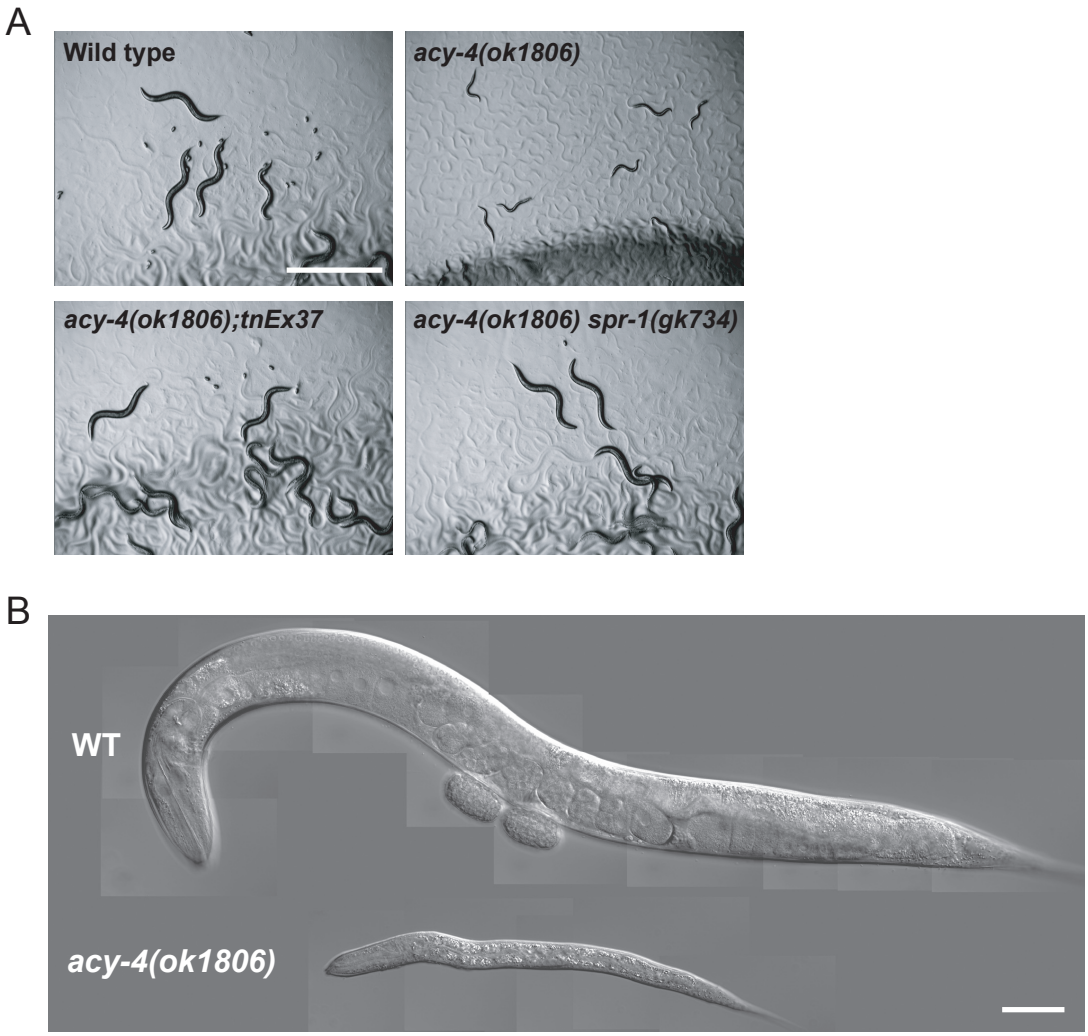

Figure S10 Growth defect of *acy-4(ok1806)* on HT115 bacteria. (A) *acy-4(ok1806)* animals exhibit larval lethality, larval arrest, or slow growth on standard NGM plates with *E. coli* HT115 as the food source. In contrast, wild-type, *acy-4(ok1806); tnEx37[acy-4(+) sur-5::gfp],* and *acy-4(ok1806) spr-1(gk734)* animals grow well with HT115 as the food source. Likewise, *spr-2, spr-4*, and *spr-5* mutations suppress the *acy-4(ok1806)* growth defect (not shown). Embryos isolated by bleach treatment were cultured on HT115-seeded plates for approximately 72 hrs. *acy-4(ok1806)* homozygotes were the GFP-negative progeny of array-bearing parents. Scale bar, 1 mm. (B) DIC images of wild type (WT) and *acy-4(ok1806)* animals grown on HT115-seeded medium for 72 hrs. Scale bar, 50 μm.

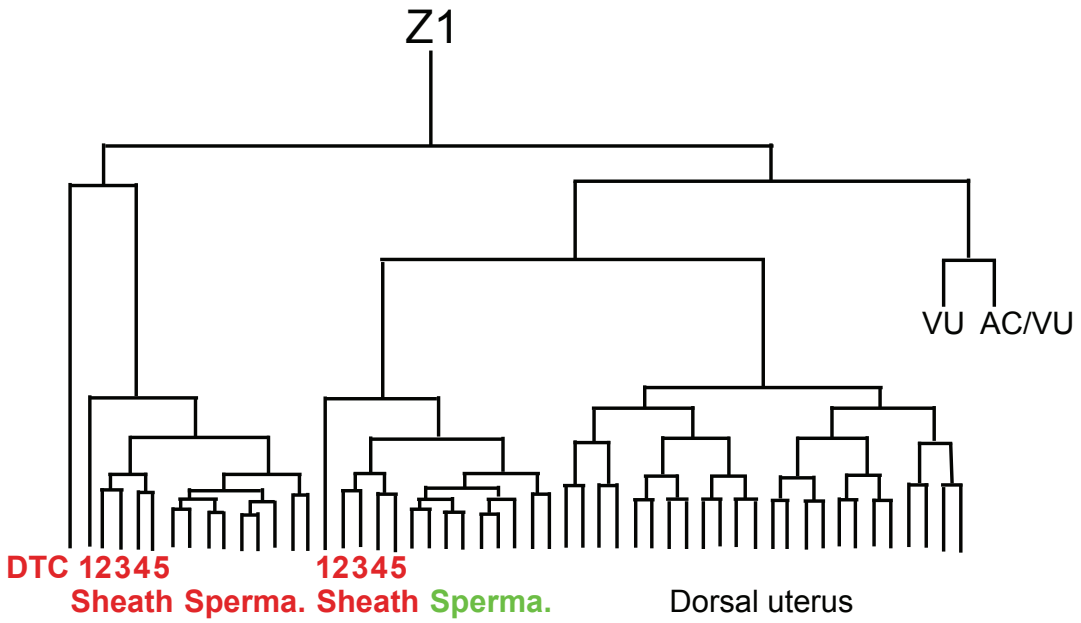

Figure S11 *twk-1* functions in the somatic gonad downstream of *acy-4*. A genetic mosaic animal resulting from multiple independent losses of the *twk-1(+)*-bearing extrachromosomal array in the anterior somatic gonadal lineage (Z1). This animal was fertile in the anterior arm, indicating suppression of *acy-4(lf)* sterility, but sterile in the posterior arm. Green characters represent the presence of the *twk-1(+)* array, and red characters represent the absence of the *twk-1(+)* array. Uterine cells were not scored.

A

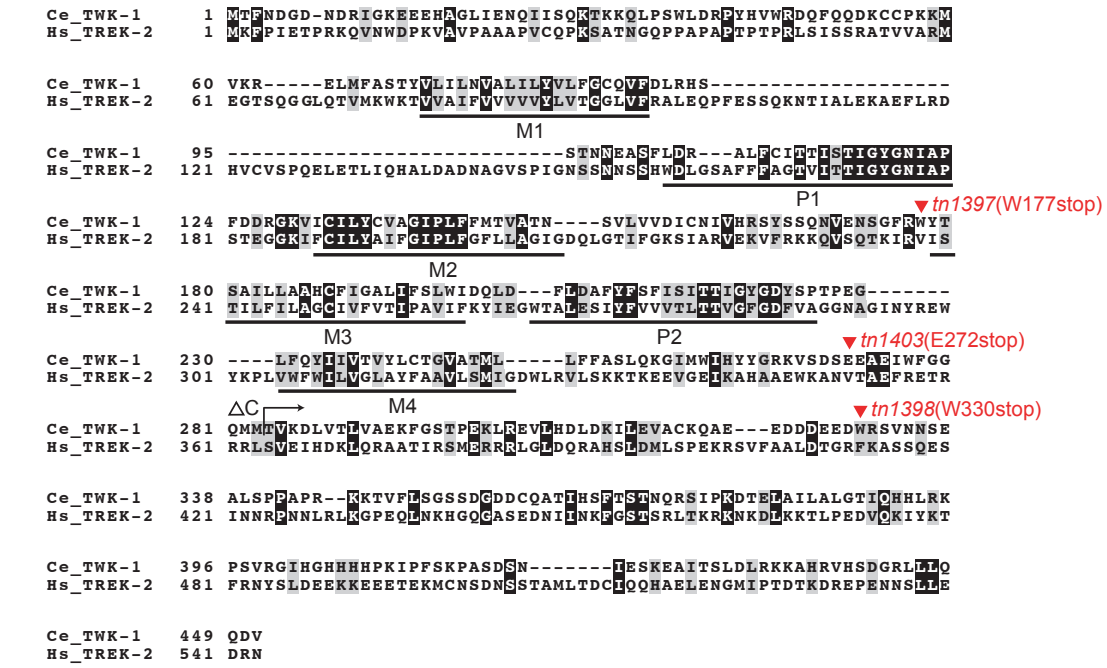

B

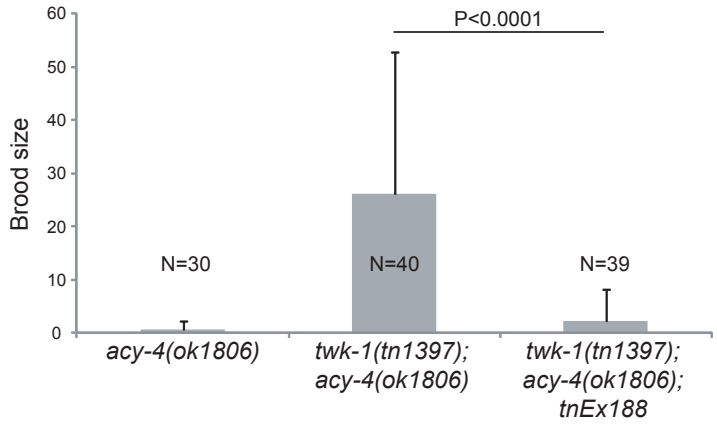

Figure S12 The TWK-1 C-terminus is not essential for function. (A) ClustalW alignment of *C. elegans* TWK-1 and human TREK-2 (NP_612190). Using RT-PCR, we found that the TWK-1 prediction (NP_492054.2) was incorrect in that a small predicted intron was found to be coding, resulting in an additional 14 amino acids. The RT-PCR data is in agreement with the gene prediction based on the FN890018 cDNA. We thank Bernard Lakowski for pointing out the discrepancy in the *twk-1* gene prediction. The four transmembrane domains (M1-M4) and two pore domains (P1 and P2) are underlined. The three *twk-1* nonsense mutations and the position of the ΔC284 deletion are indicated. TWK-1 exhibits less similarity to TREK-1 (not shown) in the C-terminal region because of the latter's smaller size. (B) The TWK-1DC284::GFP fusion (*tnEx188*) rescues *twk-1(tn1397)*. Error bars represent one standard deviation. Student's *t*-test was used for statistical analysis.

Table S1 Molecular identity of Sacy mutations in *tn* alleles

Gene	Allele	Nucleotide change	Amino acid change[a]
pde-6	*tn1237*	CAG -> **T**AG	Q668*
	tn1242	TGG -> TG**A**	W444*
	tn1336	TGG -> TG**A**	W664*
tom-1	*tn1454*	Tc1 insertion	
	tn1463	GGT -> **A**GT	G498S
sacy-1	*tn1385*	GGA -> **A**GA	G533R
	tn1391	GGA -> **A**GA	G473R
	tn1440	GGA -> **A**GA	G331R
twk-1	*tn1397*	TGG -> T**A**G	W177*
	tn1398	TGG -> TG**A**	W330*
	tn1403	GAA -> **T**AA	E272*
spr-4	*tn1383*	CGA -> **T**GA	R1230*
	tn1402	CGA -> **T**GA	R1230*
	tn1404	CAT -> **T**AT	H845Y
	tn1438	CGA -> **T**GA	R486*
	tn1444	CAG -> **T**AG	Q1128*
	tn1467	CAG -> **T**AG	Q45*
spr-5	*tn1378*	TGG -> T**A**G	W666*
	tn1379	GAG -> **A**AG	E164K
	tn1394	GGT -> G**A**T	G619D
uev-1	*tn1381*	GGA-> G**A**A	G17E
	tn1382	GGT -> G**A**T	G47D
spr-2	*tn1380*	GAT-> G**C**T	D42A
	tn1436	Tc1 insertion	

[a]Premature stop codons are indicated by asterisks. The numbering of amino acids refers to the isoforms PDE-6A, TOM-1A, SPR-4A, and SPR-2B.

Table S2 ***C. elegans*** **strains used for this study**

Strain	Genotype
N2	Wild type, Bristol isolate
CB4856	Hawaiian isolate
DG2730	*tnIr1[N2=>CB4856, acy-4(ok1806)]* V; *tnEx37[acy-4(+) sur-5::gfp]*
DG3051	*tnEx131[acy-1::gfp rol-6(su1006d)]*
DG3064	*tnEx133[acy-2::gfp rol-6(su1006d)]*
DG3066	*tnEx134[acy-3::gfp rol-6(su1006d)]*
DG3395	*tnEx175[twk-1::gfp rol-6(su1006d)]*
DG3441	*tnEx181[twk-1::gfp str-1::gfp]*
DG3521	*fog-1(e2121) sacy-1(tm5503)* I/*hT2[bli-4(e937) let-?(q782) qIs48]* (I;III)
DG3524	*fog-1(e2121) sacy-1(tn1385)* I/*hT2[bli-4(e937) let-?(q782) qIs48]* (I;III)
DG3585	*fog-3(q470)* I/*hT2[bli-4(e937) let-?(q782) qIs48]* (I;III); *acy-4(ok1806)* V; *tnEx37*
DG3186	*gsa-1(pk75)* I/*hT2[bli-4(e937) let-?(q782) qIs48]* (I;III); *fog-2(oz40)* V
DG3393	*kin-1(ok338)* I; *tnEx109[kin-1(+) sur-5::gfp]*
DG3360	*pbrm-1(gk1195)* I; *acy-4(ok1806)* V; *tnEx37*
VC10166	*pbrm-1(gk1195)* I; *octr-1(gk1196)* X
DG2292	*pde-6(tn1237)* I
DG2397	*pde-6(tn1237)* I; *unc-46(e177) acy-4(ok1806)* V
DG2096	*pde-6(tn1242)* I
DG2454	*pde-6(tn1242)* I; *unc-46(e177) acy-4(ok1806)* V
DG2111	*pde-6(tn1336)* I
DG2834	*rrf-1(pk1417)* I; *acy-4(ok1806)* V; *tnEx37*
DG3606	*rrf-1(pk1417)* I; *fog-2(oz40)* V
DG3544	*sacy-1(tm5503) fog-3(q470)* I/*hT2[bli-4(e937) let-?(q782) qIs48]* (I;III)
DG3589	*sacy-1(tm5503) fog-3(q470)* I/*hT2[bli-4(e937) let-?(q782) qIs48]* (I;III); *acy-4(ok1806)* V; *tnEx37*
DG3557	*sacy-1(tm5503) fog-3(q470)/unc-13(e1091) lin-11(n566)* I; *oma-1(zu405te33)* IV/*nT1[qIs51]* (IV;V); *oma-2(te51)* V/*nT1[qIs51]* (IV;V)
DG3492	*sacy-1(tm5503)* I/*hT2[bli-4(e937) let-?(q782) qIs48]* (I;III)
DG3587	*sacy-1(tm5503)* I/*hT2[bli-4(e937) let-?(q782) qIs48]* (I;III); *acy-4(ok1806)* V; *tnEx37*
DG3514	*sacy-1(tm5503)* I/*hT2[bli-4(e937) let-?(q782) qIs48]* (I;III); *ced-3(n717)* IV
DG3566	*sacy-1(tm5503)* I/*hT2[bli-4(e937) let-?(q782) qIs48]* (I;III); *ced-4(n1162)* III/*hT2[bli-4(e937) let-?(q782) qIs48]* (I;III)
DG3528	*sacy-1(tm5503)* I/*hT2[bli-4(e937) let-?(q782) qIs48]* (I;III); *fem-3(e1996)/unc-24(e138) dpy-20(e1282)* V
DG3570	*sacy-1(tm5503)* I/*hT2[bli-4(e937) let-?(q782) qIs48]* (I;III); *fem-3(q20gf)* V
DG3505	*sacy-1(tm5503)* I/*hT2[bli-4(e937) let-?(q782) qIs48]* (I;III); *fog-2(oz40)* V
DG3512	*sacy-1(tm5503)* I/*hT2[bli-4(e937) let-?(q782) qIs48]* (I;III); *fog-2(q71)* V
DG3486	*sacy-1(tm5503)* I/*hT2[bli-4(e937) let-?(q782) qIs48]* (I;III); *him-8(tm611)* IV
DG3561	*sacy-1(tm5503) I/hT2[bli-4(e937) let-?(q782) qIs48] (I;III); unc-24(e138) IV*

DG3560	*sacy-1(tm5503) I/hT2[bli-4(e937) let-?(q782) qIs48] (I;III); unc-32(e189) III/hT2[bli-4(e937) let-?(q782) qIs48] (I;III)*
DG3571	*sacy-1(tm5503) I/hT2[bli-4(e937) let-?(q782) qIs48] (I;III); unc-33(mn407) IV*
DG3547	*sacy-1(tm5503) I/hT2[bli-4(e937) let-?(q782) qIs48] (I;III); unc-68(e540) V*
DG3485	*sacy-1(tm5503) I; tnEx159[gfp::sacy-1 unc-119(+)]*
DG3611	*sacy-1(tm5503) I; unc-119(ed3) III; tnEx159[gfp::sacy-1 unc-119(+)]*
DG3520	*sacy-1(tm5503)/unc-13(e1091) lin-11(n566) I; fem-3(e1996) V/nT1[qIs51] (IV;V)*
DG3539	*sacy-1(tm5503)/unc-13(e1091) lin-11(n566) I; oma-1(zu405te33) IV/nT1[qIs51] (IV;V); oma-2(te51) V/nT1[qIs51] (IV;V)*
DG3543	*sacy-1(tn1385) fog-3(q470) I/hT2[bli-4(e937) let-?(q782) qIs48] (I;III)*
DG3430	*sacy-1(tn1385) I*
DG3373	*sacy-1(tn1385) I; acy-4(ok1806) V*
DG3542	*sacy-1(tn1385) I; fem-3(e1996) IV/nT1[qIs51] (IV;V)*
DG3449	*sacy-1(tn1385) I; fog-2(oz40) V*
DG3460	*sacy-1(tn1385) I; fog-2(q71) V*
DG3453	*sacy-1(tn1385) kin-1(ok338) I; tnEx109*
DG3070	*sacy-1(tn1385) pbrm-1(tn1475) I; acy-4(ok1806) V*
DG3254	*sacy-1(tn1385) pbrm-1(tn1475) I; acy-4(ok1806) V; tnEx37*
DG3249	*sacy-1(tn1391) I*
DG3060	*sacy-1(tn1391) I; acy-4(ok1806) V*
DG3414	*sacy-1(tn1391) I; fog-2(oz40) V*
DG3461	*sacy-1(tn1391) I; fog-2(q71) V*
DG3314	*sacy-1(tn1391) I; unc-119(ed3) III; acy-4(ok1806) V; tnEx37; tnEx159*
DG3431	*sacy-1(tn1440) I*
DG3362	*sacy-1(tn1440) I; acy-4(ok1806) V*
DG3478	*sacy-1(tn1440) I; fog-2(oz40) V*
DG3450	*sacy-1(tn1440) I; fog-2(q71) V*
DG3115	*sacy-1(tn1440) pbrm-1(tn1476) I; acy-4(ok1806) V*
DG3256	*sacy-1(tn1440) pbrm-1(tn1476) I; acy-4(ok1806) V; tnEx37*
DG3458	*sacy-1(tn1440) spr-5(by134) I; acy-4(ok1806) V*
DG2964	*spr-4(by105) I; acy-4(ok1806) V*
DG3073	*spr-4(tn1383) I; acy-4(ok1806) V*
DG3074	*spr-4(tn1402) I; acy-4(ok1806) V*
DG3107	*spr-4(tn1404) I; acy-4(ok1806) V*
DG3108	*spr-4(tn1438) I; acy-4(ok1806) V*
DG3109	*spr-4(tn1444) I; acy-4(ok1806) V*
DG3110	*spr-4(tn1467) I; acy-4(ok1806) V*
DG2942	*spr-5(ar197) I; acy-4(ok1806) V*
DG2941	*spr-5(by134) I; acy-4(ok1806) V*

DG3185	*spr-5(by134) I; fog-2(oz40) V*
DG3122	*spr-5(by134) kin-1(ok338) I; tnEx109*
DG2553	*spr-5(tn1378) I; acy-4(ok1806) V*
DG2564	*spr-5(tn1379) I; acy-4(ok1806) V*
DG2522	*spr-5(tn1394) I; acy-4(ok1806) V*
NM1815	*tom-1(ok188)*
DG3192	*tom-1(ok188) I; acy-4(ok1806) V; tnEx37*
RB1887	*tom-1(ok2437) I*
DG3079	*tom-1(ok2437) I; acy-4(ok1806) V*
VC223	*tom-1(ok285) I*
DG3217	*tom-1(ok285) I; acy-4(ok1806) V; tnEx37*
FX04724	*tom-1(tm4724) I*
DG3245	*tom-1(tm4724) I; acy-4(ok1806) V; tnEx37*
DG3118	*tom-1(tn1454) I; acy-4(ok1806) V*
DG3097	*tom-1(tn1463) I; acy-4(ok1806) V*
DG3408	*twk-1(tn1397) I*
DG3095	*twk-1(tn1397) I; acy-4(ok1806) V*
DG3447	*twk-1(tn1397) I; acy-4(ok1806) V/nT1[qIs51] (IV;V); tnEx180[twk-1(+) sur-5::gfp]*
DG3490	*twk-1(tn1397) I; acy-4(ok1806) V/nT1[qIs51] (IV;V); tnEx188[twk-1(ΔC284)::gfp str-1::gfp]*
DG3451	*twk-1(tn1397) kin-1(ok338) I; tnEx109*
DG3389	*twk-1(tn1398) I*
DG3083	*twk-1(tn1398) I; acy-4(ok1806) V*
DG3390	*twk-1(tn1403) I*
DG3113	*twk-1(tn1403) I; acy-4(ok1806) V*
DG3459	*twk-1(tn1403) spr-5(by134) I; acy-4(ok1806) V*
RB1976	*uev-1(ok2610) I*
DG3409	*uev-1(ok2610) I; acy-4(ok1806) V*
DG3076	*uev-1(tn1381) I; acy-4(ok1806) V*
DG3080	*uev-1(tn1382) I; acy-4(ok1806) V*
CB3778	*tra-2(e2020) II*
CB3843	*fem-3(e1996)/unc-24(e138) dpy-20(e1282) IV*
CA257	*him-8(tm611) IV*
DG2836	*spr-2(ar199) dpy-20(e1282) IV; acy-4(ok1806) V; tnEx37*
DG2943	*spr-2(ar211) dpy-20(e1282)* IV; *acy-4(ok1806)* V
DG3136	*spr-2(tm4802)* IV; *acy-4(ok1806)* V
DG2558	*spr-2(tn1380)* IV; *acy-4(ok1806)* V
DG2592	*spr-2(tn1436)* IV; *acy-4(ok1806)* V
DG3612	*acy-4(ok1806) spr-1(gk734)* V
DG3604	*acy-4(ok1806) unc-23(e25)* V; *tnEx37*

DG3145	*acy-4(ok1806)* V; *spr-3(by108)* X
DG3129	*acy-4(ok1806)* V; *spr-3(ok2525)* X
DG3391	*acy-4(ok1806)* V; *tnEx37*
BS553	*fog-2(oz40)* V
CB4108	*fog-2(q71)* V

Table S3 Primers used for this study

Name	Sequence	Use
ok1806F1	CGGGTTGATGAATCTTGTATCATTCTC	*acy-4(ok1806)* genotyping
ok1806R1	CATGATACAAGCATTGTCACGAGACTC	*acy-4(ok1806)* genotyping
ok1806F2	TCAGTCTCGTCATTGGTGTTCTGTTC	*acy-4(ok1806)* genotyping
gk1195_F1	TTCATCTGAATGGCCATTCACTCTTGATC	*pbrm-1(gk1195)* genotyping
gk1195_F2	TTTCAGGAAAGCGAAGTCGAAATGGAAG	*pbrm-1(gk1195)* genotyping
gk1195_R1	CTCTTTGTATACTCCAATTCCTCGTCTTC	*pbrm-1(gk1195)* genotyping
H27M09.1_F5	ACTGCTGGAAGATATATCACTTATCGTC	*sacy-1(tm5503)* genotyping
tm5503_F1	GTTATTGACGAATCAGAACGGCAATTAATG	*sacy-1(tm5503)* genotyping
tm5503_R1	CTTGTATCTGAATAGCTGTCGGTGTCAC	*sacy-1(tm5503)* genotyping
H27M09.1_RNAi_F	TTTTAATACGACTCACTATAGGGTCAAATCTTTGACCTGATCATTGAAATG	*sacy-1* RNAi
H27M09.1_RNAi_R	TTTTAATACGACTCACTATAGGGGACAATCTGTGATGCGATGACCCAG	*sacy-1* RNAi
H27M09.1_cDNA_F1	TTTCCCGGGAATATGAGGACCGCCGGCGAAAAATTC	*sacy-1* cDNA 5' half RNAi
H27M09.1_cDNA_R1	TTTCTCGAGCTCTAACGTCTTTAGCTTGTTCGCCAATTG	*sacy-1* cDNA 5' half RNAi
H27M09.1_cDNA_F2	TTTCCCGGGCAATTGGCGAACAAGCTAAAGACGTTAGAG	*sacy-1* cDNA 3' half RNAi
H27M09.1_cDNA_R2	TTTCTCGAGCAATGCTTGCGTCGTTTTGTTTCCGATTC	*sacy-1* cDNA 3' half RNAi
acy-1_Exon13_F	AAGGTGATGGAATACCTCCATCAATCAAGGATAACCAAGAAGACGAATTTATGAGTAAAGGAGAAGAACTTTTCAC	Recombineering for *acy-1::gfp*
acy-1_Exon13_R	TGTGAAAGGAATTATAGAAGTTTGTTTAAAGCAAAATGTATGAAAATTTATTTGTATAGTTCATCCATGCCATG	Recombineering for *acy-1::gfp*
acy-2_Exon17_F	CCGGCGAGCAACAAAACCATAGTAACAACAATAATTGTCACAGTACACTCATGAGTAAAGGAGAAGAACTTTTCAC	Recombineering for *acy-2::gfp*
acy-2_Exon17_R	GAGAGAAGGTGAATGCAGTTGAGAGGTAAAAATAACAGAACAACGAGTTATTTGTATAGTTCATCCATGCCATG	Recombineering for *acy-2::gfp*
acy-3_Exon14_F	ACAATTTCGGAGACTTTCAACTTTCAACATTTGATGATATTGATCAGGACATGAGTAAAGGAGAAGAACTTTTCAC	Recombineering for *acy-3::gfp*
acy-3_Exon14_R	AGACCTAGAGAATAGTAAGAAACATATATTTGAAAAAAATGAAATGATTATTTGTATAGTTCATCCATGCCATG	Recombineering for *acy-3::gfp*
twk-1_GalK_F2	AGGTTTCAGATTCAGAAGAAGCTGAAATTTGGTTTGGAGGGCAAATGATGCCTGTTGACAATTAATCATCGGCATAG	Recombineering for *galk* insertion in threonine284 of *twk-1*
twk-1_GalK_R2	TCCGGCGTTGATCCAAACTTTTCAGCCACCAAAGTGACCAAATCCTTGACTCAGCACTGTCCTGCTCCTTG	Recombineering for *galk* insertion in threonine284 of *twk-1*
twk-1_C-ter_trunc	AGGTTTCAGATTCAGAAGAAGCTGAAATTTGGTTTGGAGGGCAAATGATGATGAGTAAAGGAGAAGAACTTTTCACTGGAGTTG	Recombineering for C-terminal deletion of *twk-1*

	TCCCAATTCTTGTTGA	
KIN-1R 50bp	AATCAACAGTGATGCAACATTCACAAAAAAAAGTTACCGAAA CTCTGTGG	Recombineering for extending *kin-1* promoter in the WRM069aA02 fosmid
KIN-1OF 50bp	TAAGTTGGGTAACGCCAGGGTTTTCCCAGTCACGACGTTGTA AAACGACGAGAGACACTGCTCCTGGAGAGTCAC	Recombineering for extending *kin-1* promoter in the WRM069aA02 fosmid
kin-1 galk F	TAAGTTGGGTAACGCCAGGGTTTTCCCAGTCACGACGTTGTA AAACGACGCCTGTTGACAATTAATCATCGGCA	Recombineering for *galk* insertion into the WRM069aA02 fosmid
kin-1 galk R	AATCAACAGTGATGCAACATTCACAAAAAAAAGTTACCGAAA CTCTGTGGTCAGCACTGTCCTGCTCCTT	Recombineering for *galk* insertion into the WRM069aA02 fosmid
H27M09.1_gfpF1	TTTTAAGTATCTTAAAAAGTAGAACAGAAAAATTCGTTTAGTA TTCCGAAATGAGTAAAGGAGAAGAACTTTTCACTG	Recombineering for *gfp::sacy-1*
H27M09.1_gfpR1	CGCCGGCGGTCCTCATATTTTCGTCGCGCCGCTTCCACATCTG TGCTCATTTTGTATAGTTCATCCATGCCATGTG	Recombineering for *gfp::sacy-1*
twk-1_GFP_F1	AAGCTCATCGGGTACACAGTGATGGTCGACTTTTACTGCAACA AGATGTGATGAGTAAAGGAGAAGAACTTTTCACTG	Recombineering for *twk-1::gfp*
twk-1_GFP_R1	ATATCCGTTTCTTTTTTTGTTTCGAAAAATCTAAAATTGCAGAA TATCTATTTGTATAGTTCATCCATGCCATGTG	Recombineering for *twk-1::gfp*
twk-1_F1	GACAAATAATGAAGCATCCTTCTTGGATAG	*twk-1* RT-PCR
twk-1_R1	GTGACCAAATCCTTGACAGTCATCATTTG	*twk-1* RT-PCR

Table S4 *pbrm-1* is not a Sacy mutation

Genotype	Brood size (± SD)	Number of animals scored
acy-4(ok1806)	1 (± 2)	30
pbrm-1(gk1195)[a]	102 (± 86)	30
pbrm-1(gk1195); acy-4(ok1806)	0 (± 2)	35
sacy-1(tn1385); acy-4(ok1806)	14 (± 15)	39
sacy-1(tn1385) pbrm-1(tn1475)[b]*; acy-4(ok1806)*	23[c] (± 18)	30
sacy-1(tn1440); acy-4(ok1806)	20 (± 19)	39
sacy-1(tn1440) pbrm-1(tn1476)[d]*; acy-4(ok1806)*	12[e] (± 11)	30

[a]VC10166 [*pbrm-1(gk1195) I; octr-1(gk1196) X*] strain was used. *pbrm-1(gk1195)* deletes 126 nucleotides, including an intron and part of exon 6 of the *pbrm-1a* gene isoform.

[b]*pbrm-1(tn1475)* induces a missense mutation (A1182T) in the *pbrm-1a* gene isoform.

[c]P=0.025 compared to *sacy-1(tn1385); acy-4(ok1806)*.

[d]*pbrm-1(tn1476)* induces a missense mutation (A157T) in the *pbrm-1a* gene isoform.

[e]P=0.048 compared to *sacy-1(tn1440); acy-4(ok1806)*.

Student's *t*-test was used for statistical analysis.

Table S5 *pde-6* negatively regulates oocyte meiotic progression

A. *pde-6(tn1237)* is epistatic to *gsa-1(pk75)* for oocyte meiotic maturation

Genotype	Fertile gonad arms/Total
gsa-1(pk75)	0/9
gsa-1(pk75); pde-6(tn1237)	5/6

Genetic mosaics in which the sheath/spermathecal lineages were mutant for *gsa-1* were sought using *tnEx31[gsa-1(+) sur-5::gfp]* for mosaic analysis (Govindan et al., 2009).

B. *pde-6(tn1237)* extends AIR-2::GFP to oocyte chromatin in a hermaphrodite background

Genotype	Chromatin localization of AIR-2::GFP Oocyte position in the gonad arm				
	–1	–2	–3	–4	–5
Wild type (n=72)	95.8%	32%	1.4%	0%	0%
pde-6(tn1237) (n=35)	100%	97.1%	70.6%	10.3%	0%

Strains were homozygous for *itIs14*, which expresses AIR-2::GFP in the germ line. MSP and $G\alpha_s$-ACY-4 signaling promotes the localization of AIR-2::GFP to oocyte chromatin (Govindan et al., 2009). The control data were published (Govindan et al., 2009), and the *pde-6* data were from a contemporaneous experiment.

Table S6 Genetic analysis of *twk-1(lf)* for meiotic maturation and Unc phenotypes

A. *twk-1(lf)* suppresses *acy-4(lf)* sterility

Genotype	Brood size (± SD)	Number of animals scored
acy-4(ok1806)	1 (± 2)	30
twk-1(tn1397); acy-4(ok1806)	36 (± 25)	36
twk-1(tn1397); acy-4(ok1806); tnEx180[a]	2[*] (± 7)	46
twk-1(tn1397); acy-4(ok1806); tnEx181[b]	1[*] (± 1)	40

[a]*tnEx180[twk-1(+) sur-5::gfp]*. *tnEx180* itself does not reduce brood size because *twk-1(tn1397); acy-4(ok1806)/nT1[qIs51]; tnEx180* hermaphrodites have 267 ± 36 (n=25) progeny.

[b]*tnEx181[twk-1::gfp str-1::gfp]*. *twk-1(tn1397); acy-4(ok1806)/+* animals bearing *tnEx180* or *tnEx181* are not Unc, indicating rescue of the *twk-1* adult-onset Unc phenotype.

[*]P<0.00001 compared to *twk-1(tn1397); acy-4(ok1806)* using Student's *t*-test.

B. The adult-onset Unc phenotype of *twk-1(tn1397)* requires *acy-4(+)*

Genotype	Percentage of Unc animals[a]	Number of animals scored
Wild type	0	152
twk-1(tn1397)	76	106
twk-1(tn1397); tnEx180[b]	0	126
twk-1(tn1397); acy-4(ok1806)	0	93
twk-1(tn1397); acy-4(ok1806); tnEx37[c]	93	94

[a]L4 hermaphrodites were transferred to new NGM plates and observed approximately 24 hrs later for the *twk-1(tn1397)* Unc phenotype. All L4s tested did not show the Unc phenotype at the time of picking.

[b]*tnEx180[twk-1(+) sur-5::gfp]*.

[c]*tnEx37[acy-4(+) sur-5::gfp]*.

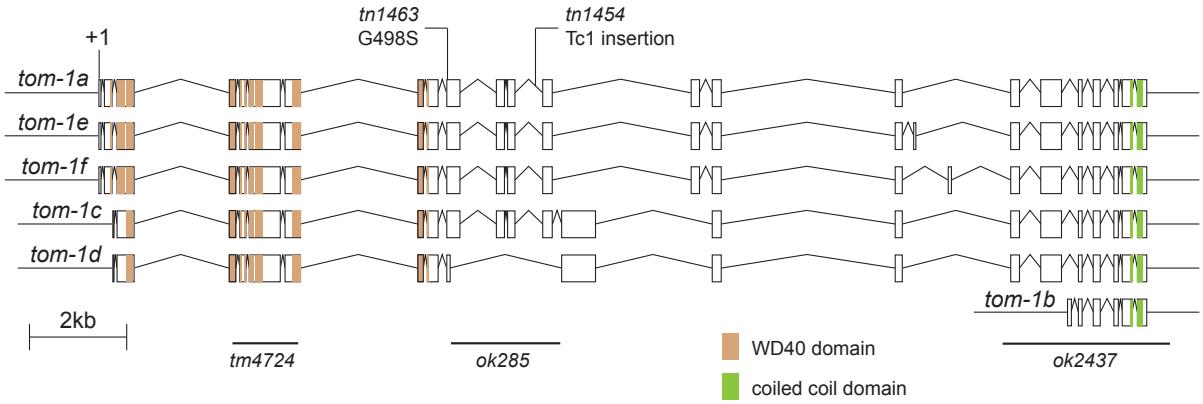

Figure S1 Location of Sacy alleles of *tom-1*. Each *tom-1* gene isoform is depicted. The start codon (+1) of the *tom-1a* gene isoform is indicated. Newly identified *tom-1 tn* alleles and the corresponding amino acid changes are shown. Deletion alleles are underlined. Apparently, *tom-1* is a complex locus and only *ok2437*, *tn1463*, and *tn1454* suppress *acy-4(lf)* sterility–the *tom-1* isoform(s) relevant to this observation are unclear.

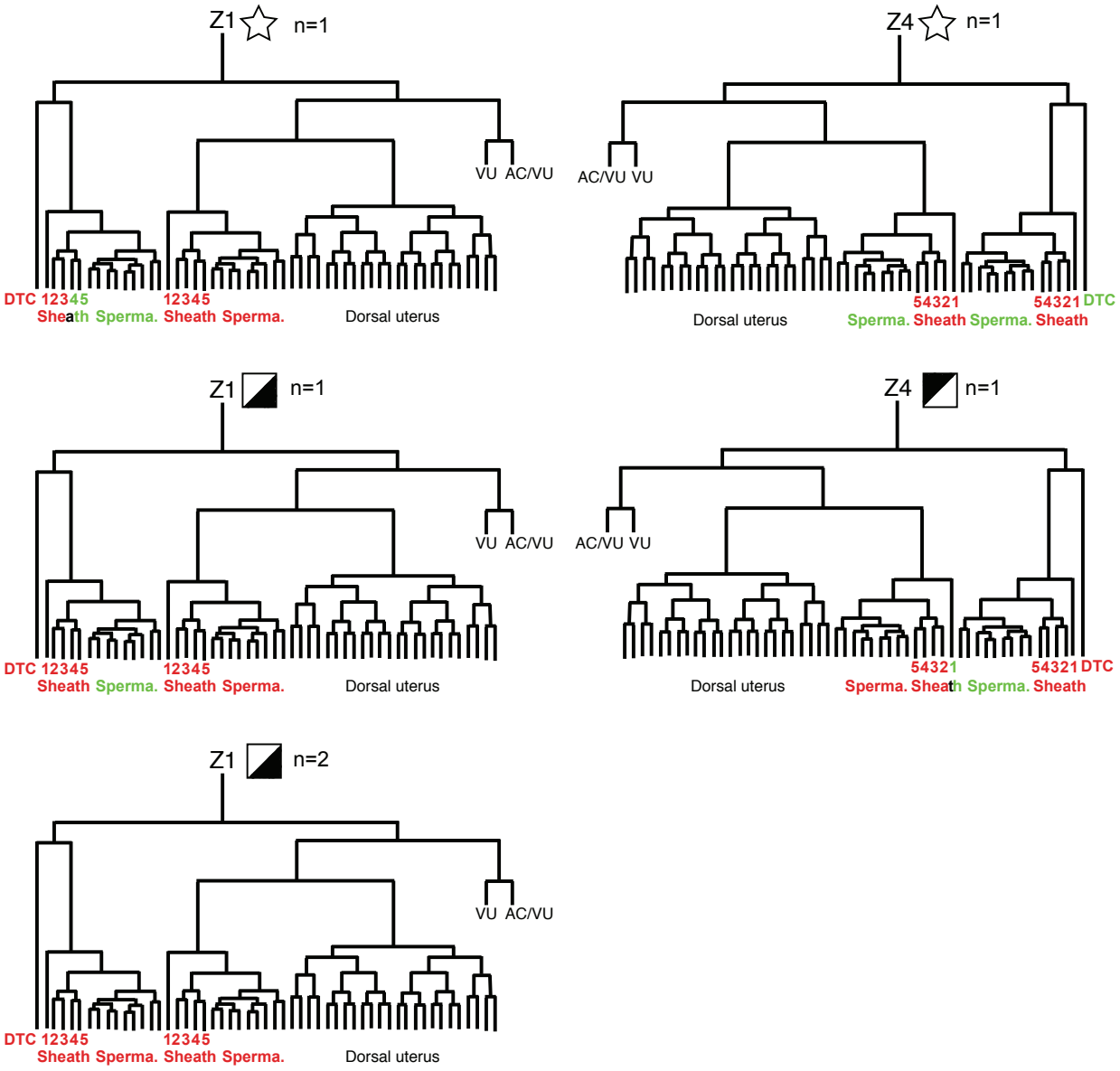

Figure S2 *kin-1* genetic mosaics with complex losses within the somatic gonadal cell lineages. Genetic-mosaic animals with complex losses of the *kin-1(+)* array in the somatic gonad (see Figure 1 in the main text) are described in more detail. Green characters represent the presence of the *kin-1(+)* array and red characters represent the absence of the *kin-1(+)* array. Uterine cells were not scored. One sterile genetic mosaic animal (star) resulted from multiple independent losses within both the Z1 and Z4 lineages. This animal is consistent with a requirement for *kin-1(+)* function in the gonadal sheath cells for meiotic maturation.

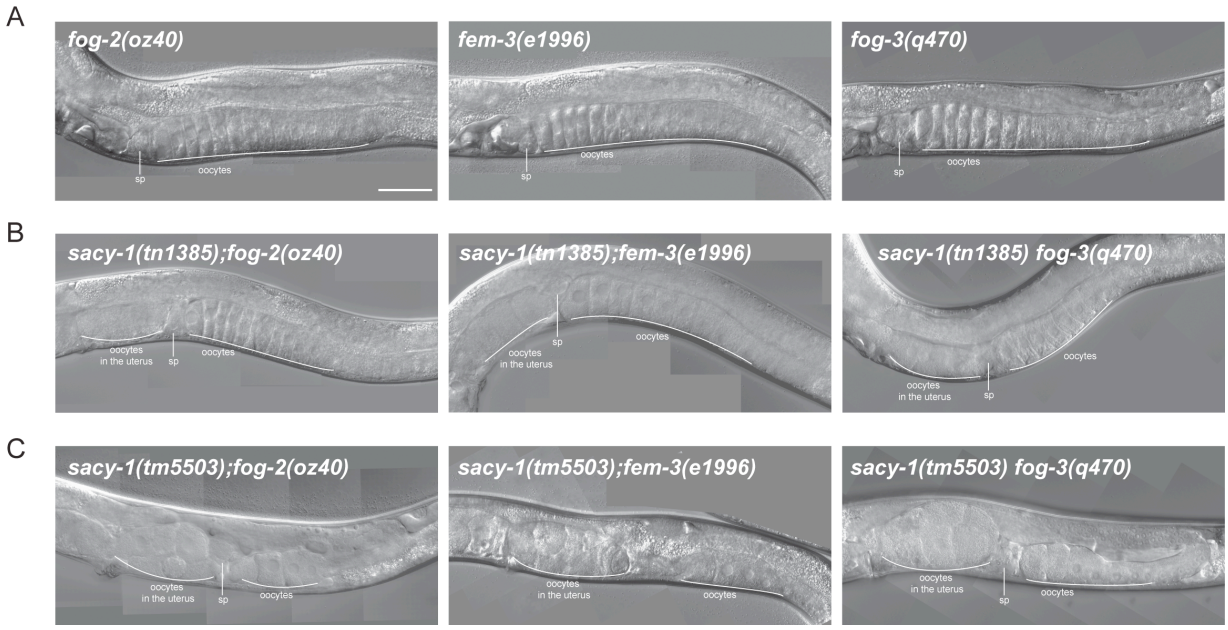

Figure S3 *sacy-1* is a negative regulator of oocyte meiotic maturation in the absence of sperm. (A) Control female mutants. Oocytes are stacked within the gonad arm and the uterus is empty. Spermatheca (sp). (B) *sacy-1(tn1385)* inhibits oocyte meiotic maturation in the absence of sperm. Oocytes undergo maturation and ovulation at an increased frequency and are observed in the uterus despite the absence of sperm. A similar phenotype was observed in *fog-1(e2121) sacy-1(tn1385)* females (S. Kim and D. Greenstein, unpublished results). (C) *sacy-1(tm5503)* is a strong negative regulator of oocyte meiotic maturation in the absence of sperm. Many unfertilized oocytes are observed in the uterus of *sacy-1(tm5503)* females, suggesting that *sacy-1* inhibits oocyte meiotic maturation in the absence of sperm. The frequent occurrence of defective ovulation in *sacy-1(tm5503)* females prevented us from directly measuring meiotic maturation rates. *fog-1(e2121) sacy-1(tm5503)* females exhibit a similar phenotype (S. Kim and D. Greenstein, unpublished results). All images were obtained from day-1 adults (24 hr post-L4) examined by DIC microscopy. *fog-3(q470)* and *sacy-1(tm5503) fog-3(q470)* images were duplicated from Figure 8 for comparison. Scale bar, 50 μm.

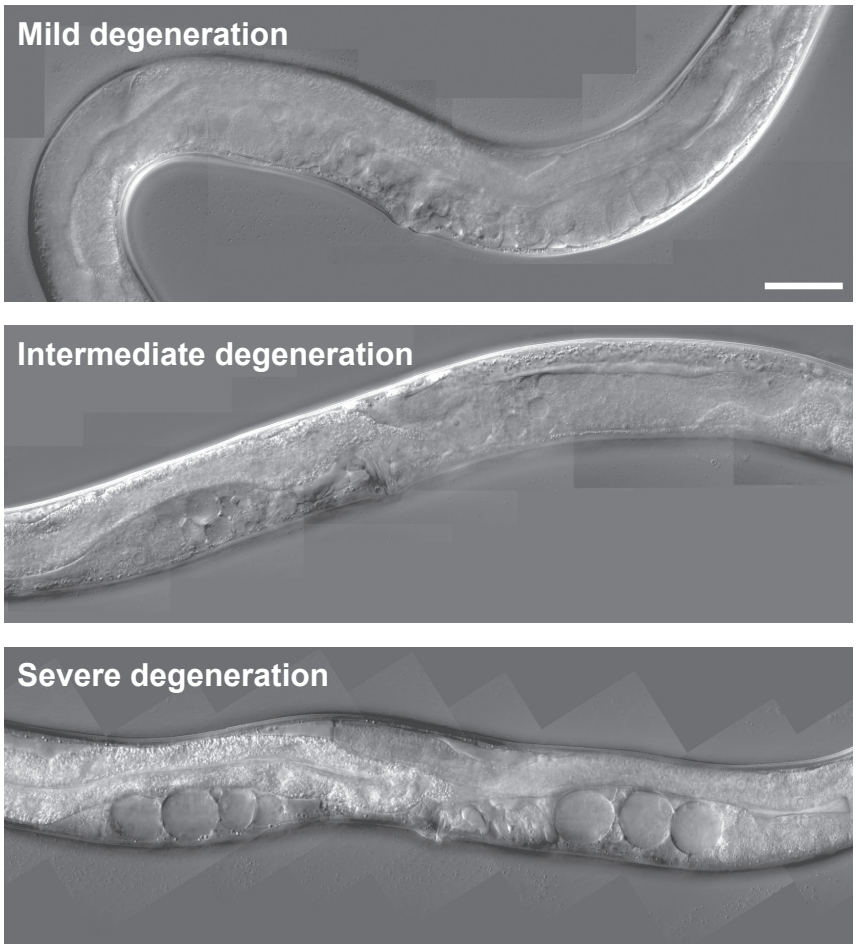

Figure S4 Representative DIC images of day-1 adults illustrating the qualitative scoring criteria used to evaluate the severity of the gamete degeneration phenotype of *sacy-1(tm5503)* hermaphrodites and females. Scale bar, 50 μm.

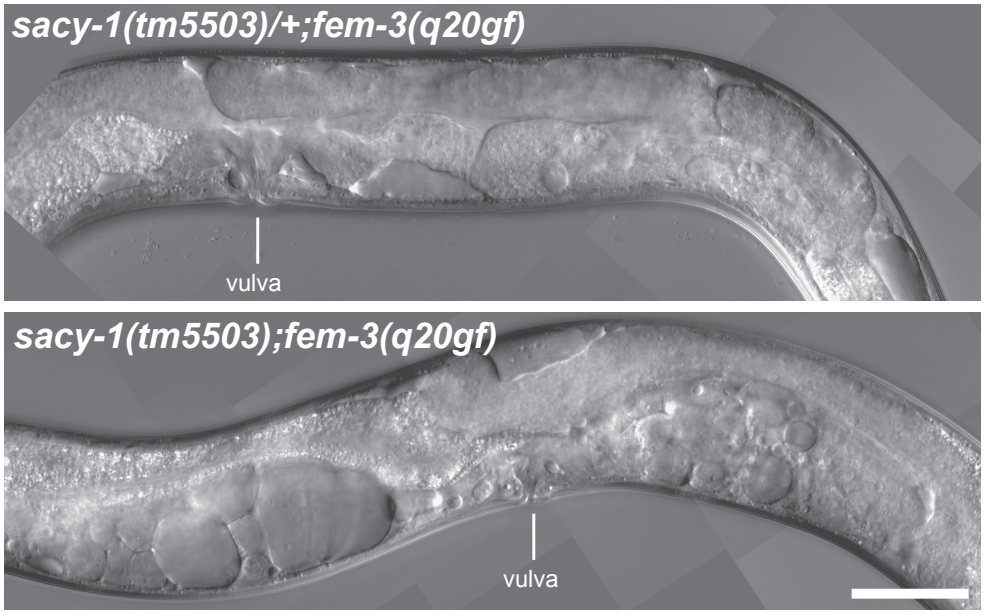

Figure S5 Masculinization of the hermaphrodite germ line does not suppress *sacy-1(tm5503)* gamete degeneration. A *sacy-1(tm5503); fem-3(q20gf)* hermaphrodite (bottom) exhibits the gamete degeneration phenotype. A *sacy-1(tm5503)/+; fem-3(q20gf)* hermaphrodite (top) produces excessive amounts of sperm. Scale bar, 50 μm.

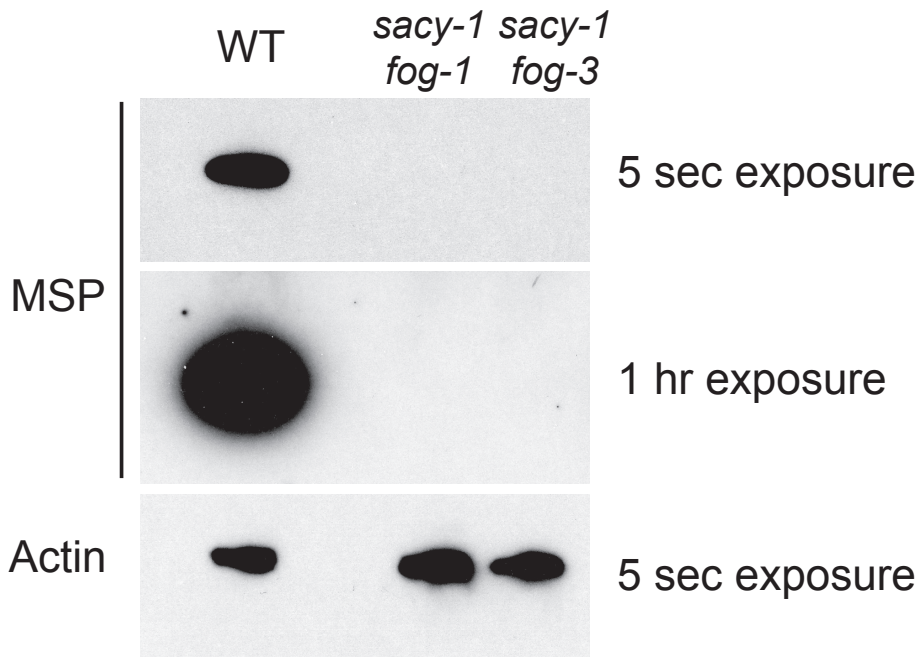

Figure S6 *sacy-1(tm5503)* females do not produce MSP. Western blot of MSP from wild-type (WT), *fog-1(e2121) sacy-1(tm5503)*, and *sacy-1(tm5503) fog-3(q470)* adults. Because oocyte meiotic maturation occurs frequently in *sacy-1(tm5503)* females despite the absence of MSP, *sacy-1* is a strong negative regulator of meiotic maturation. Ten animals of each genotype were lysed and immunoblotting was conducted using a rabbit C-terminal-specific anti-MSP antibody (C3196; 1:20,000) (Kosinski et al., 2005). Mouse anti-actin C4 antibody (Millipore; 1:20,000) served as a loading control.

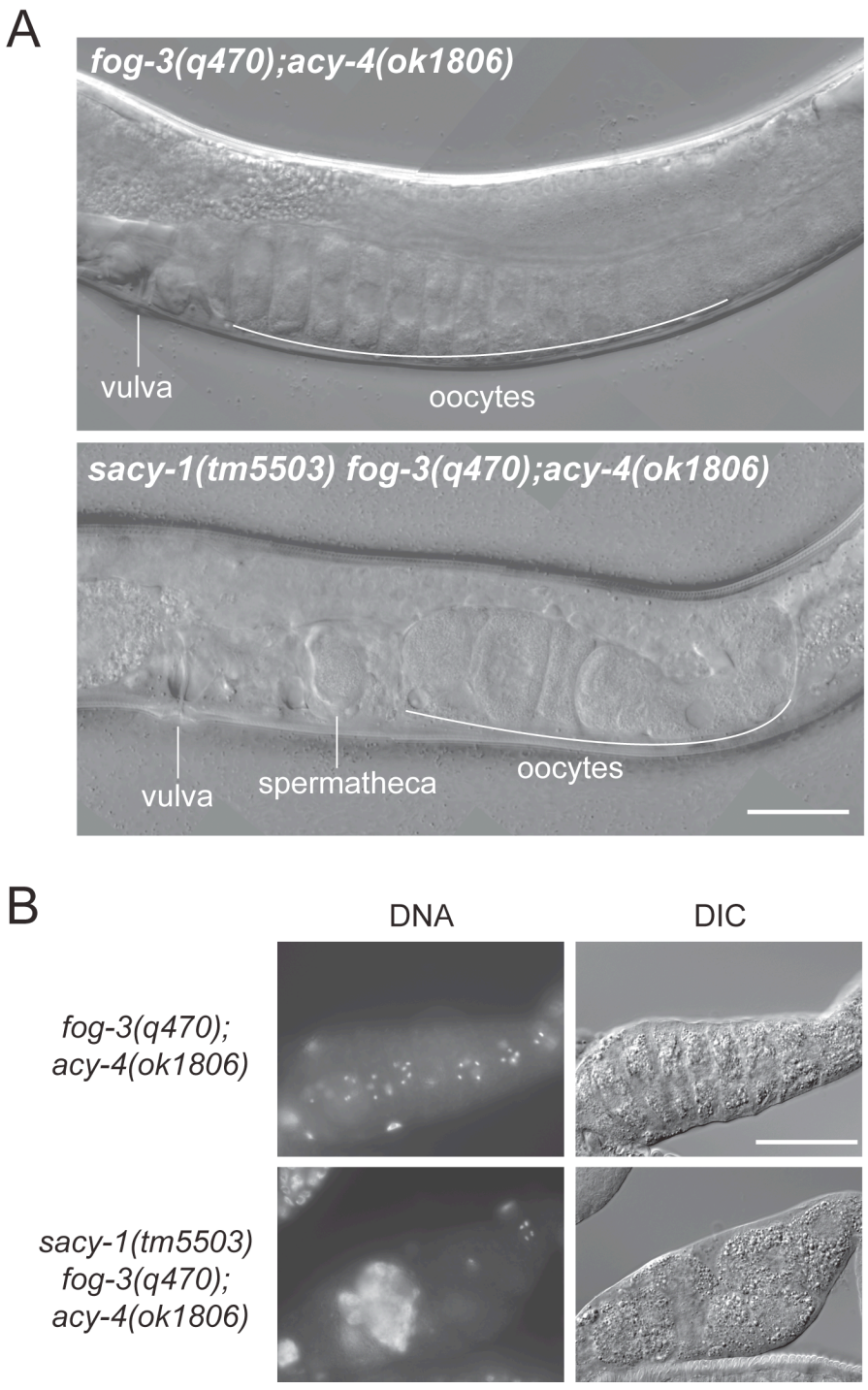

Figure S7 *sacy-1(tm5503)* is epistatic to *acy-4(ok1806)* for oocyte meiotic maturation. Oocyte meiotic maturation occurs frequently in *sacy-1(tm5503) fog-3(q470); acy-4(ok1806)* females, though ovulation often fails and endomitotic oocytes are observed in the gonad arm. In contrast, oocytes arrest in diakinesis in *fog-3(q470); acy-4(ok1806)* females. Day-1 adults were examined by DIC microscopy of living animals (A) and DNA was detected by DAPI staining of dissected and fixed gonads (B). Proximal is to the left side. Scale bar, 50 μm.

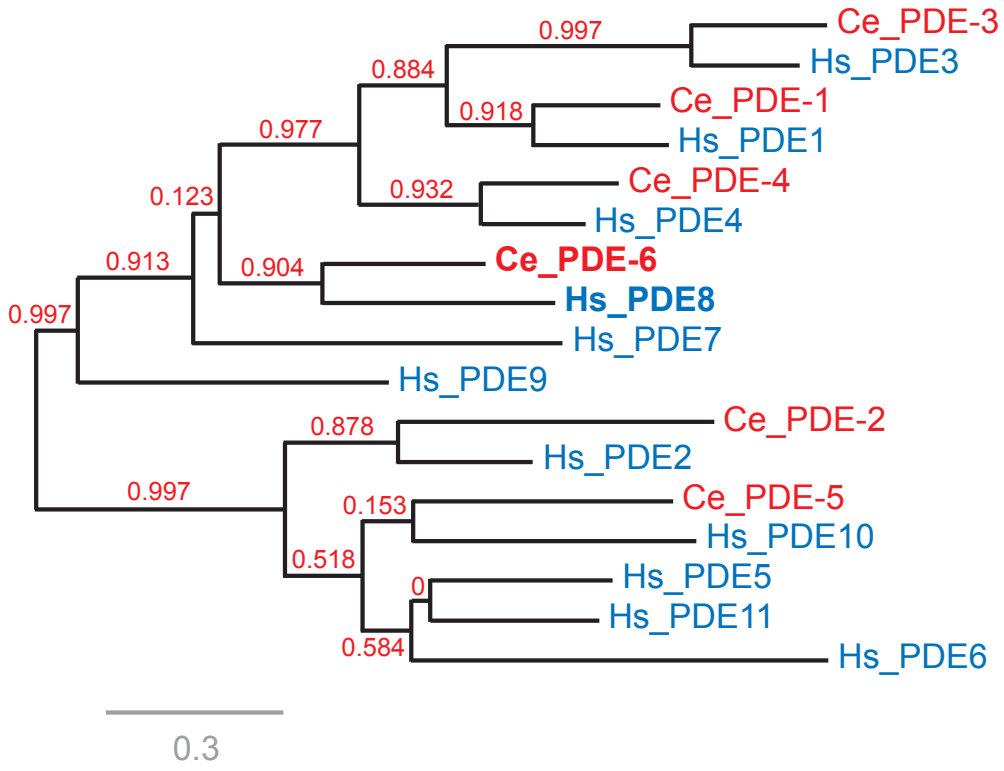

Figure S8 Phylogenetic comparison *C. elegans* and human phosphodiesterases. The likely human ortholog of *C. elegans* PDE-6 is PDE8, the high-affinity cAMP-specific phosphodiesterase. Red characters represent six *C. elegans* phosphodiesterases, and blue characters represent 11 human phosphodiesterases. The following amino acid sequences were used for the analysis; Ce_PDE-1 (NP_493343.1), Ce_PDE-2 (NP_001022705), Ce_PDE-3 (NP_871943.2), Ce_PDE-4 (NP_001040798.1), Ce_PDE-5 (NP_491544.2), Ce_PDE-6 (NP_490787.1), Hs_PDE1 (NP_000915.1), Hs_PDE2 (NP_002590.1), Hs_PDE3 (NP_000913.2), Hs_PDE4 (NP_001098101.1), Hs_PDE5 (NP_001074.2), Hs_PDE6 (NP_000274.2), Hs_PDE7 (NP_001229247.1), Hs_PDE8 (NP_001025024.1), Hs_PDE9 (NP_002597.1), Hs_PDE10 (NP_001124162.1), Hs_PDE11 (NP_058649.3).

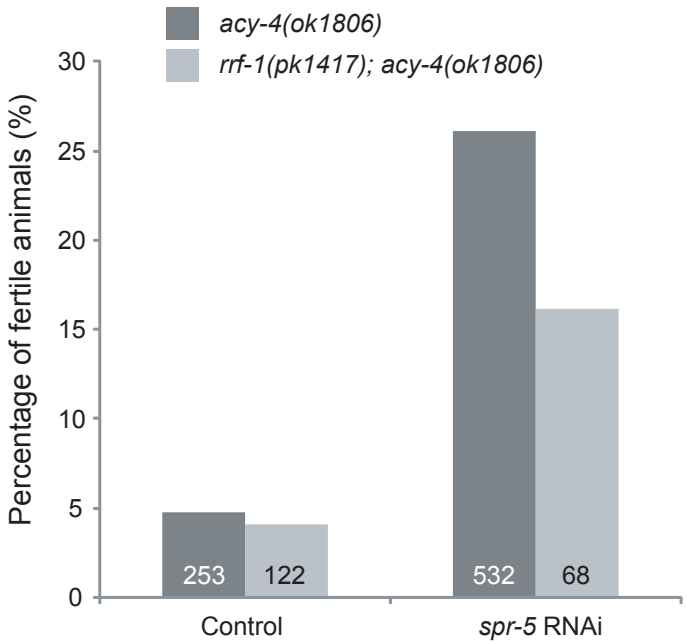

Figure S9 *spr-5* RNAi suppresses *acy-4(lf)* sterility. *spr-5* dsRNAs, or a buffer control, were injected into the gonad arms of *acy-4(ok1806); tnEx37[acy-4(+) sur-5::gfp]* or *rrf-1(pk1417); acy-4(ok1806); tnEx37[acy-4(+) sur-5::gfp]* adult hermaphrodites, and non-array-bearing F1 animals were scored by DIC microscopy for suppression of *acy-4(ok1806)* sterility. Fertile animals were defined as having more than two embryos in the spermathecae and/or uterus. The numbers of animals scored are indicated.

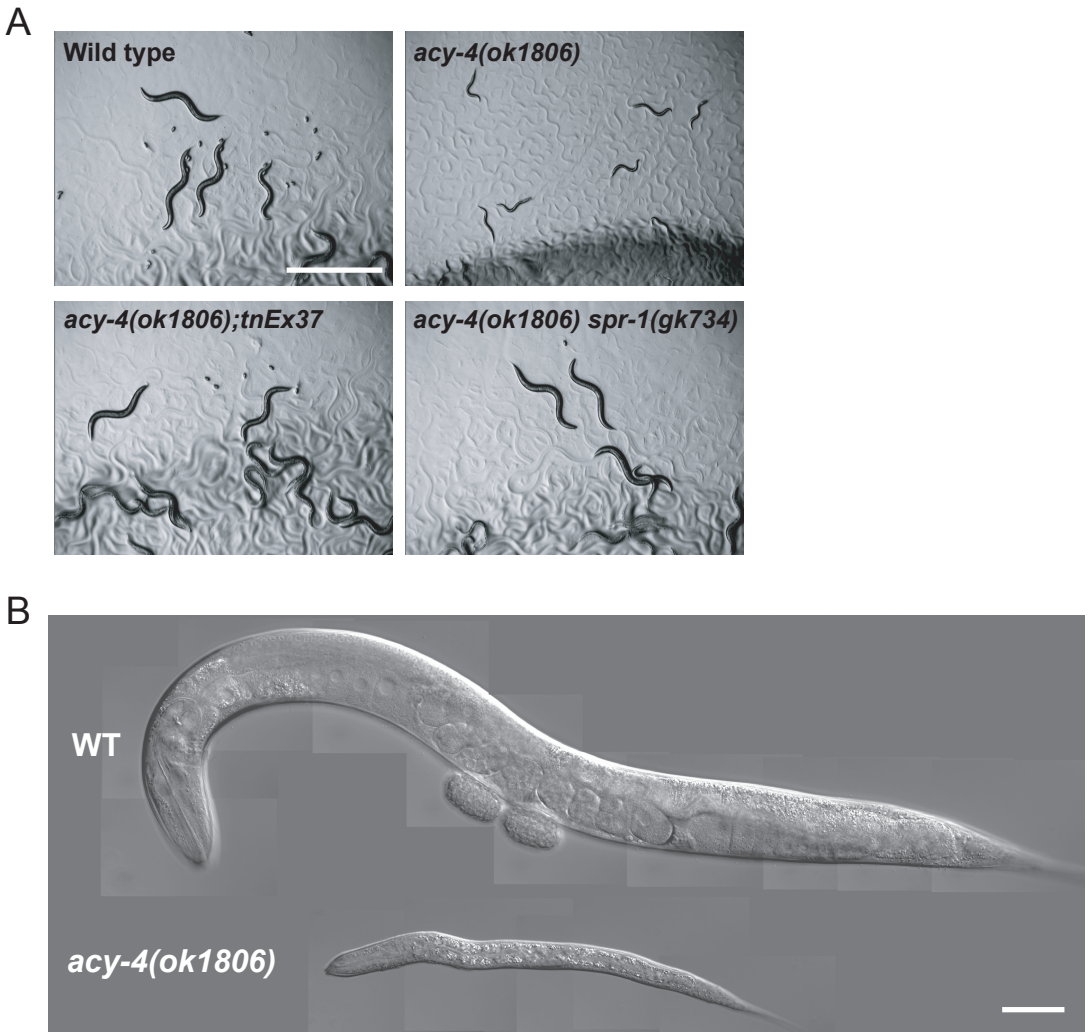

Figure S10 Growth defect of *acy-4(ok1806)* on HT115 bacteria. (A) *acy-4(ok1806)* animals exhibit larval lethality, larval arrest, or slow growth on standard NGM plates with *E. coli* HT115 as the food source. In contrast, wild-type, *acy-4(ok1806); tnEx37[acy-4(+) sur-5::gfp],* and *acy-4(ok1806) spr-1(gk734)* animals grow well with HT115 as the food source. Likewise, *spr-2, spr-4*, and *spr-5* mutations suppress the *acy-4(ok1806)* growth defect (not shown). Embryos isolated by bleach treatment were cultured on HT115-seeded plates for approximately 72 hrs. *acy-4(ok1806)* homozygotes were the GFP-negative progeny of array-bearing parents. Scale bar, 1 mm. (B) DIC images of wild type (WT) and *acy-4(ok1806)* animals grown on HT115-seeded medium for 72 hrs. Scale bar, 50 μm.

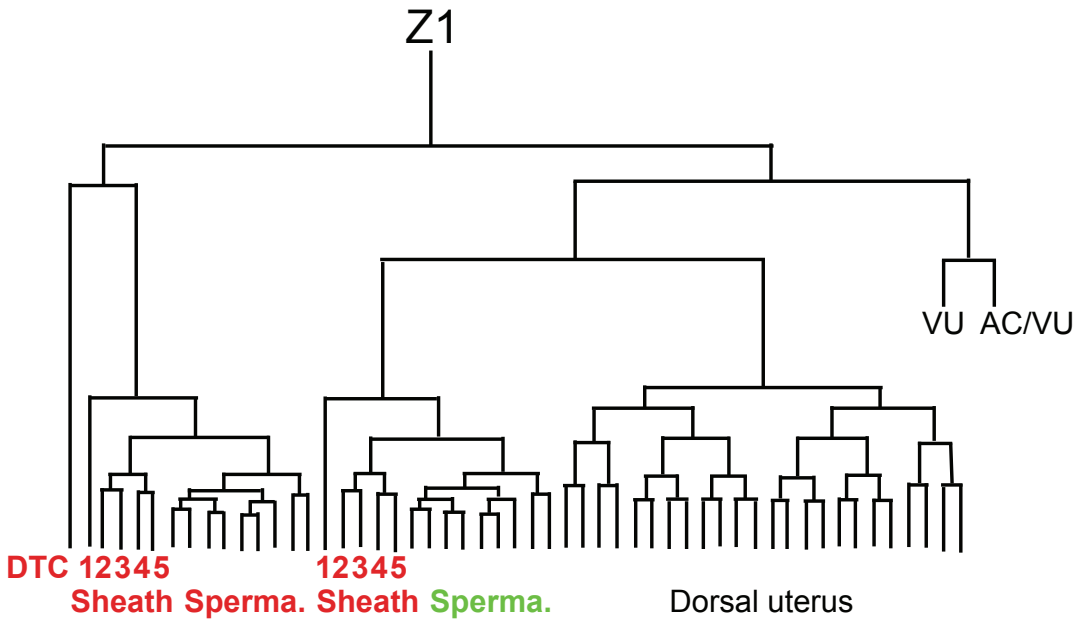

Figure S11 *twk-1* functions in the somatic gonad downstream of *acy-4*. A genetic mosaic animal resulting from multiple independent losses of the *twk-1(+)*-bearing extrachromosomal array in the anterior somatic gonadal lineage (Z1). This animal was fertile in the anterior arm, indicating suppression of *acy-4(lf)* sterility, but sterile in the posterior arm. Green characters represent the presence of the *twk-1(+)* array, and red characters represent the absence of the *twk-1(+)* array. Uterine cells were not scored.

A

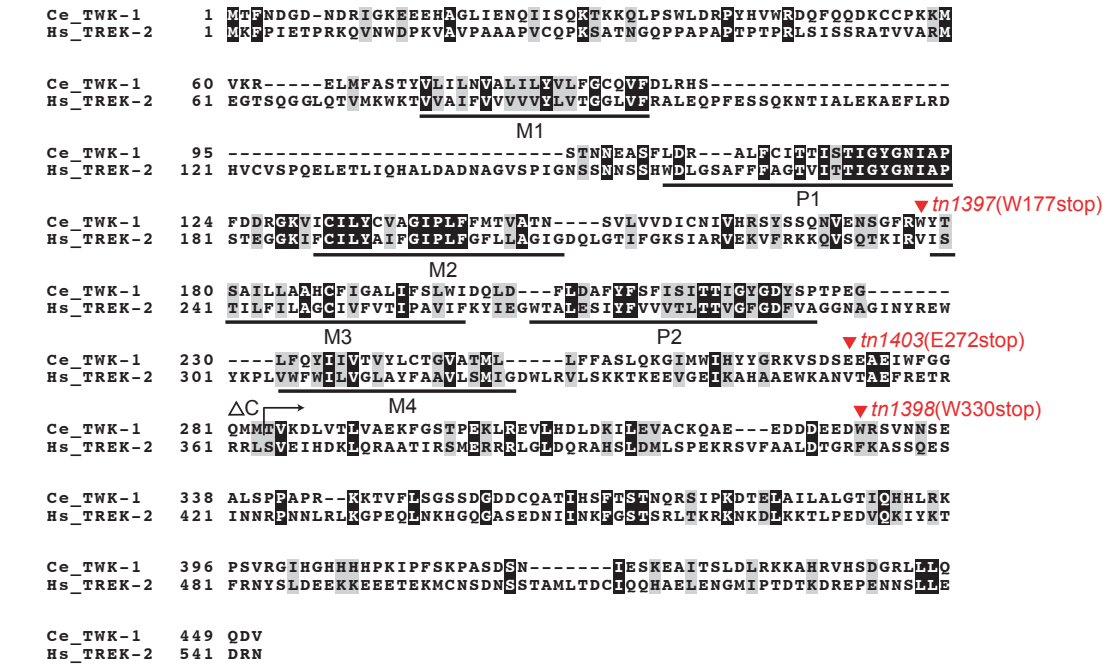

B

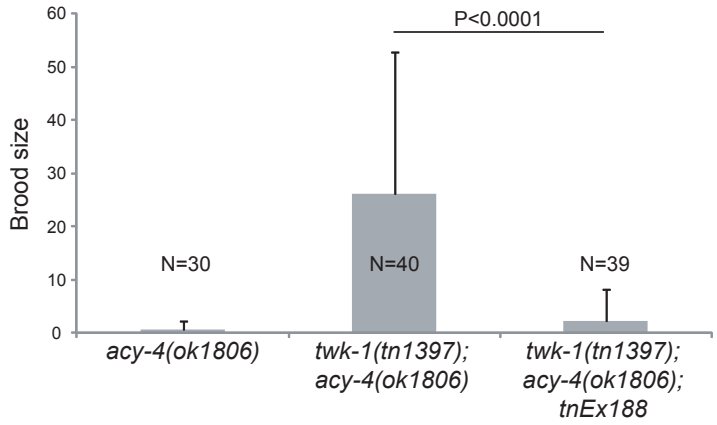

Figure S12 The TWK-1 C-terminus is not essential for function. (A) ClustalW alignment of *C. elegans* TWK-1 and human TREK-2 (NP_612190). Using RT-PCR, we found that the TWK-1 prediction (NP_492054.2) was incorrect in that a small predicted intron was found to be coding, resulting in an additional 14 amino acids. The RT-PCR data is in agreement with the gene prediction based on the FN890018 cDNA. We thank Bernard Lakowski for pointing out the discrepancy in the *twk-1* gene prediction. The four transmembrane domains (M1-M4) and two pore domains (P1 and P2) are underlined. The three *twk-1* nonsense mutations and the position of the ΔC284 deletion are indicated. TWK-1 exhibits less similarity to TREK-1 (not shown) in the C-terminal region because of the latter's smaller size. (B) The TWK-1DC284::GFP fusion (*tnEx188*) rescues *twk-1(tn1397)*. Error bars represent one standard deviation. Student's *t*-test was used for statistical analysis.

Table S1 Molecular identity of Sacy mutations in *tn* alleles

Gene	Allele	Nucleotide change	Amino acid change[a]
pde-6	*tn1237*	CAG -> **T**AG	Q668*
	tn1242	TGG -> TG**A**	W444*
	tn1336	TGG -> TG**A**	W664*
tom-1	*tn1454*	Tc1 insertion	
	tn1463	GGT -> **A**GT	G498S
sacy-1	*tn1385*	GGA -> **A**GA	G533R
	tn1391	GGA -> **A**GA	G473R
	tn1440	GGA -> **A**GA	G331R
twk-1	*tn1397*	TGG -> T**A**G	W177*
	tn1398	TGG -> TG**A**	W330*
	tn1403	GAA -> **T**AA	E272*
spr-4	*tn1383*	CGA -> **T**GA	R1230*
	tn1402	CGA -> **T**GA	R1230*
	tn1404	CAT -> **T**AT	H845Y
	tn1438	CGA -> **T**GA	R486*
	tn1444	CAG -> **T**AG	Q1128*
	tn1467	CAG -> **T**AG	Q45*
spr-5	*tn1378*	TGG -> T**A**G	W666*
	tn1379	GAG -> **A**AG	E164K
	tn1394	GGT -> G**A**T	G619D
uev-1	*tn1381*	GGA-> G**A**A	G17E
	tn1382	GGT -> G**A**T	G47D
spr-2	*tn1380*	GAT-> G**C**T	D42A
	tn1436	Tc1 insertion	

[a]Premature stop codons are indicated by asterisks. The numbering of amino acids refers to the isoforms PDE-6A, TOM-1A, SPR-4A, and SPR-2B.

Table S2 ***C. elegans*** **strains used for this study**

Strain	Genotype
N2	Wild type, Bristol isolate
CB4856	Hawaiian isolate
DG2730	*tnIr1[N2=>CB4856, acy-4(ok1806)]* V; *tnEx37[acy-4(+) sur-5::gfp]*
DG3051	*tnEx131[acy-1::gfp rol-6(su1006d)]*
DG3064	*tnEx133[acy-2::gfp rol-6(su1006d)]*
DG3066	*tnEx134[acy-3::gfp rol-6(su1006d)]*
DG3395	*tnEx175[twk-1::gfp rol-6(su1006d)]*
DG3441	*tnEx181[twk-1::gfp str-1::gfp]*
DG3521	*fog-1(e2121) sacy-1(tm5503)* I/*hT2[bli-4(e937) let-?(q782) qIs48]* (I;III)
DG3524	*fog-1(e2121) sacy-1(tn1385)* I/*hT2[bli-4(e937) let-?(q782) qIs48]* (I;III)
DG3585	*fog-3(q470)* I/*hT2[bli-4(e937) let-?(q782) qIs48]* (I;III); *acy-4(ok1806)* V; *tnEx37*
DG3186	*gsa-1(pk75)* I/*hT2[bli-4(e937) let-?(q782) qIs48]* (I;III); *fog-2(oz40)* V
DG3393	*kin-1(ok338)* I; *tnEx109[kin-1(+) sur-5::gfp]*
DG3360	*pbrm-1(gk1195)* I; *acy-4(ok1806)* V; *tnEx37*
VC10166	*pbrm-1(gk1195)* I; *octr-1(gk1196)* X
DG2292	*pde-6(tn1237)* I
DG2397	*pde-6(tn1237)* I; *unc-46(e177) acy-4(ok1806)* V
DG2096	*pde-6(tn1242)* I
DG2454	*pde-6(tn1242)* I; *unc-46(e177) acy-4(ok1806)* V
DG2111	*pde-6(tn1336)* I
DG2834	*rrf-1(pk1417)* I; *acy-4(ok1806)* V; *tnEx37*
DG3606	*rrf-1(pk1417)* I; *fog-2(oz40)* V
DG3544	*sacy-1(tm5503) fog-3(q470)* I/*hT2[bli-4(e937) let-?(q782) qIs48]* (I;III)
DG3589	*sacy-1(tm5503) fog-3(q470)* I/*hT2[bli-4(e937) let-?(q782) qIs48]* (I;III); *acy-4(ok1806)* V; *tnEx37*
DG3557	*sacy-1(tm5503) fog-3(q470)/unc-13(e1091) lin-11(n566)* I; *oma-1(zu405te33)* IV/*nT1[qIs51]* (IV;V); *oma-2(te51)* V/*nT1[qIs51]* (IV;V)
DG3492	*sacy-1(tm5503)* I/*hT2[bli-4(e937) let-?(q782) qIs48]* (I;III)
DG3587	*sacy-1(tm5503)* I/*hT2[bli-4(e937) let-?(q782) qIs48]* (I;III); *acy-4(ok1806)* V; *tnEx37*
DG3514	*sacy-1(tm5503)* I/*hT2[bli-4(e937) let-?(q782) qIs48]* (I;III); *ced-3(n717)* IV
DG3566	*sacy-1(tm5503)* I/*hT2[bli-4(e937) let-?(q782) qIs48]* (I;III); *ced-4(n1162)* III/*hT2[bli-4(e937) let-?(q782) qIs48]* (I;III)
DG3528	*sacy-1(tm5503)* I/*hT2[bli-4(e937) let-?(q782) qIs48]* (I;III); *fem-3(e1996)/unc-24(e138) dpy-20(e1282)* V
DG3570	*sacy-1(tm5503)* I/*hT2[bli-4(e937) let-?(q782) qIs48]* (I;III); *fem-3(q20gf)* V
DG3505	*sacy-1(tm5503)* I/*hT2[bli-4(e937) let-?(q782) qIs48]* (I;III); *fog-2(oz40)* V
DG3512	*sacy-1(tm5503)* I/*hT2[bli-4(e937) let-?(q782) qIs48]* (I;III); *fog-2(q71)* V
DG3486	*sacy-1(tm5503)* I/*hT2[bli-4(e937) let-?(q782) qIs48]* (I;III); *him-8(tm611)* IV
DG3561	*sacy-1(tm5503) I/hT2[bli-4(e937) let-?(q782) qIs48] (I;III); unc-24(e138) IV*

DG3560	*sacy-1(tm5503) I/hT2[bli-4(e937) let-?(q782) qIs48] (I;III); unc-32(e189) III/hT2[bli-4(e937) let-?(q782) qIs48] (I;III)*
DG3571	*sacy-1(tm5503) I/hT2[bli-4(e937) let-?(q782) qIs48] (I;III); unc-33(mn407) IV*
DG3547	*sacy-1(tm5503) I/hT2[bli-4(e937) let-?(q782) qIs48] (I;III); unc-68(e540) V*
DG3485	*sacy-1(tm5503) I; tnEx159[gfp::sacy-1 unc-119(+)]*
DG3611	*sacy-1(tm5503) I; unc-119(ed3) III; tnEx159[gfp::sacy-1 unc-119(+)]*
DG3520	*sacy-1(tm5503)/unc-13(e1091) lin-11(n566) I; fem-3(e1996) V/nT1[qIs51] (IV;V)*
DG3539	*sacy-1(tm5503)/unc-13(e1091) lin-11(n566) I; oma-1(zu405te33) IV/nT1[qIs51] (IV;V); oma-2(te51) V/nT1[qIs51] (IV;V)*
DG3543	*sacy-1(tn1385) fog-3(q470) I/hT2[bli-4(e937) let-?(q782) qIs48] (I;III)*
DG3430	*sacy-1(tn1385) I*
DG3373	*sacy-1(tn1385) I; acy-4(ok1806) V*
DG3542	*sacy-1(tn1385) I; fem-3(e1996) IV/nT1[qIs51] (IV;V)*
DG3449	*sacy-1(tn1385) I; fog-2(oz40) V*
DG3460	*sacy-1(tn1385) I; fog-2(q71) V*
DG3453	*sacy-1(tn1385) kin-1(ok338) I; tnEx109*
DG3070	*sacy-1(tn1385) pbrm-1(tn1475) I; acy-4(ok1806) V*
DG3254	*sacy-1(tn1385) pbrm-1(tn1475) I; acy-4(ok1806) V; tnEx37*
DG3249	*sacy-1(tn1391) I*
DG3060	*sacy-1(tn1391) I; acy-4(ok1806) V*
DG3414	*sacy-1(tn1391) I; fog-2(oz40) V*
DG3461	*sacy-1(tn1391) I; fog-2(q71) V*
DG3314	*sacy-1(tn1391) I; unc-119(ed3) III; acy-4(ok1806) V; tnEx37; tnEx159*
DG3431	*sacy-1(tn1440) I*
DG3362	*sacy-1(tn1440) I; acy-4(ok1806) V*
DG3478	*sacy-1(tn1440) I; fog-2(oz40) V*
DG3450	*sacy-1(tn1440) I; fog-2(q71) V*
DG3115	*sacy-1(tn1440) pbrm-1(tn1476) I; acy-4(ok1806) V*
DG3256	*sacy-1(tn1440) pbrm-1(tn1476) I; acy-4(ok1806) V; tnEx37*
DG3458	*sacy-1(tn1440) spr-5(by134) I; acy-4(ok1806) V*
DG2964	*spr-4(by105) I; acy-4(ok1806) V*
DG3073	*spr-4(tn1383) I; acy-4(ok1806) V*
DG3074	*spr-4(tn1402) I; acy-4(ok1806) V*
DG3107	*spr-4(tn1404) I; acy-4(ok1806) V*
DG3108	*spr-4(tn1438) I; acy-4(ok1806) V*
DG3109	*spr-4(tn1444) I; acy-4(ok1806) V*
DG3110	*spr-4(tn1467) I; acy-4(ok1806) V*
DG2942	*spr-5(ar197) I; acy-4(ok1806) V*
DG2941	*spr-5(by134) I; acy-4(ok1806) V*

DG3185	*spr-5(by134) I; fog-2(oz40) V*
DG3122	*spr-5(by134) kin-1(ok338) I; tnEx109*
DG2553	*spr-5(tn1378) I; acy-4(ok1806) V*
DG2564	*spr-5(tn1379) I; acy-4(ok1806) V*
DG2522	*spr-5(tn1394) I; acy-4(ok1806) V*
NM1815	*tom-1(ok188)*
DG3192	*tom-1(ok188) I; acy-4(ok1806) V; tnEx37*
RB1887	*tom-1(ok2437) I*
DG3079	*tom-1(ok2437) I; acy-4(ok1806) V*
VC223	*tom-1(ok285) I*
DG3217	*tom-1(ok285) I; acy-4(ok1806) V; tnEx37*
FX04724	*tom-1(tm4724) I*
DG3245	*tom-1(tm4724) I; acy-4(ok1806) V; tnEx37*
DG3118	*tom-1(tn1454) I; acy-4(ok1806) V*
DG3097	*tom-1(tn1463) I; acy-4(ok1806) V*
DG3408	*twk-1(tn1397) I*
DG3095	*twk-1(tn1397) I; acy-4(ok1806) V*
DG3447	*twk-1(tn1397) I; acy-4(ok1806) V/nT1[qIs51] (IV;V); tnEx180[twk-1(+) sur-5::gfp]*
DG3490	*twk-1(tn1397) I; acy-4(ok1806) V/nT1[qIs51] (IV;V); tnEx188[twk-1(ΔC284)::gfp str-1::gfp]*
DG3451	*twk-1(tn1397) kin-1(ok338) I; tnEx109*
DG3389	*twk-1(tn1398) I*
DG3083	*twk-1(tn1398) I; acy-4(ok1806) V*
DG3390	*twk-1(tn1403) I*
DG3113	*twk-1(tn1403) I; acy-4(ok1806) V*
DG3459	*twk-1(tn1403) spr-5(by134) I; acy-4(ok1806) V*
RB1976	*uev-1(ok2610) I*
DG3409	*uev-1(ok2610) I; acy-4(ok1806) V*
DG3076	*uev-1(tn1381) I; acy-4(ok1806) V*
DG3080	*uev-1(tn1382) I; acy-4(ok1806) V*
CB3778	*tra-2(e2020) II*
CB3843	*fem-3(e1996)/unc-24(e138) dpy-20(e1282) IV*
CA257	*him-8(tm611) IV*
DG2836	*spr-2(ar199) dpy-20(e1282) IV; acy-4(ok1806) V; tnEx37*
DG2943	*spr-2(ar211) dpy-20(e1282)* IV; *acy-4(ok1806)* V
DG3136	*spr-2(tm4802)* IV; *acy-4(ok1806)* V
DG2558	*spr-2(tn1380)* IV; *acy-4(ok1806)* V
DG2592	*spr-2(tn1436)* IV; *acy-4(ok1806)* V
DG3612	*acy-4(ok1806) spr-1(gk734)* V
DG3604	*acy-4(ok1806) unc-23(e25)* V; *tnEx37*

DG3145	*acy-4(ok1806)* V; *spr-3(by108)* X
DG3129	*acy-4(ok1806)* V; *spr-3(ok2525)* X
DG3391	*acy-4(ok1806)* V; *tnEx37*
BS553	*fog-2(oz40)* V
CB4108	*fog-2(q71)* V

Table S3 Primers used for this study

Name	Sequence	Use
ok1806F1	CGGGTTGATGAATCTTGTATCATTCTC	*acy-4(ok1806)* genotyping
ok1806R1	CATGATACAAGCATTGTCACGAGACTC	*acy-4(ok1806)* genotyping
ok1806F2	TCAGTCTCGTCATTGGTGTTCTGTTC	*acy-4(ok1806)* genotyping
gk1195_F1	TTCATCTGAATGGCCATTCACTCTTGATC	*pbrm-1(gk1195)* genotyping
gk1195_F2	TTTCAGGAAAGCGAAGTCGAAATGGAAG	*pbrm-1(gk1195)* genotyping
gk1195_R1	CTCTTTGTATACTCCAATTCCTCGTCTTC	*pbrm-1(gk1195)* genotyping
H27M09.1_F5	ACTGCTGGAAGATATATCACTTATCGTC	*sacy-1(tm5503)* genotyping
tm5503_F1	GTTATTGACGAATCAGAACGGCAATTAATG	*sacy-1(tm5503)* genotyping
tm5503_R1	CTTGTATCTGAATAGCTGTCGGTGTCAC	*sacy-1(tm5503)* genotyping
H27M09.1_RNAi_F	TTTTAATACGACTCACTATAGGGTCAAATCTTTGACCTGATCATTGAAATG	*sacy-1* RNAi
H27M09.1_RNAi_R	TTTTAATACGACTCACTATAGGGGACAATCTGTGATGCGATGACCCAG	*sacy-1* RNAi
H27M09.1_cDNA_F1	TTTCCCGGGAATATGAGGACCGCCGGCGAAAAATTC	*sacy-1* cDNA 5' half RNAi
H27M09.1_cDNA_R1	TTTCTCGAGCTCTAACGTCTTTAGCTTGTTCGCCAATTG	*sacy-1* cDNA 5' half RNAi
H27M09.1_cDNA_F2	TTTCCCGGGCAATTGGCGAACAAGCTAAAGACGTTAGAG	*sacy-1* cDNA 3' half RNAi
H27M09.1_cDNA_R2	TTTCTCGAGCAATGCTTGCGTCGTTTTGTTTCCGATTC	*sacy-1* cDNA 3' half RNAi
acy-1_Exon13_F	AAGGTGATGGAATACCTCCATCAATCAAGGATAACCAAGAAGACGAATTTATGAGTAAAGGAGAAGAACTTTTCAC	Recombineering for *acy-1::gfp*
acy-1_Exon13_R	TGTGAAAGGAATTATAGAAGTTTGTTTAAAGCAAAATGTATGAAAATTTATTTGTATAGTTCATCCATGCCATG	Recombineering for *acy-1::gfp*
acy-2_Exon17_F	CCGGCGAGCAACAAAACCATAGTAACAACAATAATTGTCACAGTACACTCATGAGTAAAGGAGAAGAACTTTTCAC	Recombineering for *acy-2::gfp*
acy-2_Exon17_R	GAGAGAAGGTGAATGCAGTTGAGAGGTAAAAATAACAGAACAACGAGTTATTTGTATAGTTCATCCATGCCATG	Recombineering for *acy-2::gfp*
acy-3_Exon14_F	ACAATTTCGGAGACTTTCAACTTTCAACATTTGATGATATTGATCAGGACATGAGTAAAGGAGAAGAACTTTTCAC	Recombineering for *acy-3::gfp*
acy-3_Exon14_R	AGACCTAGAGAATAGTAAGAAACATATATTTGAAAAAAATGAAATGATTATTTGTATAGTTCATCCATGCCATG	Recombineering for *acy-3::gfp*
twk-1_GalK_F2	AGGTTTCAGATTCAGAAGAAGCTGAAATTTGGTTTGGAGGGCAAATGATGCCTGTTGACAATTAATCATCGGCATAG	Recombineering for *galk* insertion in threonine284 of *twk-1*
twk-1_GalK_R2	TCCGGCGTTGATCCAAACTTTTCAGCCACCAAAGTGACCAAATCCTTGACTCAGCACTGTCCTGCTCCTTG	Recombineering for *galk* insertion in threonine284 of *twk-1*
twk-1_C-ter_trunc	AGGTTTCAGATTCAGAAGAAGCTGAAATTTGGTTTGGAGGGCAAATGATGATGAGTAAAGGAGAAGAACTTTTCACTGGAGTTG	Recombineering for C-terminal deletion of *twk-1*

	TCCCAATTCTTGTTGA	
KIN-1R 50bp	AATCAACAGTGATGCAACATTCACAAAAAAAAGTTACCGAAA CTCTGTGG	Recombineering for extending *kin-1* promoter in the WRM069aA02 fosmid
KIN-1OF 50bp	TAAGTTGGGTAACGCCAGGGTTTTCCCAGTCACGACGTTGTA AAACGACGAGAGACACTGCTCCTGGAGAGTCAC	Recombineering for extending *kin-1* promoter in the WRM069aA02 fosmid
kin-1 galk F	TAAGTTGGGTAACGCCAGGGTTTTCCCAGTCACGACGTTGTA AAACGACGCCTGTTGACAATTAATCATCGGCA	Recombineering for *galk* insertion into the WRM069aA02 fosmid
kin-1 galk R	AATCAACAGTGATGCAACATTCACAAAAAAAAGTTACCGAAA CTCTGTGGTCAGCACTGTCCTGCTCCTT	Recombineering for *galk* insertion into the WRM069aA02 fosmid
H27M09.1_gfpF1	TTTTAAGTATCTTAAAAAGTAGAACAGAAAAATTCGTTTAGTA TTCCGAAATGAGTAAAGGAGAAGAACTTTTCACTG	Recombineering for *gfp::sacy-1*
H27M09.1_gfpR1	CGCCGGCGGTCCTCATATTTTCGTCGCGCCGCTTCCACATCTG TGCTCATTTTGTATAGTTCATCCATGCCATGTG	Recombineering for *gfp::sacy-1*
twk-1_GFP_F1	AAGCTCATCGGGTACACAGTGATGGTCGACTTTTACTGCAACA AGATGTGATGAGTAAAGGAGAAGAACTTTTCACTG	Recombineering for *twk-1::gfp*
twk-1_GFP_R1	ATATCCGTTTCTTTTTTTGTTTCGAAAAATCTAAAATTGCAGAA TATCTATTTGTATAGTTCATCCATGCCATGTG	Recombineering for *twk-1::gfp*
twk-1_F1	GACAAATAATGAAGCATCCTTCTTGGATAG	*twk-1* RT-PCR
twk-1_R1	GTGACCAAATCCTTGACAGTCATCATTTG	*twk-1* RT-PCR

Table S4 *pbrm-1* is not a Sacy mutation

Genotype	Brood size (± SD)	Number of animals scored
acy-4(ok1806)	1 (± 2)	30
pbrm-1(gk1195)[a]	102 (± 86)	30
pbrm-1(gk1195); acy-4(ok1806)	0 (± 2)	35
sacy-1(tn1385); acy-4(ok1806)	14 (± 15)	39
sacy-1(tn1385) pbrm-1(tn1475)[b]*; acy-4(ok1806)*	23[c] (± 18)	30
sacy-1(tn1440); acy-4(ok1806)	20 (± 19)	39
sacy-1(tn1440) pbrm-1(tn1476)[d]*; acy-4(ok1806)*	12[e] (± 11)	30

[a]VC10166 [*pbrm-1(gk1195) I; octr-1(gk1196) X*] strain was used. *pbrm-1(gk1195)* deletes 126 nucleotides, including an intron and part of exon 6 of the *pbrm-1a* gene isoform.

[b]*pbrm-1(tn1475)* induces a missense mutation (A1182T) in the *pbrm-1a* gene isoform.

[c]P=0.025 compared to *sacy-1(tn1385); acy-4(ok1806)*.

[d]*pbrm-1(tn1476)* induces a missense mutation (A157T) in the *pbrm-1a* gene isoform.

[e]P=0.048 compared to *sacy-1(tn1440); acy-4(ok1806)*.

Student's *t*-test was used for statistical analysis.

Table S5 *pde-6* negatively regulates oocyte meiotic progression

A. *pde-6(tn1237)* is epistatic to *gsa-1(pk75)* for oocyte meiotic maturation

Genotype	Fertile gonad arms/Total
gsa-1(pk75)	0/9
gsa-1(pk75); pde-6(tn1237)	5/6

Genetic mosaics in which the sheath/spermathecal lineages were mutant for *gsa-1* were sought using *tnEx31[gsa-1(+) sur-5::gfp]* for mosaic analysis (Govindan et al., 2009).

B. *pde-6(tn1237)* extends AIR-2::GFP to oocyte chromatin in a hermaphrodite background

Genotype	Chromatin localization of AIR-2::GFP Oocyte position in the gonad arm				
	–1	–2	–3	–4	–5
Wild type (n=72)	95.8%	32%	1.4%	0%	0%
pde-6(tn1237) (n=35)	100%	97.1%	70.6%	10.3%	0%

Strains were homozygous for *itIs14*, which expresses AIR-2::GFP in the germ line. MSP and $G\alpha_s$-ACY-4 signaling promotes the localization of AIR-2::GFP to oocyte chromatin (Govindan et al., 2009). The control data were published (Govindan et al., 2009), and the *pde-6* data were from a contemporaneous experiment.

Table S6 Genetic analysis of *twk-1(lf)* for meiotic maturation and Unc phenotypes

A. *twk-1(lf)* suppresses *acy-4(lf)* sterility

Genotype	Brood size (± SD)	Number of animals scored
acy-4(ok1806)	1 (± 2)	30
twk-1(tn1397); acy-4(ok1806)	36 (± 25)	36
twk-1(tn1397); acy-4(ok1806); tnEx180[a]	2[*] (± 7)	46
twk-1(tn1397); acy-4(ok1806); tnEx181[b]	1[*] (± 1)	40

[a]*tnEx180[twk-1(+) sur-5::gfp]*. *tnEx180* itself does not reduce brood size because *twk-1(tn1397); acy-4(ok1806)/nT1[qIs51]; tnEx180* hermaphrodites have 267 ± 36 (n=25) progeny.

[b]*tnEx181[twk-1::gfp str-1::gfp]*. *twk-1(tn1397); acy-4(ok1806)/+* animals bearing *tnEx180* or *tnEx181* are not Unc, indicating rescue of the *twk-1* adult-onset Unc phenotype.

[*]P<0.00001 compared to *twk-1(tn1397); acy-4(ok1806)* using Student's *t*-test.

B. The adult-onset Unc phenotype of *twk-1(tn1397)* requires *acy-4(+)*

Genotype	Percentage of Unc animals[a]	Number of animals scored
Wild type	0	152
twk-1(tn1397)	76	106
twk-1(tn1397); tnEx180[b]	0	126
twk-1(tn1397); acy-4(ok1806)	0	93
twk-1(tn1397); acy-4(ok1806); tnEx37[c]	93	94

[a]L4 hermaphrodites were transferred to new NGM plates and observed approximately 24 hrs later for the *twk-1(tn1397)* Unc phenotype. All L4s tested did not show the Unc phenotype at the time of picking.

[b]*tnEx180[twk-1(+) sur-5::gfp]*.

[c]*tnEx37[acy-4(+) sur-5::gfp]*.